Comments on the structure and dynamics of magnetic fields in stellar convection zones

Habilitationsschrift
zur Erlangung der Lehrbefugnis im Fachgebiet
Astronomie und Astrophysik

vorgelegt dem Fachbereich Physik in der
Mathematisch-Naturwissenschaftlichen Fakultät
der Georg-August-Universität zu Göttingen

von
Manfred Schüßler
aus Weinheim

Göttingen 1990

Preliminary remark

This paper is a “Habilitationsschrift”, a second thesis required until recently by universities in Germany and in a few other countries to obtain the right to lecture. It was accepted by the University of Göttingen in 1990 after review by a number of german and international experts. Although the introduction and the references represent the state of research in 1990, most of the remaining content is still relevant and has never been published elsewhere. The most important part is the derivation of a linear stability formalism for thin magnetic flux tubes following an arbitrary path in a gravitationally stratified medium with a stationary velocity. It was found later (Ferriz-Mas & Schüssler, Geophys. Astrophys. Fluid Dyn. vol. 72, 209; 1995) that, for consistency, the inertial term in the equation of motion for the external medium should be included in Eq. (3.24), which leads to an additional term in the stability equations in the case of a spatially varying external velocity. This term is missing in the present text, but can be easily introduced into the formalism.

Summary

Some aspects of magnetic fields in stellar convection zones are investigated in this contribution. Observational and theoretical results are discussed which support the conjecture that the magnetic field structure in a convection zone is intermittent with most of the magnetic flux being concentrated in small filaments or 'flux tubes' surrounded by field-free plasma. These kind of structures can be mathematically described with aid of the 'approximation of slender flux tubes' whose general form for flux tubes which follow an arbitrary path in space is rederived and discussed.

The approximation is applied to equilibrium structures of flux tubes determined by hydrostatic equilibrium along the magnetic field lines and by a balance of buoyancy, curvature and drag forces (exerted by external velocity fields like convection, rotation and large-scale flows) perpendicular to the field. Some general properties of static equilibria (without drag forces) are derived and it is shown that such structures are incompatible with the observed properties of solar magnetic fields. We discuss methods to determine equilibrium flux tubes in practice and give analytical examples of stationary tubes in a horizontal velocity field.

In the central part of the contribution we present a linear stability analysis of general flux tube equilibria including arbitrary external velocity fields. The tube may follow a curved path in space, gradients of external velocity and gravitational acceleration are included. The general equations for Lagrangian displacements are derived and for the application to stellar convection zones we give a suitably non-dimensionalized, approximate form for large values of the plasma parameter β which represents the ratio of gas pressure to magnetic pressure. For static equilibria a symmetric form of the equations is obtained which allows the application of variational methods and a simplified numerical treatment. It also serves as a consistency check for the (somewhat lengthy) algebra. The formalism is applied to analytically tractable cases, namely horizontal flux tubes and symmetric loops with horizontal tangent at the point of extremum (maximum or minimum). Numerical examples on the basis of the properties of the solar convection zone indicate that in a superadiabatically stratified environment and in the absence of an external flow all these structures are monotonically unstable. Stabilizing external velocity fields can be constructed, but they do not seem to be of much practical importance for the case of a stellar convection zone. Additionally, we have found that overstable modes can be excited by an external velocity field in which case the drag force conspires with the curvature force with the result of oscillations with growing amplitude. Overstable modes cannot be stabilized by stratification; they appear also in subadiabatic regions like a layer of overshooting convection.

Finally, we attempt to summarize our present state of understanding of magnetic fields in stellar convection zones and, in particular, the convection zone of the Sun. We favor the picture of a strongly fragmented, intermittent field structure. While in the deep parts the individual magnetic filaments are passive with respect to large-scale velocity fields, surface fields exhibit a peculiar nature owing to thermal effects and the dominance of buoyancy. As to the dynamo problem, we find that observational and theoretical evidence is in favor of a 'boundary layer dynamo' operating in an overshoot region below the superadiabatic parts of a convection zone.

Acknowledgements

Many people have contributed to this work, be it by discussion and criticism, by moral and technical support, or by their own work which laid the foundations on which I could build by adding a small brick to the walls of an unfinished building. Let me thank in particular

V. Anton for the good time we spent calculating flux tube models,
W. Deinzer for his encouragement and support,
H. Düker for help with technical problems,
A. Ferriz-Mas for his scrutinity with mathematical details and comments on Ch. 3,
M. Knölker for sharing his knowledge on eigenvalue problems,
D. Schmitt for advice on stability problems and the energy principle,
M. Stix for discussions about ways to determine the stability of loops, and
H. Spruit for clarifying answers concerning the approximation of slender flux tubes.

This work has been carried out and written down partly at the Kiepenheuer-Institut für Sonnenphysik, Freiburg, and partly at the Universitäts-Sternwarte, Göttingen. I like to thank my colleagues at both institutions for their support and for a climate of cooperation and kindness. Moreover, I am grateful to U. Grossmann-Doerth, R. Hammer and H. Schleicher for having taken the burden of additional work in a critical phase of installation and management of the computer network at the Kiepenheuer-Institut while I was on leave in Göttingen or absorbed in writing.

Finally, I want to thank E.N. Parker for his life-long work on solar and stellar magnetic fields which revealed so many basic mechanisms, opened so many doors and possibilities for investigation and understanding – and for continuously stirring up inveterate ways of thinking by pointing out inconsistencies and throwing new ideas into the arena.

Contents

1. Introduction

The activity of the Sun and other stars with outer convection zones and the origin of their hot chromospheres, coronae, and winds is intimately related to the existence of magnetic fields in their atmospheres. Most probably, the source of the magnetic flux which is observed to pervade photospheres of late-type stars is the underlying convection zone. In the case of the Sun, magnetic flux is directly observed to emerge from the convection zone. On the other hand, the 22-year period of the solar magnetic cycle leads to a very small (skin) depth to which the alternating magnetic fields can penetrate within the electrically well-conducting, quiescent radiative region below the solar convection zone.

A complete theory of the structure, dynamics and evolution of magnetic fields in stellar convection zones does not exist – and this work does not attempt to provide one. This lack of a consistent description of a basic astrophysical situation is due to a) the impossibility of direct measurements and b) our unsufficient comprehension of turbulent flows.

In the case of the Sun, although the physics of the photosphere is much more complicated, thanks to a wealth of observational data our understanding of photospheric magnetic fields is much more advanced than the state of theory for the fields within the convection zone. Only indirect observational evidence about their state is available through photospheric observations – and due to the peculiar nature of this layer the results are not necessarily representative for the deeper parts (cf. Sec. 6.3). The situation can be illustrated by the following simile: Imagine a person who is unfamiliar with the purpose and operation of clocks. Imagine further that this person is confronted with a mechanical clock and the task to analyze the internal mechanism without opening it, just from the visual appearance of the dial, the motion of the hands and a spectral analysis of the ticking. Good luck! A person who tries to understand the structure and dynamics of the convection zone and its magnetic fields is in a similar situation: Only a shallow surface layer can be observed directly (dial and hands) while global oscillations (ticking) supply some indirect information from the deeper layers.

The large spatial extension of a stellar convection zone and the small viscosity of a stellar plasma lead to enormous values of the Reynolds number $Re = UL/\nu$ (U, L: velocity and spatial scale of the dominant convective flow, ν: kinematic viscosity) which describes the ratio of the magnitudes of inertial force and viscous force. For the granular velocity field observed in the solar photosphere ($U \approx 1$ km$\cdot$s^{-1}, $L \approx 10^3$ km, $\nu \approx 10^{-3}$ m$^2\cdot$s^{-1}) we find $Re \approx 10^{12}$. Consequently, the nonlinear inertial forces dominate and a turbulent cascade of kinetic energy to larger spatial wavenumbers ensues until scales of less than 1 cm are reached at which disspation by molecular viscosity effectively takes place. Stellar convection zones thus span a huge range of scales which reach from their global dimensions and time scales (of the order of 10^5 km and 10^6 s, respectively) to the disspation range of about 1 cm with a related dynamical time scale of less than 1 s. The problem of describing turbulent convection in a stellar convection zone is rendered even more difficult by the influences of rotation and of stratification due to gravity.

The *magnetic* Reynolds number $Re = UL/\eta$ where η denotes the magnetic diffusivity is also very large. For the solar convection zone it increases from about 10^3 in the upper layers to about 10^9 near the bottom (cf. Stix, 1976). Consequently, field line advection and stretching is much more important than Ohmic dissipation on the dominant scale of convective flows. Similar to the fluid motions, the magnetic field spans large ranges of spatial and temporal scales which extend from the global convective to the dissipative scales.

Given our insufficient understanding of turbulent convection it may seem futile to complicate things even more by introducing magnetic fields or, more precisely, by taking account of the large electrical conductivity of the stellar plasma. Besides the fact that the very presence of magnetic fields in the solar and stellar atmospheres forces us to do so, the additional complication brought about by including magnetic fields must not necessarily be prohibitive since there is a number of indications that magnetic fields do not significantly influence the global structure and dynamics of stellar convection zones. One piece of evidence is the success of the theory of stellar structure and evolution which has been developed without taking account of magnetic fields while the other line of arguments is provided by the comparatively small magnitude of observed variations of the Sun during the activity cycle.

The reversals of the polar fields, the polarity rules for active regions, and the strong variation of the frequency of occurrence of large active regions indicate a major change of the magnetic structure in the convection zone during the activity cycle. On the other hand, the change of the solar convection zone is much less significant: Variations of the surface rotation rate of both plasma and magnetic structures (at a given heliographic latitude) are smaller than a few percent (Howard, 1984; Schröter, 1985) while a velocity structure associated with the activity belts (misnamed 'torsional oscillation' by its discoverers, cf. LaBonte and Howard, 1982) has an amplitude of less than 1% of the differential rotation in latitude. Convective flow patterns do not show a significant change during the cycle either, apart from slight variations of the size distribution of granules (Müller and Roudier, 1984) and, possibly, of their temperature structure (Livingston and Holweger, 1982). It is improbable that much larger variations in the deep layers of the convection are effectively 'screened' by the surface layers since perturbations of temperature and velocity are transmitted from the bottom of the convection zone to the surface without being significantly attenuated (Stix, 1981b). Solar cycle variations of the solar radius are smaller than 200 km (Wittmann et al., 1981; Parkinson, 1983). The short-term luminosity variation is of the order of 10^{-3} and corresponds directly to the fraction of the surface covered by sunspots while a variation of about the same magnitude on the time scale of the cycle is indicated (Willson, 1984). However, larger heat flux variations on the time scale of the solar cycle in the deep layers of a convection zone may be efficiently screened due to its large thermal conductivity and heat capacity (Spruit, 1977a, 1982; Stix, 1981b).

All these results support the thesis that magnetic fields do not significantly modify the convection zone on a global scale. However, one must not conclude that magnetic forces can as well be neglected locally, i.e. at any given location. The contrary seems to be the case: A global equipartition of magnetic and kinetic energy which would lead to major changes of the convection zone during the magnetic cycle is avoided by concentration of the magnetic flux into filaments of strong field with large regions of non-magnetic, undisturbed convection between (Parker, 1984a). Such a 'phase separation' in a convecting and a magnetic phase is observed for the case of the solar photosphere: Most of the observable magnetic flux (outside sunspots) is in the form of concentrated structures of high flux density which are arranged in a network defined by the downflow regions of granulation and supergranulation, the dominant convective structures (Stenflo, 1989; Solanki, 1990).

Under the conditions prevailing in a convection zone the flux expulsion process (for a discussion and further references see Sec. 2.2) which is responsible for this separation in magnetic and convecting regions leads to *local* equipartition of the magnetic and kinetic energy *densities* which gives a flux density of about 10^4 Gauss in the deep parts of the solar convection zone. Since the amount of magnetic flux which emerges during one half cycle (11 years) is about 10^{24} mx (Howard,

1974) it fills only about 1% of convection zone volume given such a flux density. Consequently, the total magnetic energy of $E_{mag} \approx 3 \cdot 10^{35}$ erg amounts to about 1% of the total kinetic energy (E_{con}) of the convective flows. The total energy of differential rotation (E_{dr}) is of the same order of magnitude as E_{con} since the velocity differences due to differential rotation in depth and in latitude (Duvall et al., 1984, 1987) are of the same order of magnitude as the convective velocities in the deeper parts of the convection zone. Consequently, we find the following scaling of total energies within the convection zone:

$$E_{con} \approx E_{dr} \approx 10^2 E_{mag}.$$

These relations are consistent with the observed percent-level variations of the properties of the solar convection zone during the activity cycle. In the light of these considerations it seems adequate to take the convective flows as given and undisturbed by the magnetic fields for all scales which are large compared to the typical size of the magnetic flux concentrations. Small-scale flows locally are strongly affected by the presence of the field and probably convective heat exchange between a flux concentration and its environment is largely suppressed.

While a complete theory is lacking, a variety of more or less satisfactory physical descriptions and models of certain aspects of the complicated thermodynamical and (magneto)hydrodynamical system represented by a stellar convection zone can be found in the literature. We do not attempt to give a complete overview but we may roughly classify them in two complimentary groups, namely the *mean field approach* and the *model problem approach.* The contributions belonging to the first group attempt to describe the large-scale structure and dynamics of a stellar convection zone with the aid of parametrized model equations for appropriately averaged quantities which vary on large scales. Such equations typically contain parameters or functions which represent conjectures about small-scale processes. Prominent examples are Prandtl's mixing length formalism which has been used successfully in the theory of stellar structure and evolution and the mean-field approach for magnetic fields (e.g. Parker, 1979a; Krause and Rädler, 1980) which led to the presently most developed theory of the solar cycle, the theory of turbulent dynamo action.

Attempts towards a numerical simulation of the hydrodynamical and magnetic structure of the convection zone (Gilman and Miller, 1981; Gilman, 1983; Glatzmaier 1984, 1985a,b; Brandenburg et al., 1990) also fall into this category: Due to limitations of memory capacity and processor speed of presently available computers only a small part of the range of spatial and temporal scales can be covered by the simulation and the influence of the small scales is parametrized by introducing 'turbulent' values for viscosity as well as thermal and magnetic diffusivity. The effective (hydrodynamical and magnetic) Reynolds numbers for such simulations are therefore many orders of magnitude smaller than those of the real system. The results are partly in contradiction to observational data: Neither the predicted uniformity of angular velocity on cylindrical surfaces nor the large amplitude of large-scale convective flows has been borne out by measurements (Duvall et al., 1987; Brown et al. 1989; Dziembowski et al., 1989; LaBonte et al., 1981). Furthermore, the characteristic features of the solar cycle could not be reproduced by the simulations. Apparently processes operating on small scales which have not been resolved play an important rôle for the hydrodynamic and the magnetic structure of the convection zone.

In the contributions belonging to the second group, *model problem approaches*, individual processes are studied in (artificial) isolation and their relevance for the global behavior of the system is evaluated. This may lead to the introduction of new terms in model equations and to a more sensible parametrization in numerical simulations. Furthermore, one might attempt to combine a sample of reasonable well understood processes like a jigsaw puzzle in order to obtain a description of the whole system. The work of E.N. Parker (cf. Parker, 1979a) is a prominent example for the model problem approach. The theory of magnetic flux tubes (e.g. Spruit and Roberts, 1983), the work on magnetoconvection carried out by N.O. Weiss and his colleagues in Cambridge (cf. Proctor and Weiss, 1982), and the simulations of turbulence with magnetic fields performed by the Nice group around U. Frisch and A. Pouquet (e.g. Meneguzzi et al., 1981; Grappin et al., 1982; Pouquet, 1985; Meneguzzi and Pouquet, 1989) also fall in the group of model problems.

The work presented here belongs to the same class of contributions. Its motivation results from the debate on magnetic flux storage in a convection zone and the location of the dynamo process which is responsible for the solar activity cycle. Parker (1975a) argued that magnetic buoyancy leads to rapid flux loss and thus prohibits the storage of magnetic flux within the convection zone for time intervals comparable to the cycle period. This argument was strengthened by Spruit and van Ballegooijen (1982) who showed that toroidal flux tubes are unstable in a superadiabatically stratified region. Following earlier proposals (e.g. Spiegel and Weiss, 1980; Galloway and Weiss, 1981) they suggested that a slightly subadiabatic region of overshooting convection near the bottom of the solar convection zone represents a favorable place for the storage of magnetic flux and the operation of a dynamo mechanism (see also van Ballegooijen 1982a,b; Schüssler, 1983, 1984a; Durney, 1989).

However, are the arguments given so far sufficient to definitely exclude that the major part of the magnetic flux emerging in the solar activity cycle is stored within the convection zone proper? For instance, Parker (1987a-d; 1988a-c) has argued that 'thermal shadows' due to local suppression of convection can keep large portions of magnetic flux in the deep parts of the convection zone. Here we consider another possibility and investigate whether flux tubes could possibly find a stable equilibrium in the convection zone if they follow a curved path in space and/or if the influence of external flows is taken into account. Of particular interest in this respect are loop structures and sequences of loops ('sea serpents'). To this end we reconsider the general form of the approximation of slender flux tubes (Spruit, 1981a,b), determine general properties of static and stationary flux tube equilibria, and generalize the approach of Spruit and van Ballegooijen (1982, see also van Ballegooijen, 1983; van Ballegooijen and Choudhuri, 1988) to derive a stability analysis formalism for a flux tube which follows an arbitrary path in space. This analysis is embedded in a general discussion of the structure and dynamics of magnetic fields in a stellar convection zone which is necessarily tentative and far from rigorous.

We start by presenting some arguments in favor of the conjecture that magnetic fields in stellar convection zones consist of small, concentrated structures separated by field-free plasma. As a basis for this conjecture, a variety of physical processes which form and maintain such structures is discussed in Ch. 2. The small size of the magnetic flux concentrations resulting from fragmentation and expulsion processes permits their description using the approximation of slender flux tubes. In Ch. 3 we rederive the general form of this approximation for a flux tube which follows an arbitrary path in space. We use a somewhat different approach than that taken by Spruit (1981a,b) in order to elucidate some aspects of the approximation. The formalism is applied in Ch. 4 to obtain some general properties of flux tubes in static equilibrium given by the balance of buoyancy and curvature force and of flux tubes in stationary equilibrium for which the drag force exerted by an external flow field is additionally taken into account. In Ch. 5, the central part of this contribution, a formalism is derived which allows the stability analysis of a general static or stationary flux tube equilibrium with arbitrary path in space. Some basic stability properties are derived by application of this formalism to a number of special cases which can be treated analytically, in particular horizontal tubes and symmetric loops. In Ch. 6 the outcome of these calculations, the results of other investigations and further considerations are tentatively combined in a (hopefully) coherent picture which summarizes the author's present view of magnetic fields in stellar convection zones. This includes also a discussion of the consequences for the dynamo problem. Finally, an outlook on possibilities for extension and continuation of this work is given in Ch. 7.

2. Formation of structures

The work presented here is based on the hypothesis that, similar to the observed magnetic fields in the photosphere of the Sun, most of the magnetic flux within a stellar convection zone is concentrated into filaments or *flux tubes** embedded in nearly field-free plasma. Although at present this conjecture can neither be proven theoretically in a rigorous way nor undubitably demonstrated by observations it is supported by a number of observational indications and theoretical results.

Observationally, Hale's polarity rules for solar active regions are known to apply with very few exceptions (e.g. Howard, 1989). This can only be so if the magnetic fields in the convection zone are strong enough to avoid a significant deformation by convective velocity fields, i.e. if the magnetic energy density is equal to or larger than the kinetic energy density of convection. Otherwise the magnetic fields would be passively carried around at random and the erupting active region would not show a preferred orientation. Consequently, the magnetic field strength at least must be of the order of the *equipartition field strength*

$$B_e = v_c(4\pi\rho)^{1/2} \tag{2.1}$$

(v_c: convective velocity, ρ: density). Throughout the whole convection zone B_e is much larger than the average field strength of about 100 Gauss which can be estimated from the total magnetic flux emerging during one activity cycle. Consequently, if the magnetic flux in the convection zone has at least equipartition field strength it is strongly intermittent and fills only a small fraction of the volume. The observed properties of emerging active regions and the formation of sunspots by accumulation of fragments also indicate that the magnetic flux already is in a concentrated form before it appears at the solar surface (Zwaan, 1978; McIntosh, 1981; Garcia de la Rosa, 1987).

Theoretical arguments for a filamented nature of the magnetic fields in a stellar convection zone are given in the subsequent sections.

2.1 Rayleigh-Taylor instability of a magnetic layer

Beginning with Parker (1975a) a number of arguments has been put forward which support the assertion that the major part of the magnetic flux which is responsible for the solar activity cycle cannot be kept in the superadiabatic parts of the convection zone for times comparable to the cycle period. The flux rather has to be stored below in a region of overshooting convection where a magnetic layer forms which occasionally ejects magnetic flux into the convection zone proper (Spiegel and Weiss, 1980). Since the thickness of such an overshoot layer probably is less than the local pressure scale height of about $5 \cdot 10^4$ km (Shaviv and Salpeter, 1973; Schmitt et al., 1984; van Ballegooijen, 1982b; Pidatella and Stix, 1986) and thus a lot of toroidal magnetic flux (about 10^{24} mx) has to be accommodated in a rather small volume the field there is thought to be densely

* Strictly spoken, the term 'flux tube' refers to a cylindrically shaped bundle of magnetic field lines. However, in what follows we shall often use this term more loosely to generally denote a magnetic filament or flux concentration of arbitrary shape.

packed (non-filamented) and, because the flow velocities are small compared to the sound speed, in magnetostatic equilibrium.

If the (horizontal or toroidal) magnetic field decreases rapidly enough with height or even drops to zero discontinuously at some level, this equilibrium which is basically a balance between gravity and the gradient of the total (magnetic + gas) pressure becomes unstable with respect to an interchange of more and less magnetized fluid which lowers the potential energy of the system. This is the magnetic Rayleigh-Taylor instability* of a layer of magnetic field directed perpendicular to the local direction of gravity (Gilman, 1970; Cadez, 1974; Acheson and Gibbons, 1978; Acheson, 1979; Parker, 1979b; Schmitt and Rosner, 1983; Hughes, 1985a,b, 1987; Schmitt, 1985; Hughes and Cattaneo, 1987). For this kind of instability the stratification need not necessarily show a density inversion as in the case of the hydrodynamical Rayleigh-Taylor instability. The nonlinear evolution of the instability in the case of a discontinuity of the magnetic field is nicely illustrated by the numerical simulation of Cattaneo and Hughes (1988) who showed that secondary Kelvin-Helmholtz instabilities lead to the formation of intense vortices whose dynamical interaction dominates the dynamics after the first phases of the instability.

Because of the stabilizing effect of magnetic curvature forces linear stability analysis shows that the fastest growing perturbations are those with large wavelength along and small wavelength perpendicular to the equilibrium magnetic field. Consequently, the formation of *thin* structures at the upper boundary of a sheet of horizontal magnetic field (where the field strength may rapidly decrease with height) is favored. Quantitative results for the case of a stellar convection zone are difficult to obtain since most of the work done so far is restricted to linear analysis under idealized assumptions. The typical fragment sizes of a destabilized flux sheet depend on diffusive effects (thermal, viscous and magnetic) and on the detailed height dependence of field strength and entropy. Another important effect to consider is *rotation* which may drastically reduce the growth rates or even entirely suppress the instability (cf. Acheson, 1978; 1979; Roberts and Stewartson, 1977).

We shall not discuss here the complex variety of instability mechanisms which grows out of the interaction of differential rotation, magnetic field, stratification and diffusive effects (see e.g. Schmitt and Rosner, 1983). In order to give a crude estimate of typical temporal and spatial scales we consider a case which is thought to represent the typical properties of a magnetic layer in the overshoot region below the solar convection zone: Adiabatic or weakly subadiabatic temperature stratification, sound speed (≈ 500 km$\cdot$s^{-1}) large compared to rotational velocity (1.4 km$\cdot$s^{-1}) which, in turn, is large compared to the Alfvén velocity (≈ 60 m$\cdot$s^{-1} for an equipartition field of about 10^4 Gauss). Under these circumstances the magnetic Rayleigh-Taylor instability evolves near the top of the sheet, i.e. in a region where the field strength, B, decreases with height faster than density, ρ, in the form of growing magnetostrophic waves which propagate along the direction of the equilibrium magnetic field (Acheson, 1979; Schmitt, 1985). For a magnetic layer of thickness D the fastest growing wave mode is characterized by the wavenumbers n (perpendicular to both gravity and magnetic field) and k (parallel to the field) which are given by (Acheson, 1979, Ch. 3)

$$n^2D^2 = \frac{\pi}{2}\, C^{1/2} \left[-\frac{H_p}{\gamma}\, \frac{d}{dz} \ln\left(\frac{B}{\rho}\right) \right] \tag{2.2}$$

$$k^2H_p^2 = \frac{1}{2} \left[-\frac{H_p}{\gamma}\, \frac{d}{dz} \ln\left(\frac{B}{\rho}\right) \right] \tag{2.3}$$

* In the case of a discontinuous transition between a non-magnetic plasma and a vacuum magnetic field the instability is known as Kruskal-Schwarzschild instability (cf. Cap, 1976, Ch. 11).

(H_p: pressure scale height, γ: ratio of specific heats, z: height coordinate, antiparallel to the direction of gravity). The quantity C is given by

$$C = \frac{v_A^2}{2\Omega\eta}\,\frac{D^2}{H_p^2} \tag{2.4}$$

(v_A: Alfvén speed, Ω: angular velocity, η: magnetic diffusivity). Using values of $B = 10^4$ Gauss, $\Omega = 2.7\cdot 10^{-6}$ s^{-1}, the surface equatorial rotation rate, $\eta = 10^4$ cm^{2}s^{-1}, $H_p = 6\cdot 10^4$ km and $D = 10^4$ km (cf. Schmitt et al., 1984) we find $C \approx 2\cdot 10^7$. Taking the thickness of the layer, D, as typical length scale for the decrease of B/ρ with height, we find

$$-\frac{d}{dz}\ln\left(\frac{B}{\rho}\right) \approx D^{-1} \tag{2.5}$$

and from Eqs. (2.2) and (2.3)

$$n^{-1} \approx 6\cdot 10^{-3} D \approx 60 \text{ km}$$
$$k^{-1} \approx .75\ H_p \approx 4.5\cdot 10^4 \text{ km}\,.$$

Thus the fastest growing wave has a longitudinal wavelength of about a scale height and a much smaller transversal scale. With increasing amplitude the wave penetrates into the convection zone proper and its filaments become subject to the convective flows. Furthermore, they are liable to other instabilities and fragmentation processes (see Sec. 2.3). We conclude that the magnetic Rayleigh-Taylor instability of a magnetic layer in an overshoot region leads to magnetic fragments in the convection zone which have a transversal scale of the order of 100 km or less.

The growth time, τ, of the instability is given by

$$\begin{aligned}\tau &\approx \frac{4\Omega H_p^2}{v_A^2}\left[-\frac{H_p}{\gamma}\,\frac{d}{dz}\ln\left(\frac{B}{\rho}\right)\right]^{-1}\\ &\approx \frac{4\gamma\Omega H_p D}{v_A^2} \approx 35 \text{ days}\,.\end{aligned} \tag{2.6}$$

This rather large time scale reflects the stabilizing influence of rotation. The instability cannot be suppressed by the stable, subadiabatic stratification of the overshoot layer since the radiative thermal diffusivity $\kappa \approx 2\cdot 10^7$ cm^{2}s^{-1} equalizes temperature differences between a structure with $l = 60$ km diameter and its environment in a timescale $l^2/\kappa \approx 41$ days which is comparable to the growth time of the instability given by Eq. (2.6). The flux loss of a magnetic layer in the overshoot region due to the magnetic Rayleigh-Taylor instability is possibly limited by the 'turbulent diamagnetism' of the convection zone which is briefly discussed in Sec. 2.2.

The conclusions drawn above are not significantly changed if an appropriate "turbulent" value for the magnetic diffusivity is taken instead of the molecular value $\eta = 10^4$ cm^{2}s^{-1}. This is true even if the suppression of motions by the strong magnetic field in the layer is ignored. We take an appropriate "microscale" $\delta = 100$ km for the motions to be described by the turbulent diffusivity η_t which is given by

$$\eta_t \approx 0.1\,u(\delta)\,\delta \tag{2.7}$$

where $u(\delta)$ is the turbulent velocity on the spatial scale δ. Assuming a Kolmogorov spectrum with an external scale $L = 10^{10}$ cm and $u(L) = 10^4$ cm·s^{-1} as typical for the convective flows in the deep convection zone we find

$$u(\delta) \;=\; u(L)\left(\frac{\delta}{L}\right)^{1/3} \;\approx\; 10^3 \;\mathrm{cm}\cdot\mathrm{s}^{-1} \tag{2.8}$$

and using Eq. (2.7) we have $\eta_t \approx 10^9$ cm^{2}s^{-1}. Hence, the quantity C is decreased by a factor 10^5 (cf. Eq. 2.4) and we see from Eq. (2.2) that the transversal length scale n^{-1} is increased by a factor $10^{5/4}$ to about 1000 km which confirms a posteriori our choice of the microscale in Eq. (2.7). The fragment size is still much smaller than the local scale height and the typical length scales of the convective motions. While the growth time of the instability given by Eq. (2.6) is not changed, the thermal diffusion timescale is now about 30 years and radiative heating cannot remove the stabilizing effect of a subadiabatic temperature stratification.

In a much more detailed study Schmitt and Rosner (1983) come to essentially the same conclusions. The magnetic Rayleigh-Taylor instability is of "double-diffusive" nature: For molecular magnetic diffusivity we have $\eta/\kappa \ll 1$, i.e. the stabilizing effect of the subadiabatic stratification is connected with a larger diffusivity (κ) than the destabilizing magnetic field gradient (η) and instability ensues. On the other hand, if $\eta = \eta_t$ we have $\eta > \kappa$ and a sufficiently subadiabatic stratification like the one used by Schmitt and Rosner (1983) removes the magnetic instability while an adiabatic stratification as assumed by Acheson (1979) still leads to instability. Consequently, the stability properties of a magnetic layer depend sensitively on the entropy gradient within the overshoot region. Model results for this quantity have been presented, among others, by Shaviv and Salpeter (1973), Schmitt et al. (1984) and Pidatella and Stix (1986). All these authors find that the subadiabaticity is rather small ($\nabla - \nabla_{ad} \approx -10^{-6} ... - 10^{-7}$) in the overshoot layer.

Schmitt and Rosner (1983) propose the following scenario: During a first phase magnetic flux is accumulated and amplified by dynamo processes but the field strength stays below the equipartition value and the turbulent motions are not strongly affected by the magnetic field. Consequently, turbulent diffusivities are appropriate and, given a sufficiently large subadiabaticity, the configuration is stable. As the field strength increases (e.g. by differential rotation) the turbulent motions are more and more affected by the field and the magnetic diffusivity approaches its molecular value. As we have seen above, this quenches the stabilizing effect of the stratification, the magnetic layer sheet becomes unstable and is ejected into the convection zone in the form of small filaments.

The important point for this work which mainly deals with the magnetic structure *within* the convection zone proper is that in any case very small structures with diameters between 100 and 1000 km are formed when the instability sets in.

2.2 Flux expulsion

Independent of having entered from below or being generated in place magnetic flux within a convection zone interacts with the convective flows, a situation which the theory of magnetoconvection attempts to describe (see Proctor and Weiss, 1982, for a review). An important result of this interaction is *flux expulsion*, a process which has first been demonstrated in the kinematical case (passive magnetic field) by Parker (1963). He showed that in an electrically well-conducting plasma with a stationary velocity field a magnetic field is excluded from the regions of closed streamlines. Starting with the work of Weiss (1966) a number of numerical studies have been performed (e.g. Galloway et al., 1978; Weiss, 1981a,b). They showed that in a convecting medium at high magnetic Reynolds number $R_m = UL/\eta$ (U, L: Velocity and size of the dominating convective cell, η: magnetic diffusivity) permeated by a magnetic field, the magnetic flux is concentrated into filaments between the convection cells. This effect is related to the phenomenon of 'intermittency' for magnetic fields in turbulent flow (e.g. Kraichnan, 1976; Orszag and Tang, 1979; Meneguzzi et al., 1981).

In a compressible, stratified fluid the magnetic flux concentrations formed by flux expulsion are found in the convective downflow regions (Nordlund, 1983; 1986; Hurlburt et al., 1984; Hurlburt and Toomre, 1988). Observations demonstrate that the flux expulsion process operates in the solar (sub-)photosphere: On both the granular (Title et al., 1987) and the supergranular scale (the well-known network fields) magnetic flux is predominantly located and concentrated in the downflow regions.

The nonlinear back-reaction of the magnetic field on the convective flows via the Lorentz force limits the flux density which can be achieved by flux expulsion to a value which is roughly given by the equipartition of magnetic and kinetic energy density. This limit may be modified by compressibility, diffusive and thermal effects (e.g. Galloway et al., 1978; Schüssler, 1990). Furthermore, motion is excluded from strong flux concentrations and a kind of "phase separation" between field-free, convecting fluid and magnetic, almost stagnant regions evolves. Such a situation seems to be favored energetically (Parker, 1984): The interference of the magnetic field with the convective energy transport is minimized and the total energy is smaller than for a state with a diffuse field and the same convective energy flux. The exclusion of motion for fields stronger than equipartition suppresses the convective heat exchange between the magnetic structure and its surroundings. Thermal interaction with the environment is reduced to radiative energy transport.

The properties of nonlinear magnetoconvection are much more complicated than can be discussed here (see Proctor and Weiss, 1982). For our purposes it suffices to state that a magnetic field permeating a convecting fluid at high magnetic Reynolds number inevitably is concentrated into structures of about equipartition field strength. In the convection zone the magnetic Reynolds number for the dominating convective flows is everywhere large: It increases from about 10^3 in the upper layers to about 10^9 near the bottom (cf. Stix, 1976). Consequently, flux expulsion is relevant throughout the whole convection zone and we have to expect a concentrated, filamented magnetic field structure.

The well-known formal analogy between the MHD induction equation and the equation which determines the time evolution of *vorticity* supports the conjecture that the expulsion effect operates also for vorticity and leads to the formation of intense whirls or vortices. An example in cylindrical geometry has been given by Galloway (1978) while Schüssler (1984a) showed that a full analogy between *kinematic* expulsion of magnetic field and vorticity holds for two-dimensional flow in cartesian geometry. Numerical simulations of turbulence (e.g. McWilliams, 1984) and laboratory experiments in rotating, turbulent fluids (McEwan, 1973; 1976; Hopfinger et al., 1982) have clearly demonstrated vorticity expulsion for rotationally dominated flows (i.e. flows with small Rossby number $U/(2\Omega L)$ with U, L: velocity and size of the dominating eddy, Ω: angular velocity). A similar effect occurs in the simulations of solar granulation carried out by Nordlund (1984b, 1985a) who found that narrow granular 'fingers' come into rapid rotation. At least in the surface layers of the Sun magnetic field and vorticity are concentrated in the same locations such that magnetic flux concentrations become surrounded by rapidly rotating, descending whirl flows.

In a general context flux expulsion is related to the idea of *turbulent diamagnetism* which goes back to Zel'dovich (1957) and Spitzer (1957). This means a transport of magnetic field antiparallel to the gradient of turbulent intensity in inhomogeneous turbulence. The effect tends to expel a magnetic field into the boundary parts of a confined turbulent region (like a convection zone). Adopting a two-scale approach turbulent diamagnetism has been studied by Rädler (1968), Moffatt (1983) and Cattaneo et al. (1988). Again, we may conjecture that the effect operates in a similar way for vorticity. For the illustrative case of spatially periodic velocity field in two dimensions with a perpendicular shear flow Schüssler (1984a) applied a mean-field treatment for the kinematic case and showed that vorticity is transported and expelled in the same way as a magnetic field. He also gave an estimate for the effect of this mechanism on the depth dependence of rotation in the lower half of the solar convection zone where rotation is dominant (Rossby number ≈ 0.3). A stationary profile of the angular velocity Ω could be determined by assuming a balance between the 'negative viscosity' effect of vorticity expulsion and normal (turbulent) viscosity.

For the solar and stellar convection zones we may conjecture that flux expulsion has two major effects in a stellar convection zone: It leads to a filamentary state of magnetic fields by generating local concentrations of magnetic flux and vorticity *and* it pushes both magnetic field and vorticity (angular momentum in a rotating system) to the boundaries. This generates a magnetic shear layer at the bottom of the convection zone, a region which is favorable for the operation of a dynamo mechanism (see Sec. 6.4).

2.3 Instabilities and fragmentation of single flux tubes

Having shown some evidence in favor of a concentrated and filamented state of magnetic fields in a stellar convection zone we may ask for the typical size of a flux concentration. The size distribution of magnetic structures depends not only on the initial sizes of the flux tubes injected into the region but also on fragmentation, accumulation and coagulation processes operating in the convection zone itself (Bogdan, 1985; Bogdan and Lerche, 1985). Large-scale convective flows tend to accumulate magnetic flux by way of the flux expulsion mechanism discussed in the preceding section but a number of processes counteracts this tendency to form large structures in the form of single, coherent flux tubes.

A first mechanism to mention is, again, the *magnetic Rayleigh-Taylor instability:* If a magnetic structure is oriented mainly horizontally, it may be fragmented by this instability if it is larger than the scale given by Eq. (2.2). However, the rather large growth time (Eq. 2.6) must be compared with the time scales of other processes in order to evaluate the relevance of this instability. Of particular importance in this connection are the hydromagnetic interchange instability and a special form of the Kelvin-Helmholtz instability.

The *interchange instability* is well known from laboratory plasmas (e.g. Krall and Trivelpiece, 1973, Ch. 5; Cap, 1976, Ch. 11). As a simple example consider the interface between a non-magnetic plasma and a vacuum magnetic field where in equilibrium gas pressure and magnetic pressure are equal. This equilibrium is unstable if, looking from the plasma side, the boundary is concave: the potential energy of the system can be diminished by exchanging magnetic and non-magnetic volume elements because this procedure decreases the magnetic tension. Conversely, if the boundary is convex with respect to the plasma, the equilibrium is stable. These considerations apply in a similar way to a non-vacuum magnetic field. For cylindrical or rotationally symmetric configurations the instability is often referred to as *fluting* or *flute instability* since the most rapidly growing perturbations are reminiscent to the flutes of classical columns.

The interchange instability is important for magnetic fields in the convection zone in at least three respects. Firstly, it increases the efficiency of magnetic field line reconnection (Parker, 1979a, Ch. 15); secondly, it can lead to fragmentation of vertical magnetic structures in the uppermost (subphotospheric) layers: Since the gas pressure decreases rapidly with height, a vertical flux tube (e.g. a sunspot) flares out with height. Consequently, the interface becomes concave with respect to the non-magnetic plasma and the configuration is liable to the interchange instability (Parker, 1975b; Piddington, 1975). Meyer et al. (1977) showed that the stratification of the fluid (due to gravity) stabilizes large flux tubes (magnetic flux larger than about $5 \cdot 10^{19}$ mx): Interchanging magnetic and non-magnetic fluid entails lifting dense material above light material which gives a positive contribution to the potential energy. Similarly, small flux tubes (magnetic flux below about $5 \cdot 10^{17}$ mx) may be stabilized by surrounding whirl flows (Schüssler, 1984b). In this case, the dynamical stability of the angular momentum distribution at the boundary compensates the destabilizing effect of field line curvature.

The third aspect – which is most important for the discussion here – is the interchange instability of deformed magnetic structures in the deep convection zone. Because of the large electrical conductivity and due to hydrodynamic coupling, magnetic structures follow the fluid motions (convection, differential rotation) until the curvature forces have grown strong enough to resist further deformation. However, for the curvature force to come into play a flux tube must be significantly deformed (cf. Sec. 6.2). As a simple example, consider an initially vertical flux tube subject to a horizontal, localized jet-like flow. The tube is deformed to the shape sketched in Fig. 1 and reaches an equilibrium which, in the absence of gravity, is determined by the balance of the hydrodynamic drag force and the magnetic curvature force (cf. Sec. 4.2).

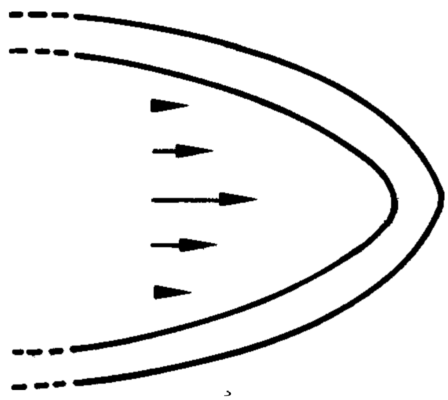

Fig. 1: Sketch of a flux tube under the influence of a horizontal, jet-like velocity field. An equilibrium is reached if the curvature force balances the hydrodynamic drag force. The interface on the upstream side is liable to the interchange instability.

The interface between the flux tube and the surrounding plasma is unstable on the upstream side which faces the flow and in the absence of stabilizing effects the flux tube splits up into smaller fragments. Linear stability analysis in the case of vanishing magnetic diffusivity gives for the growth time, τ, of the instability (cf. Cap, 1976)

$$\tau(n) \;=\; \left(\frac{\rho R}{2\,\Delta p\, n}\right)^{1/2} \tag{2.9}$$

(Δp: gas pressure difference at the interface; n: perturbation wave number, perpendicular to equilibrium magnetic field; R: radius of curvature of the interface). Since the gas pressure difference is equal to the magnetic pressure of the flux tube, i.e. $\Delta p = B^2/8\pi$, we find from Eq. (2.9)

$$\tau(n) \;=\; (v_A)^{-1}\left(\frac{R}{n}\right)^{1/2} \tag{2.10}$$

where $v_A = B/(4\pi\rho)^{1/2}$ is the Alfvén velocity. An upper limit for the growth time can be obtained by specifying a lower limit for n, i.e. $n \geq (2a)^{-1}$ where a is the radius of the flux tube. This leads to

$$\tau \;\leq\; \frac{(2R\,a)^{1/2}}{v_A} \tag{2.11}$$

Consequently, the growth time is smaller than the travel time of an Alfvén wave over a distance given by the geometric mean of flux tube diameter and its radius of curvature. For a strongly deformed tube with $R \approx a$ we find $\tau \approx a/v_A$. As an example consider a large tube, $a = 10^4$ km, in the lower convection zone of the Sun with $B = B_e$, $v_A = 100$ m·s^{-1} which is moderately deformed, $R \approx H_p \approx 6 \cdot 10^4$ km, by convective flows or differential rotation. According to Eq. (2.11) we find a growth time of $\tau \approx 3$ days. Hence, even a moderately curved structure fragments within a few days.

Since the growth time decreases for smaller perturbation wavelength (cf. Eq. 2.10), equality with the time scale of magnetic diffusion is reached only for very small fragment size. For this size, $d = 1/n_0$, inhomogeneities are as rapidly smoothed out by diffusion as they are formed due to interchange instability. d can be estimated by equating $\tau(n_0)$ with the diffusion time $\tau_d = d^2\eta^{-1}$ which gives

$$d = \left(\frac{2R\eta^2}{v_A^2}\right)^{1/3}. \qquad (2.12)$$

For the large flux tube discussed above we find $d \approx 40$ km even if we use the turbulent diffusivity derived after Eq. (2.8). The growth time for such a structure is only a few hours. Consequently, the interchange instability constitutes a very efficient fragmentation mechanism which leads to splitting of even moderately deformed flux tubes in a time scale of hours to days. The resulting fragment sizes are of the same order of magnitude as those generated by the magnetic Rayleigh-Taylor instability at the upside of a horizontal flux tube but the growth time of the latter is much larger.

Another important fragmentation mechanism is related to the *Kelvin-Helmholtz instability* (Tsinganos, 1980). Assume a flux tube embedded in an external velocity field as sketched in Fig. 2a. A small perturbation near the stagnation point leads to the flow geometry sketched in Fig. 2b. The centrifugal force due to the curved streamlines near the stagnation point leads to a pressure gradient which causes a local pressure maximum at the interface. Very similar to the interchange instability, this causes growth of the perturbation and fragmentation of the flux tube. This process is nicely demonstrated by laboratory experiments with rising gas bubbles in liquids (see the photographs reproduced in Tsinganos, 1980) and is also visible in a numerical simulation of buoyant, rising flux tubes (Schüssler, 1979).

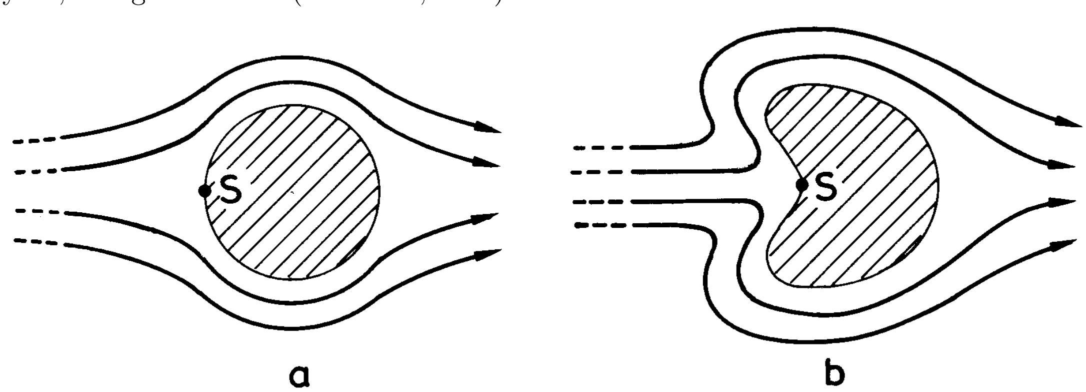

Fig. 2: Dynamical fragmentation of a flux tube. **a**: Flux tube embedded in an external flow field. A small perturbation near the stagnation point S leads to the situation sketched in **b**: The the centrifugal force causes a pressure gradient such that a local pressure maximum evolves at the interface. This leads to growth of the perturbation and fragmentation of the tube.

All these considerations lead us to expect strongly fragmented magnetic structures of the size of a few tens of km in the solar convection zone. Converging flows could possibly accumulate them in loose bundles but they are unable to produce large, monolithic structures since we have seen that the flows themselves cause fragmentation (see also Schüssler, 1984b, and the discussion in Sec. 6.1).

However, could possibly a *twisted* flux tube escape from being fragmented? With an azimuthal component, B_ϕ, of the magnetic field the internal pressure gradient is changed and, furthermore, perturbations which do not bend magnetic field lines are no longer possible. A sufficiently large B_ϕ may suppress all fragmentation processes discussed so far. For the interchange instability the necessary magnitude can be estimated by equating the (stabilizing) tension force due to B_ϕ with the (destabilizing) curvature force exerted by the longitudinal field B_z

$$\frac{B_\phi^2}{4\pi a} \quad \approx \quad \frac{B_z^2}{4\pi R}$$

which gives for the ratio of the field components

$$\frac{B_\phi}{B_z} \quad \approx \quad \left(\frac{a}{R}\right)^{1/2} . \tag{2.13}$$

For the large flux tube discussed above Eq. (2.13) gives a $B_\phi/B_z \approx 0.4$, i.e. the azimuthal field must be of the order of the longitudinal field in order to stabilize a moderately deformed flux tube ($R = H_p$) with respect to the interchange instability. With such large azimuthal fields, however, kink instabilities become relevant at perturbation wavelengths along the flux tube which are comparable to the diameter of the structure, i.e. the flux tubes buckles, reconnects and evolves rapidly on a dynamical time scale. Presumably this instability either leads directly to fragmentation or it removes most of the twist and leaves the flux tube unprotected against the other instabilities discussed above. A twisted flux tube is kink unstable for longitudinal wavelengths λ which satisfy the inequality (Cap, 1976, Ch. 11)

$$\frac{\lambda}{a} \quad > \quad \frac{B_z}{B_\phi} . \tag{2.14}$$

Using this and Eq. (2.13) we find that a flux tube which is stabilized against interchanging by an azimuthal field is kink unstable for

$$\lambda \quad > \quad (a\,R)^{1/2} . \tag{2.15}$$

In our example we have $\lambda > 2.4 \cdot 10^4$ km. The time scale for the kink instability is of the same order of magnitude as that of the interchange instability. On the other hand, slightly deformed *small* flux tubes can be stabilized by a much smaller amount of twist. For $a = 100$ km and $R = H_p = 6 \cdot 10^4$ km, a ratio $B_\phi/B_z = 0.04$ is sufficient. The helical kink instability would set in on a scale of $\lambda \approx 2500$ km which is much larger than the flux tube diameter and could possibly, as conjectured by Parker (1979a, Ch. 9.2), saturate in a stable, cork-screw shaped form of the flux tube. In the uppermost layers of the convection zone, such a modest amount of twisting could conceivably be produced by a surrounding whirl flow which itself exerts a stabilizing influence (Schüssler, 1984b).

3. The approximation of slender flux tubes

The considerations presented in the preceding chapter support the view that the magnetic flux in a convection zone consists of an ensemble of thin (diameter < 100 km $\ll H_p$), concentrated (at least equipartition field strength) filaments. Such structures allow a simplification of the MHD equations if all quantities do not vary significantly within each cross section and if the spatial scales of variations *along* the filament are large compared to its diameter. In particular, this approximation requires that the diameter is small compared to pressure scale height, radius of curvature, and to the longitudinal length scales of all dynamical processes (e.g. longitudinal wavelengths, scale of variation of flows). Under these circumstances the global statics and dynamics of a filament (excluding processes like body waves which involve a significant structure within a cross-section, cf. Ferriz-Mas et al., 1989) can be described using truncated Taylor expansions of the lateral variation of all quantities. A truncation of the resulting set of equations at *zeroth* order leads to the *approximation of slender flux tubes* (ASF) which involves only the values of the quantities along a representative curve (e.g. the axis of a flux tube with circular cross section) or averages over the cross section.

For *vertical, axisymmetric* flux tubes with straight axis the ASF has been systematically derived by Roberts and Webb (1978; see also Defouw, 1976). For this case, the general properties of the expansion procedure are discussed by Ferriz-Mas and Schüssler (1989). Spruit (1981a,b) gives a general form of the ASF for flux tubes with curved axis. For the application to extragalactic jets, Achterberg (1982, 1988) has derived a similar approximation which he calls the 'firehose limit'. In what follows we shall rederive the ASF in a way somewhat different from Spruit's approach in order to introduce the formalism and notation to be used in the subsequent chapters and hopefully also to elucidate the nature of the approximation.

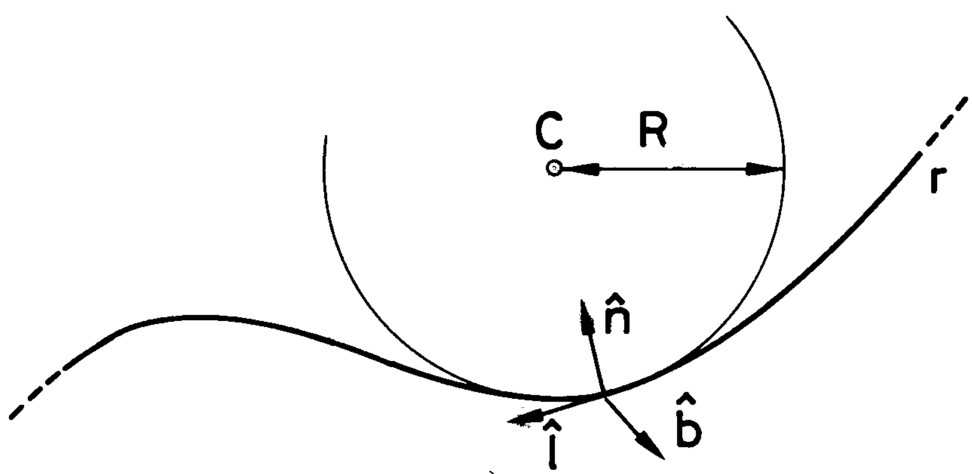

Fig. 3: Sketch of a space curve $\mathbf{r}(l)$ described in each point P by the orthogonal unit vectors $\hat{\mathbf{l}}$ (tangent), $\hat{\mathbf{n}}$ (normal), $\hat{\mathbf{b}}$ (binormal, perpendicular to the plane of the paper), and by the radius of curvature, R.

Consider a space curve whose path is described by the variation of the radius vector $\mathbf{r} = \mathbf{r}(l)$ with the arc length, l, along the curve.* As indicated in Fig. 3 the curve is described at every point, P, by the triad of unit vectors $\hat{\mathbf{l}}$ (*tangent*), $\hat{\mathbf{n}}$ (*normal*), and $\hat{\mathbf{b}}$ (*binormal*) which are given by

$$\hat{\mathbf{l}} = \frac{\partial \mathbf{r}}{\partial l} \tag{3.1}$$

$$\hat{\mathbf{n}} = R \frac{\partial \hat{\mathbf{l}}}{\partial l} \tag{3.2}$$

$$\hat{\mathbf{b}} = \hat{\mathbf{l}} \times \hat{\mathbf{n}} \tag{3.3}$$

The *radius of curvature* is given by

$$R = \left| \frac{\partial \hat{\mathbf{l}}}{\partial l} \right|^{-1} . \tag{3.4}$$

The vectors $\hat{\mathbf{l}}$ and $\hat{\mathbf{n}}$ define the local plane of the curve (plane of the paper in Fig. 3) which contains the local center of curvature, C. The change of the local plane of the curve is described by the derivative of the binormal unit vector which defines the *radius of torsion*, R_t:

$$\frac{\partial \hat{\mathbf{b}}}{\partial l} = \hat{\mathbf{l}} \times \frac{\partial \hat{\mathbf{n}}}{\partial l} = R_t^{-1}\, \hat{\mathbf{n}} \, . \tag{3.5}$$

In the ASF we consider a flux tube as a coherently moving bundle of magnetic field lines whose paths can be represented by one single space curve $\mathbf{r}(l,t)$. For such a description to be valid, the variation of tangent, $\hat{\mathbf{l}}$, radius of curvature, R, and all physical quantities within the cross section of the tube in the plane perpendicular to $\hat{\mathbf{l}}$ has to be sufficiently small. Since it allows a better readable presentation, in what follows we assume a circular cross section of the flux tube and take its axis as representative space curve and as origin of Taylor expansions. However, the following considerations are valid for any shape of the cross section and can easily be generalized as long as the flux tube remains sufficiently thin in any direction perpendicular to its local tangent. Note in particular that we do *not* (and in general are not allowed to) assume axial symmetry.

The natural coordinates within any cross section of the tube are defined along the normal and binormal directions with the axis as origin. Using ξ for the coordinate in the direction of the local normal, $\hat{\mathbf{n}}$, we may write for the differences ΔR and $|\Delta \hat{\mathbf{l}}|$ between axis ($\xi = 0$) and boundary ($\xi = a$) of the flux tube in the normal direction

$$\frac{|\Delta R|}{R} = \left| \frac{\partial R}{\partial \xi} \right|_{\xi=0} \frac{a}{R} \tag{3.6}$$

$$|\Delta \hat{\mathbf{l}}| = \left| \frac{\partial \hat{\mathbf{l}}}{\partial \xi} \right|_{\xi=0} a \, . \tag{3.7}$$

The quantities on the left of Eqs. (3.6) and (3.7), respectively, can be made arbitrarily small if a is chosen small enough, in particular if the diameter of the flux tube is everywhere small compared to

* In general, the path and all other quantities depend explicitly on time. We take this into account by writing all spatial derivatives partial but we do not especially indicate the time dependence unless it actually matters.

the local radius of curvature of the axis. Similar relations are valid for the variation in the binormal direction and for the variation of torsion which are satisfied also by a sufficiently thin flux tube.

For the (zeroth order) ASF we consider the values of the variables (and possibly their first spatial derivatives, see below) on the axis of the tube. The combined equations of induction and continuity (Walén equation for zero resistivity) and the equation of motion for the fluid *within* the flux tube in Lagrangian form read

$$\frac{d}{dt}\left(\frac{\mathbf{B}}{\rho}\right) = \left(\frac{\mathbf{B}}{\rho}\cdot\nabla\right)\mathbf{u} \tag{3.8}$$

$$\rho\frac{d\mathbf{u}}{dt} = -\nabla p + \rho\mathbf{g} + \frac{1}{4\pi}(\nabla\times\mathbf{B})\times\mathbf{B} + \mathbf{F}_D \tag{3.9}$$

where $\mathbf{u}$ denotes fluid velocity, ρ density, p gas pressure, $\mathbf{g}$ gravitational acceleration, and $\mathbf{B}$ the magnetic flux density vector. $\mathbf{F}_D$ is the drag force which results from the motion of the flux tube relative to the surrounding, non-magnetic fluid. For a sufficiently thin tube we may write for the flux density on the axis (the representative space curve)

$$\mathbf{B}(l) = B(l)\,\hat{\mathbf{l}} \tag{3.10}$$

and Eq. (3.8) can be rewritten

$$\frac{B}{\rho}\frac{d\hat{\mathbf{l}}}{dt} + \hat{\mathbf{l}}\frac{d}{dt}\left(\frac{B}{\rho}\right) = \frac{B}{\rho}(\hat{\mathbf{l}}\cdot\nabla)\mathbf{u} \equiv \frac{B}{\rho}\frac{\partial\mathbf{u}}{\partial l} \tag{3.11}$$

By scalar multiplication with $\hat{\mathbf{l}}$ and noting that a unit vector is perpendicular to its derivative we find from Eq. (3.11)

$$\frac{d}{dt}\left(\frac{B}{\rho}\right) = \frac{B}{\rho}\,\hat{\mathbf{l}}\cdot\frac{\partial\mathbf{u}}{\partial l} = \frac{B}{\rho}\left(\frac{\partial\mathbf{u}\cdot\hat{\mathbf{l}}}{\partial l} - \mathbf{u}\cdot\frac{\partial\hat{\mathbf{l}}}{\partial l}\right). \tag{3.12}$$

We write $\mathbf{u}\cdot\hat{\mathbf{l}}\equiv u_l$, $\mathbf{u}\cdot\hat{\mathbf{n}}\equiv u_n$ and use Eq. (3.2) to obtain

$$\frac{d}{dt}\left(\frac{\rho}{B}\right) = \frac{\rho}{B}\left(\frac{u_n}{R} - \frac{\partial u_l}{\partial l}\right) . \tag{3.13}$$

Eq. (3.13) represents the ASF form of the Walén equation. Multiplication of Eq. (3.11) with $\hat{\mathbf{n}}$ and $\hat{\mathbf{b}}$, respectively, gives the normal and binormal components of the time derivative of the tangent vector which describes the change of the flux tube path in time, namely

$$\hat{\mathbf{n}}\cdot\frac{d\hat{\mathbf{l}}}{dt} = \frac{\partial u_n}{\partial l} + \frac{u_l}{R} + \frac{u_b}{R_t} \tag{3.14}$$

$$\hat{\mathbf{b}}\cdot\frac{d\hat{\mathbf{l}}}{dt} = \frac{\partial u_b}{\partial l} - \frac{u_n}{R_t} \tag{3.15}$$

where we have used the general relation $\hat{\mathbf{n}} = -\hat{\mathbf{l}}\times\hat{\mathbf{b}}$ and defined $\mathbf{u}\cdot\hat{\mathbf{b}}\equiv u_b$.

The equation of motion requires somewhat more consideration. Let us first write down the Lorentz force on the axis using Eq. (3.10)

$$\frac{1}{4\pi}(\nabla\times\mathbf{B})\times\mathbf{B} \;=\; \frac{1}{4\pi}\Big[\,(\nabla B)\times\hat{\mathbf{l}}+B\,\nabla\times\hat{\mathbf{l}}\,\Big]\times B\,\hat{\mathbf{l}}$$

$$= \frac{1}{4\pi}\Big[\,B(\nabla B\times\hat{\mathbf{l}})\times\hat{\mathbf{l}}\;+\;B^2(\nabla\times\hat{\mathbf{l}})\times\hat{\mathbf{l}}\,\Big] \tag{3.16}$$

Using $(\nabla\times\hat{\mathbf{l}})\times\hat{\mathbf{l}} = R^{-1}\,\hat{\mathbf{n}}$ (e.g. Smirnov, 1968, Ch. V) and

$$(\nabla B\times\hat{\mathbf{l}})\times\hat{\mathbf{l}} \;=\; -\nabla B+\hat{\mathbf{l}}\,(\hat{\mathbf{l}}\cdot\nabla B) \;\equiv\; -(\nabla B)_\perp \tag{3.17}$$

where $(\nabla B)_\perp$ denotes the projection of the gradient on the plane perpendicular to the tangential direction (i.e. the cross section of the tube) we find for the Lorentz force

$$\mathbf{F}_L \;\equiv\; \frac{1}{4\pi}(\nabla\times\mathbf{B})\times\mathbf{B} \;=\; -\left[\nabla\left(\frac{B^2}{8\pi}\right)\right]_\perp + \frac{B^2}{4\pi R}\hat{\mathbf{n}}\,. \tag{3.18}$$

The projections of $\mathbf{F}_L$ on the three directions defined by the triad of unit vectors are given by

$$\mathbf{F}_L\cdot\hat{\mathbf{l}} \;=\; 0 \tag{3.19a}$$

$$\mathbf{F}_L\cdot\hat{\mathbf{n}} \;=\; -\frac{\partial}{\partial n}\left(\frac{B^2}{8\pi}\right) \;+\; \frac{B^2}{4\pi R} \tag{3.19b}$$

$$\mathbf{F}_L\cdot\hat{\mathbf{b}} \;=\; -\frac{\partial}{\partial b}\left(\frac{B^2}{8\pi}\right)\;. \tag{3.19c}$$

Here we have defined $\hat{\mathbf{n}}\cdot\nabla\equiv\partial/\partial n$ and $\hat{\mathbf{b}}\cdot\nabla\equiv\partial/\partial b$. We recognize the two familiar constituents of the Lorentz force, i.e. the magnetic pressure force in the plane perpendicular to the axis and the curvature force in the normal direction. There is no curvature force in the binormal direction and no magnetic force at all in the tangential direction. Note that the derivatives in the normal and binormal directions generally do not vanish since, in contrast to the ASF for vertical flux tubes, a curved flux tube cannot assumed to be axisymmetric.

Using the expressions derived for the Lorentz force in Eq. (3.19) we write for the components of the equation of motion (Eq. 3.9)

$$\rho\,\frac{d\mathbf{u}}{dt}\cdot\hat{\mathbf{l}} \;=\; -\frac{\partial p}{\partial l} \;+\; \rho\,\mathbf{g}\cdot\hat{\mathbf{l}} \tag{3.20}$$

$$\rho\,\frac{d\mathbf{u}}{dt}\cdot\hat{\mathbf{n}} \;=\; -\frac{\partial}{\partial n}(p+\frac{B^2}{8\pi}) \;+\; \rho\,\mathbf{g}\cdot\hat{\mathbf{n}} \;+\; \frac{B^2}{4\pi R} \;+\; \mathbf{F}_D\cdot\hat{\mathbf{n}} \tag{3.21}$$

$$\rho\,\frac{d\mathbf{u}}{dt}\cdot\hat{\mathbf{b}} \;=\; -\frac{\partial}{\partial b}(p+\frac{B^2}{8\pi}) \;+\; \rho\,\mathbf{g}\cdot\hat{\mathbf{b}} \;+\;\;+\,\mathbf{F}_D\cdot\hat{\mathbf{b}}\,. \tag{3.22}$$

The component along the flux tube (Eq. (3.20)) is already in a suitable form for the ASF. The other components contain derivatives in the normal and binormal directions which have to be determined by considering the external fluid. This is achieved by assuming that at the interface between flux tube and its environment instantaneous pressure equilibrium (more precisely, continuity of normal stress) is maintained permanently, viz.

$$p + \frac{B^2}{8\pi} = p_e \, . \tag{3.23}$$

Since the time required to establish pressure equilibrium is of the order of the travel time of a fast magneto-acoustic wave across the tube given by $2a/\sqrt{v_A^2 + v_S^2}$ (v_A: Alfvén speed, v_S: sound speed) it can be made arbitrarily small compared to any other dynamical time scale of the system if the flux tube is sufficiently thin.

Let us first assume a straight flux tube embedded in a static external fluid of constant pressure p_e, without gravity. We see from Eq. (3.23) that under these conditions pressure equilibrium entails $p+B^2/8\pi =$ const. in each cross section which is identical with the condition for static equilibrium of the *internal* fluid since all terms vanish on the r.h.s. of Eqs. (3.21) and (3.22) except the derivatives of total pressure.

In the case of a curved flux tube, non-vanishing gravity and stratification of the external fluid, pressure equilibrium at the interface and static equilibrium of the fluid in the interior of the flux tube generally cannot be reached simultaneously and a lateral acceleration of the fluid in the tube results. Since we deal with the zeroth-order ASF, only the terms involving first derivatives are retained in the Taylor expansion of total pressure within the cross section which is inserted into Eqs. (3.21) and (3.22). On the other hand, these derivatives are already fixed by Eq. (3.23) since a linear profile of total pressure along the normal and binormal directions is determined by the values of p_e at the intersections with the boundary of the flux tube. We can therefore formally insert Eq. (3.23) in Eqs. (3.21) and (3.22). Note that this procedure is legitimate only for linear pressure profiles, i.e. if the requirements for the validity of the ASF are met. If we take the external stratification to be hydrostatic (assuming all motions to be far subsonic), i.e.

$$\nabla p_e = \rho_e \mathbf{g} \tag{3.24}$$

(ρ_e: density of the external fluid), we obtain for the three components of the ASF form of the equation of motion*

$$\rho \frac{d\mathbf{u}}{dt} \cdot \hat{\mathbf{l}} = -\frac{\partial p}{\partial l} + \rho \, \mathbf{g} \cdot \hat{\mathbf{l}} \tag{3.20) = (3.25}$$

$$\rho \frac{d\mathbf{u}}{dt} \cdot \hat{\mathbf{n}} = (\rho - \rho_e) \, \mathbf{g} \cdot \hat{\mathbf{n}} + \frac{B^2}{4\pi R} + \mathbf{F}_D \cdot \hat{\mathbf{n}} \tag{3.26}$$

$$\rho \frac{d\mathbf{u}}{dt} \cdot \hat{\mathbf{b}} = (\rho - \rho_e) \, \mathbf{g} \cdot \hat{\mathbf{b}} + \mathbf{F}_D \cdot \hat{\mathbf{b}} \tag{3.27}$$

The first terms on the r.h.s. of Eqs. (3.26/27) represent the components of the buoyancy force which are proportional to the density difference between internal and external fluid. The magnetic field enters explicitly only by way of the curvature force in Eq. (3.26) and in the pressure balance condition (Eq. 3.23).

Let us now discuss the drag term, $\mathbf{F}_D$, which has been introduced to describe the dynamical effect of a motion of the flux tube relative to the surrounding fluid. Spruit (1981a,b) considered

* The transversal force (per unit length along the tube) can also be obtained by assuming static equilibrium *within* the flux tube (in the comoving frame) and integrating the resulting total pressure difference over the circumference of the cross section. For a thin tube the result is identical to Eqs. (3.26/27). In contrast to the procedure described in the text, this method is as well applicable for non-thin tubes as long as the assumption of internal hydrostatic equilibrium is valid. It has been used to calculate the buoyancy force on a circular flux tube of arbitrary radius (Schüssler, 1979).

impulsive motions of a flux tube in an initially static environment in which case this effect can be described by a larger effective inertia of the tube with respect to perpendicular motions. This is introduced into the equations by changing $\rho \rightarrow \rho + \rho_e$ on the l.h.s. of Eqs. (3.26) and (3.27). In our case we wish to include arbitrary flow fields around the flux tube (convection, differential rotation, dynamical motion of the tube itself). Their effect on the tube has to be described explicitly by considering an aerodynamic drag force (e.g. Parker, 1975a; Schüssler 1977; 1979; Moreno-Insertis, 1983; 1986; Chou and Fisher, 1989). Since the drag force has its origin in pressure differences between the upstream and the downstream sides of the interface between flux tube and its environment, for the ASF there is no component along the tube ($\mathbf{F}_D \cdot \hat{\mathbf{l}} = 0$). In the simplest case we may use the expression for the drag force acting on a rigid circular cylinder of radius a (cf. Batchelor, 1967), viz.

$$(\pi a^2)\,\mathbf{F}_D \;=\; C_D\,\rho_e\,a\,v_\perp^2\,\hat{\mathbf{k}}\,. \tag{3.28}$$

C_D is the (dimensionless) drag coefficient and $v_\perp^2$ is given by

$$v_\perp^2 \;=\; (\mathbf{v}\cdot\hat{\mathbf{k}})^2 \;=\; \left[\mathbf{v} - \hat{\mathbf{l}}\,(\mathbf{v}\cdot\hat{\mathbf{l}})\right]^2 \tag{3.29}$$

where $\mathbf{v} = \mathbf{v}_e - \mathbf{u}$ is the relative velocity between the flux tube and the surrounding fluid moving with velocity $\mathbf{v}_e$, and $\hat{\mathbf{k}}$ is the unit vector in the direction of the component of $\mathbf{v}$ perpendicular to the tube. Eq. (3.28) has been derived for laminar flows in which case wind tunnel measurements give $C_D \approx 1$ for a wide range ($10^2 < Re < 10^5$) of the hydrodynamic Reynolds number $Re = v_\perp a/\nu$ (ν: kinematic viscosity). For turbulent flows the effective Reynolds number of the flow is determined by the turbulent viscosity which can be orders of magnitude larger than the molecular value. Similar to the discussion of the turbulent magnetic diffusivity in the preceding chapter, the turbulent viscosity must be determined taking into account the spatial scale of the flow to be described. For $v_\perp$ given by large-scale convection on spatial scale L and a flux tube of radius a, the relevant turbulent viscosity is of the order of $0.1\,u(\delta)\,\delta$ where $u(\delta)$ is the turbulent velocity on a scale δ which is somewhat smaller than a. For $\delta = a/10$ and using Eq. (2.8) we find for the Reynolds number calculated with turbulent viscosity: $Re = 100(L/\delta)^{1/3}$. With $a = 100$ km and $L = 10^4$ km we finally estimate $Re \approx 10^3$. Hence, the effective Reynolds number for turbulent flow is such that we could hope to stay in the range of validity of Eq. (3.28) with $C_D \approx 1$ (see also the detailed discussion by Moreno-Insertis, 1984).

An enhanced inertia for perpendicular motions as introduced by Spruit (1981a,b) is not used here since it cannot be easily specified for turbulent flows which we expect in a convection zone. This may introduce errors if impulsive perpendicular motions like those connected with transversal tube waves are relevant.

For some applications it is more convenient to write the inertial terms in Eqs. (3.25-3.27) in the form of Lagrangian derivatives of the velocity components.* For example, the longitudinal component of the inertial term in Eq. (3.25) can be rewritten using Eqs. (3.14/15) in the form

$$\begin{aligned}\rho\,\frac{d\mathbf{u}}{dt}\cdot\hat{\mathbf{l}} \;&=\; \rho\,\frac{d\mathbf{u}\cdot\hat{\mathbf{l}}}{dt} \;-\; \rho\,\mathbf{u}\cdot\frac{d\hat{\mathbf{l}}}{dt} \;= \\ &=\; \rho\,\frac{du_l}{dt} \;-\; \rho\left(u_n\,\frac{\partial u_n}{\partial l} + \frac{u_n\,u_l}{R} + \frac{u_n\,u_b}{R_t}\right) \;-\; \rho\left(u_b\,\frac{\partial u_b}{\partial l} - \frac{u_b\,u_n}{R_t}\right)\,. \end{aligned} \tag{3.30}$$

* Note that there is an error in the expressions given by Chou and Fisher (1989) who treated a plane flux tube ($R_t \rightarrow \infty$, $u_b = 0$). The terms involving the derivative of the normal velocity, $\partial u_n/\partial l$, are missing in their equations (1) and (2).

Similar expressions can be derived for the other components of the inertial force. The set of equations for the ASF derived so far, i.e. the equations of motion, Eqs. (3.25-3.27), continuity, Eq. (3.13), flux tube shape, Eqs. (3.14/15), and instantaneous pressure balance, Eq. (3.23), are complemented by the condition of magnetic flux conservation along the tube, namely

$$A \cdot B \; = \; \Phi_{mag} \; = \; \text{const.} \tag{3.31}$$

where A is the cross-sectional area. For a flux tube with circular cross section of radius a we have $A = \pi a^2$. The form of the energy equation and the equation of state is determined by the particular problem to be treated. Since we shall only consider adiabatic changes we do not specify more complicated forms of the energy equation here. In most cases the derivation of the appropriate ASF form is straightforward.

4. Flux tubes in equilibrium

The comparatively long lifetime and slow evolution of large solar active regions after a much shorter phase of flux eruption and dynamical evolution give rise to the conjecture that the magnetic structures in the convection zone reach a static or stationary (i.e. with a surrounding flow) equilibrium which is characterized by a time-independent shape of the tube and hydrostatic equilibrium along its longitudinal direction. Trivial examples of *static* equilibria (for constant direction of gravity, $\mathbf{g}$) are:

a) a horizontal ($\mathbf{g}\cdot\hat{\mathbf{l}}=0$), straight flux tube with constant pressure and density ($\rho=\rho_e$), and

b) a vertical ($\mathbf{g}\cdot\hat{\mathbf{n}}=0$), straight flux tube in hydrostatic equilibrium ($dp/dz=-\rho g$; z: vertical coordinate).

An example for a *stationary* equilibrium is a straight, horizontal flux tube with a density difference, $\rho-\rho_e$, such that the resulting buoyancy force compensates the drag force due to a constant vertical velocity, $\mathbf{v}_e$, in the exterior. The force balance, Eq. (3.26), can be determined using Eq. (3.28) and gives

$$1 \;-\; \frac{\rho}{\rho_e} \;=\; \frac{C_D\, v_e^2}{\pi\, a\, g}\,\mathrm{sgn}(\mathbf{g}\cdot\mathbf{v}_e) \tag{4.1}$$

with $v_e\equiv|\mathbf{v}_e|$ and $g\equiv|\mathbf{g}|$. For a downflow, i.e. $\mathrm{sgn}(\mathbf{g}\cdot\mathbf{v}_e)=+1$, the density of the fluid in the tube has to be smaller than that of the surroundings and the resulting upward directed buoyancy force is balanced by the drag force. In the case of an upflow the buoyancy force is directed downwards.

In general, we expect more complicated shapes of equilibrium flux tubes in the solar convection zone. For example, van Ballegooijen (1982a) calculated static and stationary equilibrium solutions for flux tubes forming loops which are "anchored" in a horizontal flux system below the convection zone. Anton (1984) determined equilibrium flux tubes which reside completely within the convection zone for a variety of internal and external temperature stratifications. We shall not perform detailed calculations here but rather derive some general properties of equilibrium flux tubes and give a few illustrative examples.

4.1 Static equilibrium

The equations describing the static equilibrium of a flux tube in a hydrostatically stratified environment are obtained by setting the inertial and the drag terms to zero in Eqs. (3.25-3.27). In the direction of the binormal the equilibrium condition reads

$$(\rho-\rho_e)\,\mathbf{g}\cdot\hat{\mathbf{b}} \;=\; 0\,. \tag{4.2}$$

Unless we have $\mathbf{g}\cdot\hat{\mathbf{b}}=0$ this equation can only be satisfied if the density difference between flux tube and exterior vanishes everywhere along the flux tube. From the equilibrium condition in the normal direction,

$$(\rho-\rho_e)\,\mathbf{g}\cdot\hat{\mathbf{n}} \;+\; \frac{B^2}{4\pi R} \;=\; 0\,, \tag{4.3}$$

we see that in this case the curvature force vanishes, $R \to \infty$, i.e. the tube has to be straight. Hydrostatics of the environment, Eq. (3.24), and along the tube, Eq. (3.25), together with $\rho = \rho_e$ entail

$$\frac{\partial}{\partial l}\,(p - p_e) = 0 \tag{4.4}$$

and from Eq. (3.23) we find

$$\frac{\partial}{\partial l}\,\frac{B^2}{8\pi} \;=\; 0\,. \tag{4.5}$$

Consequently, the magnetic field strength is constant. Using the perfect gas law and assuming the molecular weight to be the same inside and outside the flux tube we find from Eq. (3.23) for the ratio of internal temperature, T, and external temperature, T_e:

$$\frac{T}{T_e} \;=\; 1 - \frac{B^2}{8\pi p_e}\,. \tag{4.6}$$

For a constant direction of gravity, a horizontal flux tube with no variation of p_e in its longitudinal direction, and a subadiabatic stratification of the external medium such a temperature reduction might be achieved by an adiabatically expanding, rising flux tube. For an oblique tube with a concomitant variation of p_e along its length we can hardly imagine a thermodynamic process which precisely leads to a temperature variation along the tube as prescribed by Eq. (4.6).

In a real star the direction of $\mathbf{g}$ varies spatially since gravity is directed towards the center. In this case, a longitudinally uniform flux tube assumes circular (toroidal) shape with finite R and therefore we have $\rho \neq \rho_e$. Thus in practice straight flux tubes with $\rho = \rho_e$ are irrelevant and we can conclude from Eq. (4.2) that $\mathbf{g} \cdot \hat{\mathbf{b}} = 0$ is necessary, i.e. static flux tubes lie in planes which contain the vector of gravitational acceleration. For the spherical geometry of a star we may state:

> *In a spherical star with radial gravity magnetic flux tubes in static equilibrium lie in planes which contain the center of the star. The singular case of straight tubes without density contrast is of no practical importance.*

For example, a toroidal flux tube in a plane parallel to but outside the equatorial plane does not fulfill this condition. It cannot find a static equilibrium since the component of the buoyancy force perpendicular to the plane of the tube is not balanced and leads to a poleward drift (Pneuman and Raadu, 1972; Spruit and van Ballegooijen, 1982).

Another important property of static flux tubes is obtained by rewriting the Lorentz force in its familiar form

$$\frac{1}{4\pi}(\nabla \times \mathbf{B}) \times \mathbf{B} \;=\; -\nabla\left(\frac{B^2}{8\pi}\right) \;+\; \frac{1}{4\pi}\,\mathbf{B}\cdot\nabla\mathbf{B}\,. \tag{4.7}$$

We may use this to obtain the static form of the equation of motion, Eq. (3.9), viz.

$$-\nabla\left(p + \frac{B^2}{8\pi}\right) \;+\; \rho\,\mathbf{g} \;+\; \frac{1}{4\pi}\,\mathbf{B}\cdot\nabla\mathbf{B} \;=\; 0 \tag{4.8}$$

and with Eqs. (3.23/24) we get

$$(\rho - \rho_e)\,\mathbf{g} \;+\; \frac{1}{4\pi}\,\mathbf{B}\cdot\nabla\mathbf{B} \;=\; 0\,. \tag{4.9}$$

We now consider the general case of a spatially varying direction of gravity and denote by $\hat{\mathbf{g}}$ the unit vector in the direction of local gravitational acceleration. We define $\hat{\mathbf{h}}$ as unit vector perpendicular to $\hat{\mathbf{g}}$ within the local plane of the flux tube (spanned by $\hat{\mathbf{n}}$ and $\hat{\mathbf{l}}$). Since $\mathbf{g} \cdot \hat{\mathbf{b}} = 0$ for a static tube we have

$$\hat{\mathbf{h}} \;=\; \hat{\mathbf{g}} \times \hat{\mathbf{b}}\,. \tag{4.10}$$

$\hat{\mathbf{h}}$ defines the *local horizontal direction*. We multiply Eq. (4.9) by $\hat{\mathbf{h}}$, use Eq. (3.10), and find

$$\hat{\mathbf{h}} \cdot (\hat{\mathbf{l}} \cdot \nabla)\, B\, \hat{\mathbf{l}} \;=\; 0\,. \tag{4.11}$$

This may be written as

$$0 \;=\; \hat{\mathbf{h}} \cdot \frac{\partial B\, \hat{\mathbf{l}}}{\partial l} \;=\; \frac{\partial}{\partial l} B(\hat{\mathbf{h}} \cdot \hat{\mathbf{l}}) \;-\; B\, \hat{\mathbf{l}} \cdot \frac{\partial\, \hat{\mathbf{h}}}{\partial l}\,. \tag{4.12}$$

Using Eqs. (4.10), (3.3) and (3.5) we find

$$\frac{\partial\, \hat{\mathbf{h}}}{\partial l} \;=\; \frac{\partial\, \hat{\mathbf{g}}}{\partial l} \times \hat{\mathbf{b}} \;+\; \hat{\mathbf{g}} \times \frac{\partial\, \hat{\mathbf{b}}}{\partial l} \;=\; \frac{\partial\, \hat{\mathbf{g}}}{\partial l} \times (\hat{\mathbf{l}} \times \hat{\mathbf{n}}) \;+\; R_t^{-1} \hat{\mathbf{g}} \times \hat{\mathbf{n}} \;=$$

$$=\; \hat{\mathbf{l}} \left(\frac{\partial\, \hat{\mathbf{g}}}{\partial l} \cdot \hat{\mathbf{n}} \right) \;-\; \hat{\mathbf{n}} \left(\frac{\partial\, \hat{\mathbf{g}}}{\partial l} \cdot \hat{\mathbf{l}} \right) \;+\; R_t^{-1} \hat{\mathbf{g}} \times \hat{\mathbf{n}}\,.$$

Consequently, we have

$$\hat{\mathbf{l}} \cdot \frac{\partial\, \hat{\mathbf{h}}}{\partial l} \;=\; \frac{\partial\, \hat{\mathbf{g}}}{\partial l} \cdot \hat{\mathbf{n}}$$

and defining $B_h \equiv B(\hat{\mathbf{h}} \cdot \hat{\mathbf{l}}) = \mathbf{B} \cdot \hat{\mathbf{h}}$ we write Eq. (4.12) as

$$\frac{\partial B_h}{\partial l} \;=\; B \left(\frac{\partial\, \hat{\mathbf{g}}}{\partial l} \cdot \hat{\mathbf{n}} \right)\,. \tag{4.13}$$

This equation couples the variation of the strength of the field component in the local horizontal direction to the variation of the direction of gravity along the flux tube. In the case of a constant direction of gravitation along the tube we find from Eq. (4.13)

$$\frac{\partial B_h}{\partial l} \;=\; 0\,, \tag{4.14}$$

i.e. the component of the magnetic field perpendicular to gravity is constant in static equilibrium (see also Parker, 1979, Sec. 8.6, and van Ballegooijen, 1982a).

As we have seen above, static flux tubes in a sphere with radially directed gravity lie in planes which contain the center. If we introduce polar coordinates (r, φ) within such a plane, we have $\hat{\mathbf{g}} = (-1\,, 0)$, $\hat{\mathbf{h}} = (0\,, 1)$, $\hat{\mathbf{l}} = (l_r\,, l_\varphi)$, and

$$\frac{\partial\, \hat{\mathbf{g}}}{\partial l} \;=\; \hat{\mathbf{l}} \cdot \nabla \hat{\mathbf{g}} \;=\; \left(0\,, \frac{-l_\varphi}{r} \right)\,.$$

Hence, we find from Eq. (4.13) with $B_h = B(\hat{\mathbf{h}} \cdot \hat{\mathbf{l}}) = B l_\varphi \equiv B_\varphi$:

$$\frac{\partial B_\varphi}{\partial l} \;=\; -B\, \frac{l_\varphi n_\varphi}{r} \;=\; -B_\varphi\, \frac{n_\varphi}{r}\,. \tag{4.15}$$

For $r \to \infty$ this passes over into Eq. (4.14). We may use Eq. (4.15) to estimate the difference between the spherical and the plane-parallel case. If we denote by δB_φ the change of B_φ over a length interval δL along the tube an upper limit for this quantity given by Eq. (4.15) is

$$\frac{\delta B_\varphi}{B_\varphi} \leq \frac{\delta L}{r} . \tag{4.16}$$

As an example, for a flux tube extending nearly vertically through the whole depth of the convection zone we have $\delta L = 2 \cdot 10^5$ km and $r = 5 \cdot 10^5$ km. Consequently, the change of B_φ between top and bottom of the convection zone is smaller than $0.4\, B_\varphi$. If this flux tube is anchored in a toroidal flux system near the bottom of the convection zone with $B_\varphi \approx B_e \approx 10^4$ Gauss, the toroidal field strength at the top (in the photosphere) cannot be smaller than 6000 Gauss for a tube in static equilibrium. Since photospheric magnetic fields and sunspots are basically vertical with very small net inclination of the magnetic structures as a whole (the mean horizontal field component is less than 100 Gauss) this excludes *static* flux tubes rooted in a toroidal equipartition field deep in the convection zone as models for sunspots and solar active regions. Since flux expulsion always tends to establish equipartition field strengths which are much larger than 100 Gauss the concept of large-scale *static* magnetic structures in the convection zone has to be abandoned.

In spite of these pessimistic remarks we shall continue the discussion of static equilibrium in the remainder of this section because this case is well suited to demonstrate the mathematical methods which are used to calculate flux tube equilibria in practice. Furthermore, static equilibrium is only excluded on a large scale for flux tubes extending through the whole convection zone but it might well be *locally* a reasonable approximation, for instance for nearly vertical flux tubes in the photosphere. For such a small region we neglect the spherical geometry of the star and assume a constant direction of gravity. The subsequent considerations follow the approach first proposed by van Ballegooijen (1982a; see also Parker, 1975c).

Consider cartesian coordinates (x, z) in a plane which contains the vector of gravitational acceleration, $\mathbf{g} = (0\,, -g)$. If the external medium is in plane-parallel hydrostatic equilibrium the path of a static flux tube is given by a curve $z = z(x)$ which satisfies Eq. (4.3). This situation is sketched in Fig. 4. Hydrostatic equilibrium along the flux tube is described by Eq. (3.25) which gives*

$$-\frac{dp}{dl} + \rho\,\mathbf{g} \cdot \hat{\mathbf{l}} = 0 . \tag{4.17}$$

Uniformity of the horizontal field component entails, by virtue of Eq. (4.14)

$$B_x = \text{const.} \tag{4.18}$$

Since we may measure the arc length in both directions along the tube, we remove this ambiguity by requiring $\hat{\mathbf{l}} \times \hat{\mathbf{x}} > 0$ where $\hat{\mathbf{x}}$ is the unit vector in x-direction. If the shape of the tube is such that it has a vertical tangent somewhere and turns backwards with respect to x this part of the tube has to be treated separately in the same way as described below after transforming $\hat{\mathbf{l}} \to -\hat{\mathbf{l}}$. We use the angle $\gamma(l)$ between the local tangent of the flux tube and the positive x-axis defined by

$$\frac{dz}{dx} = \frac{B_z}{B_x} = \tan\gamma \quad ; \quad \frac{d}{dl} = \sin\gamma\,\frac{d}{dz} \tag{4.19}$$

to write

$$\hat{\mathbf{l}} = (\cos\gamma, \sin\gamma) \tag{4.20}$$

* Since we deal with time-independent quantities we may write non-partial derivatives.

$$\hat{\mathbf{n}} \;=\; R\,(-\sin\gamma, \cos\gamma)\,\frac{d\gamma}{dl} \tag{4.21}$$

$$R^{-1} \;=\; \left|\frac{d\gamma}{dl}\right| \;=\; \left|-\frac{d\cos\gamma}{dz}\right| \;=\; \left(-\frac{d\cos\gamma}{dz}\right)\,\mathrm{sgn}\left(\frac{d\gamma}{dl}\right)\,. \tag{4.22}$$

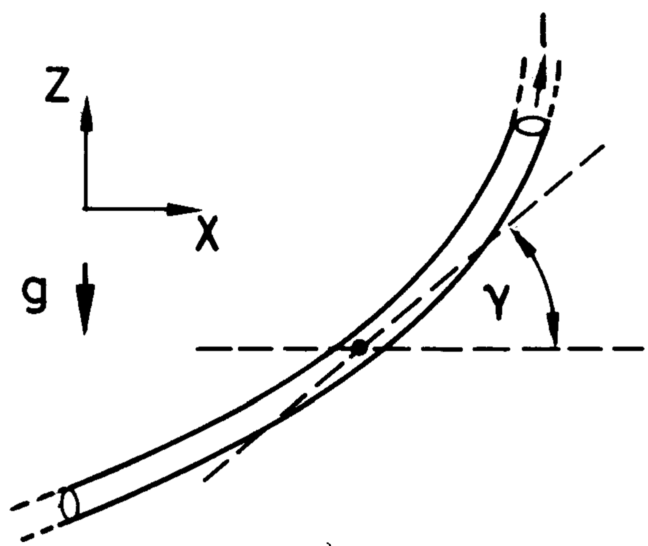

Fig. 4: Flux tube in cartesian geometry with gravity directed downward. $\gamma(l)$ is the angle between the flux tube (direction of increasing arc length) and the x-axis.

Since $\mathbf{g}\cdot\hat{\mathbf{l}} = -g\sin\gamma$ we can rewrite Eq. (4.17) using Eq. (4.19)

$$\frac{dp}{dz} \;=\; -\rho g \tag{4.23}$$

and in the external medium we have

$$\frac{dp_e}{dz} \;=\; -\rho_e g\;. \tag{4.24}$$

Consequently, for given external plane-parallel stratification and given internal temperature profile, $T(z)$, pressure and density *within* the flux tube depend only on z and can be determined without prior knowledge of its path. This applies also to the field strength, viz.

$$\frac{d}{dz}\left(\frac{B^2}{8\pi}\right) \;=\; \frac{d}{dz}(p_e - p) \;=\; (\rho - \rho_e)g\,. \tag{4.25}$$

With $\mathbf{g}\cdot\hat{\mathbf{n}} = -g\cos\gamma\,\mathrm{sgn}(d\gamma/dl)$ and using Eq. (4.25) we find for the sum of the curvature and buoyancy forces which determines the force balance in normal direction (cf. Eq. 4.3)

$$0 \;=\; -\frac{d}{dz}\left(\frac{B^2}{8\pi}\right)\cos\gamma \;-\; \frac{B^2}{4\pi}\frac{d}{dz}\cos\gamma \;=\; -\frac{B}{4\pi}\frac{d}{dz}(B\cos\gamma) \;=\; -\frac{B}{4\pi}\frac{dB_x}{dz}\,. \tag{4.26}$$

We see that the uniformity of the horizontal component of the magnetic field is sufficient for static equilibrium if the internal stratification along the flux tube is hydrostatic. We can use this property to reduce the calculation of the flux tube path, $z = z(x)$, to a quadrature. Since

$$8\pi(p_e - p) \; = \; B^2 \; = \; B_z^2 + B_x^2 \tag{4.27}$$

we can write

$$\frac{dz}{dx} \; = \; \frac{B_z}{B_x} \; = \; \left(\frac{8\pi(p_e - p)}{B_x^2} - 1 \right)^{1/2} . \tag{4.28}$$

Since $B_x = \text{const.}$ and the pressures are known functions of z, the function $x(z)$ can be determined by integration:

$$x(z) - x(z_0) \; = \; \int_{z_0}^{z} \left(\frac{8\pi(p_e - p)}{B_x^2} - 1 \right)^{-1/2} d\tilde{z} \tag{4.29}$$

The resulting function may be inverted to yield the path, $z = z(x)$. For special cases, analytical solutions of Eq. (4.29) can be obtained (e.g. Parker, 1979a, Sec. 8.6).

4.2 Stationary equilibrium

As we have seen above, flux tubes in static equilibrium do not seem to be particularly relevant for the description of magnetic structures in the convection zone. On the other hand, the slow evolution of active regions after the vigorous dynamical phase of flux eruption indicates some kind of underlying equilibrium structure. Therefore it seems worthwhile to include the effect of large scale external velocity fields (convection, differential rotation) and to consider stationary equilibria of flux tubes. In practice, such an equilibrium can be determined either by direct (numerical) integration of a second order ordinary differential equation or by solving a first order equation and subsequent quadrature. Let us first consider the latter method (van Ballegooijen, 1982a).

We start from the plane-parallel geometry used in the preceding section and introduce a relative velocity, $\mathbf{v}$, between flux tube and external medium. $\mathbf{v}$ is assumed to lie in the xz-plane. The unit vector $\hat{\mathbf{k}}$ defined in Eqs. (3.28/29) in this case is given by

$$\hat{\mathbf{k}} \; = \; \hat{\mathbf{n}} \, \mathrm{sgn}(\mathbf{v} \cdot \hat{\mathbf{n}}) \, . \tag{4.30}$$

We now determine

$$\mathbf{v} \cdot \hat{\mathbf{n}} \; = \; (-v_x \sin\gamma + v_z \cos\gamma) \, \mathrm{sgn}\left(\frac{d\gamma}{dl} \right) \; \equiv \; v_\perp \, \mathrm{sgn}\left(\frac{d\gamma}{dl} \right)$$

and find

$$\mathrm{sgn}(\mathbf{v} \cdot \hat{\mathbf{n}}) \; = \; \mathrm{sgn}(v_\perp) \, \mathrm{sgn}\left(\frac{d\gamma}{dl} \right) . \tag{4.31}$$

Using Eqs. (3.26) and (3.28) force balance in the normal direction leads to

$$(\rho - \rho_e) \, \mathbf{g} \cdot \hat{\mathbf{n}} \; + \; \frac{B^2}{4\pi R} \; + \; \frac{C_D \rho_e v_\perp^2}{\pi \, a} \, \hat{\mathbf{k}} \cdot \hat{\mathbf{n}} \; = \; 0 \, . \tag{4.32}$$

In analogy to Eq. (4.26) we find using Eqs. (4.30/31)

$$\frac{B}{4\pi} \frac{dB_x}{dz} \; = \; \frac{C_D \rho_e v_\perp^2}{\pi \, a} \, \mathrm{sgn}(v_\perp) \, . \tag{4.33}$$

In principle, this equation can be used to determine the variation of the horizontal field component with height which then can be inserted in Eq. (4.29) to determine the path of the flux tube. However, since $v_\perp$ depends on γ, the differential equation (4.33) in general is not easily solved, especially if $\mathbf{v}$ varies spatially.

As an example, let us consider the case of a purely horizontal velocity field $\mathbf{v} = (v(z), 0)$ which may represent a depth-dependent differential rotation. We have $v_\perp = -v \sin\gamma$ and assume $v \geq 0$. Eq. (4.33) now reads

$$\frac{B}{4\pi}\frac{dB_x}{dz} = \frac{C_D \rho_e v^2}{\pi a} \sin^2\gamma \,. \tag{4.34}$$

With $\pi a^2 B = \Phi_{mag} = \text{const.}$ and $B_x/B = \cos\gamma$ we find

$$\frac{dB_x}{dz} = -4C_D\rho_e v^2 \left(\frac{\pi}{\Phi_{mag}B}\right)^{1/2}\left(1 - \frac{B_x^2}{B^2}\right). \tag{4.35}$$

In the special case of a *constant magnetic field*, $B(z) = B_0$, the variables can be separated and defining $y \equiv B_x/B_0$ we may write

$$\frac{dy}{1-y^2} = -\alpha\,\rho_e v^2\,dz \tag{4.36}$$

with

$$\alpha = 4C_D\left(\frac{\pi}{\Phi_{mag}B_0^3}\right)^{1/2}. \tag{4.37}$$

As we have discussed in the preceding section the case of a constant magnetic field generally is of not much practical interest because it requires $\rho = \rho_e$ and, therefore, a very special internal temperature profile. However, if the scale height is much larger than the height range covered by the flux tube equilibrium path the variation of density is small and the assumption of a constant field may be tenable. Such a situation can be expected near the bottom of the solar convection zone. Integration of Eq. (4.36) yields

$$\frac{1}{2}\ln\left(\frac{1}{c_0}\frac{y-1}{y+1}\right) = \int_0^z \alpha\,\rho_e(\tilde{z})v^2(\tilde{z})\,d\tilde{z} \equiv f(z) \tag{4.38}$$

where c_0 is a constant of integration which is determined by a boundary condition at $z = 0$. Obviously we must have $y \neq 1$ in Eq. (4.38). The case $y = 1$ is a singular solution of Eq. (4.36) and represents a horizontal flux tube for which all forces vanish individually. Excluding this case we can determine $y(z)$ from Eq. (4.38)

$$y(z) = \frac{1 + c_0 e^{2f(z)}}{1 - c_0 e^{2f(z)}} \tag{4.39}$$

and determine c_0 by specifying $y(0) = y_0 < 1$, i.e.

$$c_0 = \frac{y_0 - 1}{y_0 + 1}\,. \tag{4.40}$$

For $y_0 \in [0, 1)$ the value of c_0 passes through the interval $c_0 \in [-1, 0)$. In the case $y_0 = 0$ (vertical tube at $z = 0$) we have $c_0 = -1$ and Eq. (4.39) gives

$$y(z) = -\tanh[f(z)]\,. \tag{4.41}$$

Since we have

$$z'(x) \;=\; \tan\gamma \;=\; \frac{(B^2 - B_x^2)^{1/2}}{B_x} \;=\; \frac{(1-y^2)^{1/2}}{y} \tag{4.42}$$

integration yields

$$x(z) \;=\; \int_0^z \frac{y}{(1-y^2)^{1/2}}\, d\tilde{z} \tag{4.43}$$

where we have assumed $x(0) = 0$. Inserting Eq. (4.39) into Eq. (4.43) we find

$$x(z) \;=\; \int_0^z \frac{1 + c_0 e^{2f(\tilde{z})}}{2\sqrt{-c_0}\, e^{f(\tilde{z})}}\, d\tilde{z} \tag{4.44}$$

and the special case $c_0 = -1$ gives

$$x(z) \;=\; \int_0^z - \sinh[f(\tilde{z})]\, d\tilde{z}\ . \tag{4.45}$$

We give two examples for which Eq. (4.44) can be directly integrated. First assume a velocity field with constant kinetic energy density, i.e. $(\rho_e v^2)(z) = \text{const}$. Consequently, we have from Eq. (4.38) that $f(z) = \alpha\rho_e v^2 z \equiv \hat{\alpha} z$ and thus

$$x(z) \;=\; \frac{1}{2\hat{\alpha}\sqrt{-c_0}} \Big(c_0 e^{\hat{\alpha} z} - e^{-\hat{\alpha} z} + 1 - c_0 \Big)\,. \tag{4.46}$$

For an initially vertical tube, i.e. $c_0 = -1$, we have

$$x(z) \;=\; \hat{\alpha}^{-1} \Big(1 \;-\; \cosh(\hat{\alpha} z) \Big) \tag{4.47}$$

and normalizing length by $1/\hat{\alpha}$, viz. $\hat{z} \equiv \hat{\alpha} z$ and $\hat{x} \equiv \hat{\alpha} x$, we find

$$\hat{x} \;=\; 1 \;-\; \cosh \hat{z}\,. \tag{4.48}$$

This solution has earlier been given by Parker (1979d). Another directly solvable example is the case of kinetic energy density being proportional to z, viz.

$$(\rho_e v^2)(z) \;=\; (\rho_e v^2)(z_0) \left(\frac{z}{z_0} \right) \tag{4.49}$$

with some reference level z_0. Inserting Eq. (4.49) into Eq. (4.38) we have

$$f(z) \;=\; \frac{\alpha(\rho_e v^2)(z_0)}{2z_0}\, z^2 \;\equiv\; \tilde{\alpha} z^2 \tag{4.50}$$

and thus write Eq. (4.44) as

$$x(z) \;=\; \frac{1}{2\sqrt{-\tilde{\alpha} c_0}} \left(\int_0^{\sqrt{\tilde{\alpha}} z} e^{-w^2}\, dw + c_0 \int_0^{\sqrt{\tilde{\alpha}} z} e^{w^2}\, dw \right)\,. \tag{4.51}$$

The first integral essentially represents the error function $\mathbf{\Phi}(\sqrt{\tilde{\alpha}} z)$ and the second is related to the Dawson integral $\mathbf{\Psi}$ (cf. Abramowitz and Stegun, 1965)

$$\mathbf{\Psi}(u) = e^{-u^2} \int_0^u e^{w^2}\, dw\ . \tag{4.52}$$

For $c_0 = -1$ we have

$$\hat{x} \;=\; \frac{1}{2}\left(\frac{\sqrt{\pi}}{2}\mathbf{\Phi}(\hat{z}) \;-\; e^{\hat{z}^2}\mathbf{\Psi}(\hat{z})\right) \tag{4.53}$$

with $\hat{z} = \sqrt{\tilde{\alpha}}\, z$, $\hat{x} = \sqrt{\tilde{\alpha}}\, x$. For both examples, Fig. 5 shows the resulting flux tube shape.

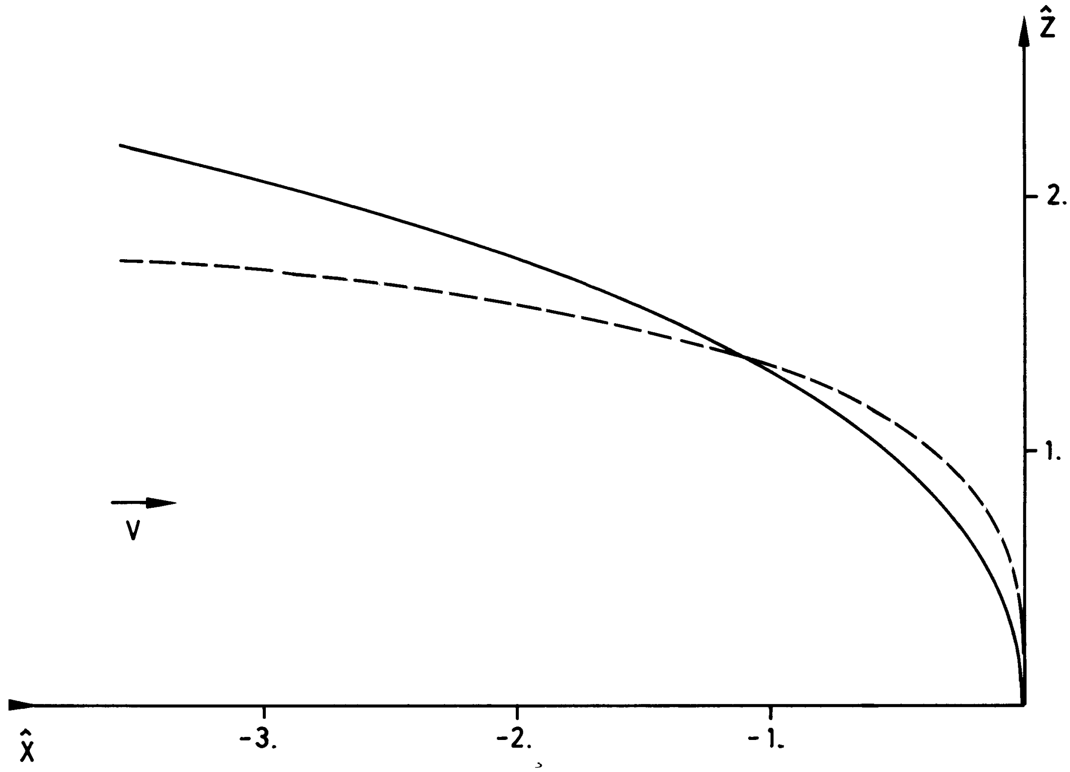

Fig. 5: Stationary equilibrium shape of flux tubes under the influence of a horizontal velocity field with kinetic energy density ρv^2 constant with height z (full line) and proportional to z (dashed line). The direction of the flow is from left to right. Note that generally the length scales are not equal for both examples.

We see that the flux tube turns *towards* the flow because only in this way a balance of forces is possible. This is in contrast to a tree bent by a storm for which the differential tension force due to bending acts in the opposite direction of the normal vector. The path given by Eq. (4.53) and shown by the dashed line has a smaller curvature for small $\hat{z}$ than that for constant kinetic energy density (Eq. 4.48, full line) but as $\hat{z}$ increases it quickly bends over. In the case $2z_0 = 1/\hat{\alpha}$ the length scales for both cases are equal and the curves can be directly compared. We may use these results to estimate the influence of velocity fields on slender flux tubes in the lower parts of the solar convection zone. Using the values

$\rho_e = 0.2$ g$\cdot$cm^{-3}
$B_0 = 10^4$ Gauss (equipartition)
$\Phi_{mag} = 10^{18}...10^{20}$ mx ($a = 6 \cdot 10^6 ... 6 \cdot 10^7$ cm)
$v_0 = 10^4$ cm$\cdot$s^{-1}(convective flow, differential rotation)

$z_0 = 6 \cdot 10^9$ cm (equal to the pressure scale height)

we find

$$\hat{\alpha}^{-1} \approx 10^7 ... 10^8 \text{ cm}$$
$$\tilde{\alpha}^{-1/2} \approx 3 \cdot 10^8 ... 10^9 \text{ cm.}$$

We see in Fig. 5 that the flux tube paths become almost horizontal at typical heights $\hat{z} \approx 1...3$ which refers to heights of the order of $\hat{\alpha}^{-1}$ and $\tilde{\alpha}^{-1/2}$, respectively, for the two cases. This means that in equilibrium an initially vertical flux tube cannot intrude significantly into a layer of horizontal flow unless either the field strength is much larger than the equipartition value, the horizontal flow speed is much smaller than the typical convective velocities, or the radius of the flux tube is of the order of the scale height. The dominant rôle of external flow fields in the dynamics of thin flux tubes is an important effect which must be taken into account when discussing the properties of magnetic structures in stellar convection zones (see Ch. 6).

For other velocity fields $\mathbf{v}(x, z)$, Eq. (4.33) in most cases has to be solved by numerical forward integration in height starting from a suitable initial point. The appropriate value of $v_\perp$ for each point is calculated using the earlier determined angle γ and location $x(z)$. The value of B_x which results from Eq. (4.33) can then be used to calculate the values of γ and $x(z)$ at the next point using Eqs. (4.19) and (4.28/29). Both steps of this procedure which correspond to two integrations can be combined in the solution of a second order differential equation for the path $z(x)$ (cf. Schüssler, 1980a; Parker, 1982c; Anton, 1984). To this end we use the relation between radius of curvature and the derivatives, $z' \equiv dz/dx$, $z'' \equiv d^2z/dx^2$, and write for the curvature force

$$\frac{B^2}{4\pi R}\,\hat{\mathbf{n}} \;=\; \frac{B^2}{4\pi}\,\frac{z''}{(1+z'^2)^{3/2}}\,\hat{\mathbf{n}}\,. \tag{4.54}$$

Since we have $\cos\gamma = (1+z'^2)^{-1/2}$ the condition for stationary equilibrium, Eq. (4.32), can be written as

$$(\rho - \rho_e)\,g \;+\; \frac{B^2}{4\pi}\,\frac{z''}{1+z'^2} \;+\; \frac{C_D \rho_e v_\perp^2}{\pi\, a}\,(1+z'^2)^{1/2}\mathrm{sgn}(v_\perp) \;=\; 0 \tag{4.55}$$

Sometimes it proves useful to rewrite the buoyancy term with aid of the relation

$$\frac{4\pi(\rho_e - \rho)g}{B^2} \;=\; -\frac{4\pi}{B^2}\frac{d}{dz}\left(\frac{B^2}{8\pi}\right) \;=\; \frac{1}{2}\frac{d}{dz}\ln\left(\frac{B^2}{4\pi}\right)\,. \tag{4.56}$$

It depends on the properties of the particular problem which of the two possible ways to calculate the path $z(x)$, i.e. Eqs. (4.29/4.33) or Eq. (4.55), is more appropriate. Other examples for the calculation of stationary flux tube equilibria have been given by Parker (1979d; 1982c,d) for horizontal flows and for idealized cellular velocity fields, by van Ballegooijen (1982a) for a constant horizontal drift of flux tubes in the solar convection zone, and by Anton and Schüssler (unpublished) for giant convective cell patterns (see also Moreno-Insertis, 1984).

5. Stability of flux tubes

Static or stationary equilibrium configurations of flux tubes can only have a practical relevance if they are at least linearly stable, i.e. if the flux tube returns to its equilibrium position and shape after a small displacement. In Ch. 2 we have discussed mechanisms which lead to fragmentation of large magnetic structures and to the formation of flux tubes which are much smaller than the scale height in the deep parts of a convection zone. Such tubes are strongly influenced by motions in their environment like convection, differential rotation, and meridional circulation. Even if a flux tube is stable with respect to fragmentation and reaches a static or stationary equilibrium characterized by a balance of buoyancy, tension, drag and rotationally induced (Coriolis, centrifugal) forces, this equilibrium might be unstable due to

a) superadiabaticity of the environment,

b) loop formation with downflows from the crests to the troughs with concomitant perturbations of magnetic buoyancy (akin to the instability discussed by Parker, 1966),

c) gradients of the drag force exerted by external flows,

d) differential rotation.

These instabilities lead to motion and deformation of the flux tube as a whole and can be treated within the framework of the approximation of slender flux tubes. This allows a considerable simplification of the mathematics and simultaneously excludes the fragmentation instabilities (Rayleigh-Taylor, Kelvin-Helmholtz) discussed in Ch. 2.

5.1 Previous work

Vertical flux tubes in the (sub)photosphere of the Sun are liable to a convective instability (convective collapse) caused by the superadiabatic stratification of the surrounding fluid (Parker, 1978; Webb and Roberts, 1978; Spruit and Zweibel, 1979; Unno and Ando, 1979). It is believed that this process is responsible for the amplification of small-scale solar magnetic fields far beyond the equipartition field strength (for a more detailed discussion see Schüssler, 1990).

Apart from preliminary studies (e.g. Schüssler, 1980a) the first detailed stability analysis of flux tubes *within* a convection zone has been presented by Spruit and van Ballegooijen (1982) who analyzed the stability of horizontal, non-buoyant ($\rho = \rho_e$) flux tubes in cartesian geometry and of toroidal flux tubes in static equilibrium between buoyancy and tension force in spherical geometry. They found instabilities which represent a mixture between the convective and the (Parker type) kink* instabilities (*a* and *b* above). The perturbations leading to kink instability must have a finite wavelength in the direction along the tube. It turns out that all flux tubes embedded in a superadiabatic environment are unstable and that kink instability occurs even for slightly subadiabatic stratification. Moreno-Insertis (1984, 1986) performed numerical simulations of the nonlinear evolution of kink-unstable horizontal flux tubes at the bottom of the solar convection

* Not to be confused with the "classical" kink instability of a plasma pinch caused by the azimuthal magnetic field component: The kink instability discussed here is driven by magnetic buoyancy and superadiabaticity.

zone. He found that while the upper part of the unstable loop rises towards the solar surface, the lower part sinks down and enters the subadiabatic region below the convection zone where it reaches a stable equilibrium. Moreno-Insertis (1984) also investigated the influence of the drag force exerted by a prescribed giant convective velocity cell on the evolution of the instability. Recently, Choudhuri (1989; see also Choudhuri and Gilman, 1987) has included rotation in a numerical study of kink-unstable flux tubes in the solar convection zone. He found in most cases that the Coriolis force dominates the dynamics and leads to a trajectory of the rising loop which is parallel to the axis of rotation. Consequently, the unstable loops break through the surface far away from the equatorial regions where solar activity predominantly is observed. A more radial eruption of unstable loops is only achieved for quite strong fields (about 10^5 Gauss) for which buoyancy becomes the dominating force.

Van Ballegooijen (1983) continued the analytical stability study of toroidal flux tubes by including (differential) rotation of the external medium and a difference between the rotation rate of the gas within and outside of the flux tube. Such a difference (a longitudinal flow along the tube with respect to a coordinate system which corotates with the external gas) may arise due to conservation of angular momentum if the flux tube is carried by an equatorward meridional circulation in the lower part of the convection zone and thus increases its distance from the axis of rotation (cf. van Ballegooijen, 1982b). The Coriolis force caused by slower rotation of the internal gas helps to balance the component of the buoyancy force perpendicular to the axis of rotation. For flux tubes situated in the equatorial plane, *rigid* rotation and longitudinal flow have a stabilizing effect. However, in the parameter regime relevant for the lower convection zone of the Sun the stability properties are determined by *differential* rotation: The flux tube is stable if $\partial\Omega_e/\partial r > 0$, i.e. if the angular velocity of the external medium increases radially outward; it is unstable with respect to non-axisymmetric disturbances (growing waves along the tube) if Ω_e decreases. Similar to the buoyancy-driven kink instability it is the downflow along the legs of a loop which triggers the instability due to differential rotation, in this case by introducing differential Coriolis forces in the radial direction.

The more general case of toroidal flux tubes outside the equatorial plane including meridional circulation has been treated by van Ballegooijen and Choudhuri (1988). In equilibrium, the component of the drag force perpendicular to the plane of the tube balances the corresponding component of the buoyancy force and thus removes the 'poleward slip instability' (Pneuman and Raadu, 1972; Spruit and van Ballegooijen, 1982). The authors found that an increase of the velocity of meridional circulation in radial direction has a stabilizing effect on the flux tube. However, their analysis is restricted to rigid rotation of the exterior and to axisymmetric perturbations such that the whole class of kink instabilities induced by buoyancy or differential rotation is neglected. The stability properties of toroidal flux tubes under these conditions remain to be investigated.

For a totally different application, the stability and interaction of jets from active galactic nuclei, Achterberg (1982, 1988) has derived a formalism which is similar to these approaches and also to the formalism developed in this work.

In this chapter we present a formalism which can be used to analyze the stability of general static and stationary flux tube equilibria in a plane with constant direction of gravity. It can be applied to any given plane equilibrium path $\mathbf{r}(l)$ along which all quantities may vary. Such a formalism is needed in order to determine the stability properties of a number of non-trivial flux tube equilibria like the examples given in Sec. 4.2 or the loop structures calculated by van Ballegooijen (1982a) and Anton (1984). We include a velocity field of arbitrary structure but, in order to limit the complication of the already somewhat involved formalism, we have refrained from treating the spherical case and also ignored rotation. However, this restriction is not fundamental and will be dropped in future work.

5.2 Equilibrium

We assume a plane flux tube in static or stationary equilibrium described by the time-independent form of Eqs. (3.25) and (3.26). We take $\mathbf{g} \cdot \hat{\mathbf{b}} = 0$ and assume that the external velocity is restricted to the plane of the equilibrium tube such that both terms on the r.h.s. of Eq. (3.27) (binormal direction) vanish. We continue to use the notation introduced in Chs. 3 and 4. Denoting all equilibrium quantities by a suffix '0', the equilibrium path of the flux tube is given by $\mathbf{r}_0(l_0)$ and the normal, $\hat{\mathbf{n}}_0(l_0)$, and tangential, $\hat{\mathbf{l}}_0(l_0)$, unit vectors as well as the radius of curvature, R_0, are defined in the usual way as functions of the equilibrium path length, l_0:

$$\hat{\mathbf{l}}_0 \;=\; \frac{\partial\,\mathbf{r}_0}{\partial l_0}, \quad \hat{\mathbf{n}}_0 \;=\; R_0\,\frac{\partial\,\hat{\mathbf{l}}_0}{\partial l_0}, \quad R_0 \;=\; \left|\frac{\partial\,\hat{\mathbf{l}}_0}{\partial l_0}\right|^{-1}. \tag{5.1}$$

The equilibrium state is characterized by hydrostatic equilibrium in the longitudinal direction (cf. Eq. 3.25)

$$0 \;=\; -\frac{\partial p_0}{\partial l_0} \;+\; \rho_0\,\mathbf{g}_0 \cdot \hat{\mathbf{l}}_0 \tag{5.2}$$

and by a balance of buoyancy, curvature and drag force in the normal direction (cf. Eq. 3.26)

$$0 \;=\; (\rho_0 - \rho_{e0})g_0(\hat{\mathbf{g}}_0 \cdot \hat{\mathbf{n}}_0) \;+\; \frac{B_0^2}{4\pi R_0} \;+\; \frac{C_D\rho_{e0}(\mathbf{v}_{e0} \cdot \hat{\mathbf{n}}_0)^2 \mathrm{sgn}(\mathbf{v}_{e0} \cdot \hat{\mathbf{n}}_0)}{\pi a_0} \tag{5.3}$$

($\mathbf{g}_0 = g_0\hat{\mathbf{g}}_0$). Eqs. (5.2/3) are complemented by the conditions of pressure balance, Eq. (3.23), and flux conservation, Eq. (3.31), and by hydrostatic equilibrium of the external medium, Eq. (3.24). Note that all quantities may depend on l_0. Since the external velocity, $\mathbf{v}_e$, has no component perpendicular to the plane of the tube the drag force given by Eqs. (3.28/29) can be written in the simpler form shown in Eq. (5.3). We may express the equilibrium condition in terms of the relative density contrast between exterior and interior of the flux tube by rewriting Eq. (5.3) in the form

$$\beta\left(\frac{\rho_{e0}}{\rho_0} - 1\right)(\hat{\mathbf{g}}_0 \cdot \hat{\mathbf{n}}_0) \;=\; \frac{2H_{p0}}{R_0} \;+\; \beta r\,\mathrm{sgn}(\mathbf{v}_{e0} \cdot \hat{\mathbf{n}}_0) \tag{5.4}$$

where $\beta = 8\pi p_0/B_0^2$, H_{p0} is the internal pressure scale height defined by $p_0/H_{p0} = \rho_0 g_0$, and r is given by

$$r \;=\; \frac{\rho_{e0}}{\rho_0}\,\frac{C_D(\mathbf{v}_{e0} \cdot \hat{\mathbf{n}}_0)^2}{\pi a_0 g_0}. \tag{5.5}$$

The product βr can be written in the form

$$\beta r \;=\; \left(\frac{2C_D}{\pi}\right)\left(\frac{\rho_{e0}}{\rho_0}\right)\left(\frac{(\mathbf{v}_{e0} \cdot \hat{\mathbf{n}}_0)^2}{v_{A0}^2}\right)\left(\frac{H_{p0}}{a_0}\right) \tag{5.6}$$

where $v_{A0} = B_0/\sqrt{4\pi\rho_0}$ is the Alfvén velocity. For equipartition fields ($B_0 = 10^4 ... 10^5$ Gauss) near the bottom of the solar convection zone ($p_0 = 6 \cdot 10^{13}\,\mathrm{dyn} \cdot \mathrm{cm}^{-2}$) we have very large values of $\beta \approx 1.5 \cdot 10^5 ... 1.5 \cdot 10^7$. We shall use this property in Sec. 5.3 to derive a simplified version of the perturbation equations in the limit $\beta \gg 1$. In most cases relevant for the deep convection zone, the density contrast in Eq. (5.4) is very small such that $\beta(\rho_{e0}/\rho_0 - 1)$, H_{p0}/R_0, and βr are all of order unity or at least have moderate values.

5.3 Perturbation equations

In order to determine the linear stability of the equilibrium we introduce Lagrangean displacements in the normal and tangential directions described by the functions $\varepsilon(l_0)$ and $\eta(l_0)$, respectively, and write for the perturbed path*

$$\mathbf{r} \;=\; \mathbf{r}_0 \;+\; \mathbf{r}_1 \;\equiv\; \mathbf{r}_0(l_0) \;+\; \varepsilon(l_0)\,\hat{\mathbf{n}}_0 \;+\; \eta(l_0)\,\hat{\mathbf{l}}_0\,. \tag{5.7}$$

Similar to the analyses of Spruit and van Ballegooijen (1982) and of van Ballegooijen (1983), a displacement in the binormal direction decouples from the rest of the equations and gives rise to (stable) transversal flux tube waves which are of no further interest here. We therefore consider only displacements within the plane of the equilibrium flux tube path.

First we determine the perturbed *geometry* of the flux tube. The relation between the arc length of the perturbed tube, l, and the arc length in equilibrium, l_0, to first order in the perturbations is given by

$$\frac{\partial l}{\partial l_0} \;=\; 1 - \frac{\varepsilon}{R_0} + \frac{\partial \eta}{\partial l_0}\,. \tag{5.8}$$

The perturbed tangent vector, $\hat{\mathbf{l}}$, is

$$\hat{\mathbf{l}} \;=\; \frac{\partial \mathbf{r}}{\partial l} \;=\; \frac{\partial \mathbf{r}}{\partial l_0}\,\frac{\partial l_0}{\partial l} \;=\; \hat{\mathbf{l}}_0 \;+\; \hat{\mathbf{n}}_0\left(\frac{\eta}{R_0} \;+\; \frac{\partial \varepsilon}{\partial l_0}\right). \tag{5.9}$$

Now we can calculate the curvature vector, $\mathbf{c} \equiv \hat{\mathbf{n}}/R$:

$$\mathbf{c} \;=\; \frac{\partial \hat{\mathbf{l}}}{\partial l} \;=\; \frac{\partial \hat{\mathbf{l}}}{\partial l_0}\,\frac{\partial l_0}{\partial l} \;=\; \frac{\hat{\mathbf{n}}_0}{R_0}\left(1 + \frac{\varepsilon}{R_0} + R_0\frac{d^2\varepsilon}{dl_0^2} - \frac{\eta}{R_0}\,\frac{\partial R_0}{\partial l_0}\right) \;-\; \frac{\hat{\mathbf{l}}_0}{R_0}\left(\frac{\eta}{R_0} + \frac{\partial \varepsilon}{\partial l_0}\right). \tag{5.10}$$

Taking the absolute value of Eq. (5.10) gives the perturbed radius of curvature, R, and the perturbed normal vector, viz.

$$R \;=\; R_0\left(1 + \frac{\varepsilon}{R_0} + R_0\frac{d^2\varepsilon}{dl_0^2} - \frac{\eta}{R_0}\,\frac{\partial R_0}{\partial l_0}\right)^{-1} \tag{5.11}$$

$$\hat{\mathbf{n}} \;=\; \hat{\mathbf{n}}_0 - \hat{\mathbf{l}}_0\left(\frac{\eta}{R_0} \;+\; \frac{\partial \varepsilon}{\partial l_0}\right). \tag{5.12}$$

We now proceed by determining the *gravitational acceleration,* $\mathbf{g}$, in the perturbed state. We assume a power law for the dependence of g_0 on height, z, and write

$$\mathbf{g}_0 \;=\; -g_m\left(\frac{z_0}{z_m}\right)^s \hat{\mathbf{z}} \;\equiv\; -g_0\hat{\mathbf{z}} \tag{5.13}$$

($\hat{\mathbf{z}}$: unit vector in direction of height; g_m: gravitational acceleration at some reference height, z_m; $z_0(l_0)$: height of equilibrium flux tube). With the height displacement, z_1, given by

$$z_1 \;\equiv\; \mathbf{r}_1\cdot\hat{\mathbf{z}} \;=\; -\mathbf{r}_1\cdot\hat{\mathbf{g}}_0 \;=\; -\varepsilon\,(\hat{\mathbf{g}}_0\cdot\hat{\mathbf{n}}_0) - \eta\,(\hat{\mathbf{g}}_0\cdot\hat{\mathbf{l}}_0) \tag{5.14}$$

where $\hat{\mathbf{g}}_0 = -\hat{\mathbf{z}}$ denotes the unit vector in the direction of gravity we find, to first order in z_1,

* The perturbations of all quantities which have a non-vanishing equilibrium value are indicated by a suffix ‘1’. Perturbed quantities (equilibrium value + perturbation) are written without suffix.

$$
\begin{aligned}
\mathbf{g} \;=\; \mathbf{g}_0 + \mathbf{g}_1 \;&=\; -g_m \left(\frac{z_0 + z_1}{z_m} \right)^s \hat{\mathbf{z}} \;=\; -g_m \left(\frac{z_0}{z_m} \right)^s \left(1 + \frac{z_1}{z_0} \right)^s \hat{\mathbf{z}} \\
&=\; \mathbf{g}_0 \left(1 - s \, \frac{\varepsilon\,(\hat{\mathbf{g}}_0 \cdot \hat{\mathbf{n}}_0) + \eta\,(\hat{\mathbf{g}}_0 \cdot \hat{\mathbf{l}}_0)}{z_0} \right) . \qquad (5.15)
\end{aligned}
$$

Defining

$$
\Delta \;\equiv\; \frac{-z_1}{z_0} \;=\; \frac{\varepsilon\,(\hat{\mathbf{g}}_0 \cdot \hat{\mathbf{n}}_0) + \eta\,(\hat{\mathbf{g}}_0 \cdot \hat{\mathbf{l}}_0)}{z_0} \qquad (5.16)
$$

we write for the component of gravity along $\hat{\mathbf{l}}$ with aid of Eqs. (5.9) and (5.15)

$$
\mathbf{g} \cdot \hat{\mathbf{l}} \;=\; (1 - s\Delta)\, \mathbf{g}_0 \cdot \left[\hat{\mathbf{l}}_0 \;+\; \hat{\mathbf{n}}_0 \left(\frac{\eta}{R_0} \;+\; \frac{\partial \varepsilon}{\partial l_0} \right) \right] \qquad (5.17)
$$

which gives for the perturbation of longitudinal component of $\mathbf{g}$

$$
(\mathbf{g} \cdot \hat{\mathbf{l}})_1 \;=\; g_0 \left[(\hat{\mathbf{g}}_0 \cdot \hat{\mathbf{n}}_0) \left(\frac{\eta}{R_0} \;+\; \frac{\partial \varepsilon}{\partial l_0} \right) \;-\; (\hat{\mathbf{g}}_0 \cdot \hat{\mathbf{l}}_0) s\Delta \right] . \qquad (5.18)
$$

For the perturbation of the normal component of $\mathbf{g}$ we find using Eqs. (5.12) and (5.15)

$$
(\mathbf{g} \cdot \hat{\mathbf{n}})_1 \;=\; -g_0 \left[(\hat{\mathbf{g}}_0 \cdot \hat{\mathbf{n}}_0) s\Delta \;+\; (\hat{\mathbf{g}}_0 \cdot \hat{\mathbf{l}}_0) \left(\frac{\eta}{R_0} \;+\; \frac{\partial \varepsilon}{\partial l_0} \right) \right] . \qquad (5.19)
$$

We now consider the *longitudinal component of the equation of motion,* Eq. (3.25). To first order in the displacements, the inertial term on its l.h.s. can be written using $\mathbf{u} = d\mathbf{r}_1/dt \equiv (\dot{\eta}, \dot{\varepsilon})$ in the form

$$
\rho \frac{d\mathbf{u}}{dt} \cdot \hat{\mathbf{l}} \;=\; \rho \frac{d\mathbf{u} \cdot \hat{\mathbf{l}}}{dt} \;-\; \rho \mathbf{u} \cdot \frac{d\hat{\mathbf{l}}}{dt} \;=\; \rho \left(\frac{d}{dt} (\dot{\eta}\, \hat{\mathbf{l}}_0 + \dot{\varepsilon}\, \hat{\mathbf{n}}_0) \right) \cdot \hat{\mathbf{l}} \;-\; \rho \mathbf{u} \cdot \left(\frac{d\hat{\mathbf{l}}_0}{dt} + \frac{d\hat{\mathbf{l}}_1}{dt} \right) \;=\; \rho_0 \ddot{\eta} \, . \qquad (5.20)
$$

The perturbation of the longitudinal pressure gradient is given by

$$
\left(\frac{\partial p}{\partial l} \right)_1 \;=\; \frac{\partial p_1}{\partial l_0} \;+\; \frac{\partial p_0}{\partial l_0} \left(\frac{\varepsilon}{R_0} - \frac{\partial \eta}{\partial l_0} \right) \qquad (5.21)
$$

and the perturbation of the gravity force reads

$$
\begin{aligned}
(\rho\, \mathbf{g} \cdot \hat{\mathbf{l}})_1 \;&=\; \rho_0 (\mathbf{g} \cdot \hat{\mathbf{l}})_1 + \rho_1 g_0 (\hat{\mathbf{g}}_0 \cdot \hat{\mathbf{l}}_0) \\
&=\; \rho_0 g_0 \left[(\hat{\mathbf{g}}_0 \cdot \hat{\mathbf{n}}_0) \left(\frac{\eta}{R_0} + \frac{\partial \varepsilon}{\partial l_0} \right) - (\hat{\mathbf{g}}_0 \cdot \hat{\mathbf{l}}_0) s\Delta \right] \;+\; \frac{\rho_1}{\rho_0} \frac{\partial p_0}{\partial l_0} \, . \qquad (5.22)
\end{aligned}
$$

where we have used Eqs. (5.2) and (5.18). Inserting Eqs. (5.20-5.22) into Eq. (3.25) we find for the longitudinal equation of motion, to first order in the perturbations:

$$
\begin{aligned}
\ddot{\eta} \;=\; &-\frac{1}{\rho_0} \frac{\partial p_1}{\partial l_0} \;-\; \frac{1}{\rho_0} \frac{\partial p_0}{\partial l_0} \left(\frac{\varepsilon}{R_0} - \frac{\partial \eta}{\partial l_0} - \frac{\rho_1}{\rho_0} \right) \\
&+\; g_0 \left[(\hat{\mathbf{g}}_0 \cdot \hat{\mathbf{n}}_0) \left(\frac{\eta}{R_0} + \frac{\partial \varepsilon}{\partial l_0} \right) - (\hat{\mathbf{g}}_0 \cdot \hat{\mathbf{l}}_0) s\Delta \right] . \qquad (5.23)
\end{aligned}
$$

Similar to Eq. (5.20) the inertial term in Eq. (3.26), the *normal component of the equation of motion,* reduces to $\rho_0\ddot{\varepsilon}$.* Using Eq. (5.19) the perturbation of the buoyancy force on the r.h.s. of Eq. (3.26) is given by

$$[(\rho - \rho_e)\mathbf{g}\cdot\hat{\mathbf{n}}]_1 = (\rho_1 - \rho_{e1})g_0(\hat{\mathbf{g}}_0\cdot\hat{\mathbf{n}}_0) - (\rho_0 - \rho_{e0})g_0\left[(\hat{\mathbf{g}}_0\cdot\hat{\mathbf{n}}_0)s\Delta + (\hat{\mathbf{g}}_0\cdot\hat{\mathbf{l}}_0)\left(\frac{\eta}{R_0} + \frac{\partial\varepsilon}{\partial l_0}\right)\right]. \tag{5.24}$$

The perturbation of the external density, ρ_{e1}, in our Lagrangian approach is

$$\rho_{e1} = -\rho_{e0}z_1 H_{\rho e}^{-1} = -\rho_{e0}z_1(1-\nabla)H_{pe}^{-1} \tag{5.25}$$

($H_{\rho e}$: external density scale height; H_{pe}: external pressure scale height; ∇: logarithmic temperature gradient in the external medium; all these quantities are taken at $z = z_0$). The relation $H_{pe} = (1-\nabla)H_{\rho e}$ is valid if the molecular weight is constant, an assumption which is well justified in the lower parts of the solar convection zone. With aid of Eq. (5.11) the perturbation of the curvature force can be written

$$\left(\frac{B^2}{4\pi R}\right)_1 = \frac{B_0B_1}{2\pi R_0} + \frac{B_0^2}{4\pi R_0}\left(\frac{\varepsilon}{R_0} + R_0\frac{d^2\varepsilon}{dl_0^2} - \frac{\eta}{R_0}\frac{\partial R_0}{\partial l_0}\right). \tag{5.26}$$

The perturbation of the drag force is slightly more complicated to determine. We start by noting that for linear analysis we may take $\mathrm{sgn}(\mathbf{v}_e\cdot\hat{\mathbf{n}}) = \mathrm{sgn}(\mathbf{v}_{e0}\cdot\hat{\mathbf{n}}_0)$ since the displacement can always be made sufficiently small. In the case $\mathbf{v}_{e0}\cdot\hat{\mathbf{n}}_0 = 0$ the perturbation of the drag term vanishes identically as one can see in Eqs. (5.31/33) below. The perturbed relative velocity between flux tube and environment is given by

$$\mathbf{v}_e = \mathbf{v}_{e0} + (\mathbf{r}_1\cdot\nabla)\mathbf{v}_e|_{\mathbf{r}_0} - \mathbf{u}\,. \tag{5.27}$$

The third term on the r.h.s. represents the motion of the tube due to the displacement while the second term describes the spatial change of $\mathbf{v}_e$ which is written in cartesian coordinates (x, z):

$$\mathbf{w}_{e1} \equiv (\mathbf{r}_1\cdot\nabla)\mathbf{v}_e|_{\mathbf{r}_0} = x_1\left.\frac{\partial\mathbf{v}_e}{\partial x}\right|_{\mathbf{r}_0} + z_1\left.\frac{\partial\mathbf{v}_e}{\partial z}\right|_{\mathbf{r}_0} \tag{5.28}$$

with

$$\begin{aligned} x_1 &= \mathbf{r}_1\cdot\hat{\mathbf{x}} = \varepsilon\,(\hat{\mathbf{x}}\cdot\hat{\mathbf{n}}_0) + \eta\,(\hat{\mathbf{x}}\cdot\hat{\mathbf{l}}_0) \\ z_1 &= \mathbf{r}_1\cdot\hat{\mathbf{z}} = -\varepsilon\,(\hat{\mathbf{g}}_0\cdot\hat{\mathbf{n}}_0) - \eta\,(\hat{\mathbf{g}}_0\cdot\hat{\mathbf{l}}_0). \end{aligned} \tag{5.29}$$

$\hat{\mathbf{x}}$ is the unit vector in direction of the x coordinate, i.e. the horizontal direction. Next we determine the perturbation of $(\mathbf{v}_e\cdot\hat{\mathbf{n}})^2$. Using Eqs. (5.12) and (5.27) we write

$$(\mathbf{v}_e\cdot\hat{\mathbf{n}})^2 = \left[(\mathbf{v}_{e0} + \mathbf{w}_{e1} - \mathbf{u})\cdot\left(\hat{\mathbf{n}}_0 - \hat{\mathbf{l}}_0\left(\frac{\eta}{R_0} + \frac{\partial\varepsilon}{\partial l_0}\right)\right)\right]^2 \tag{5.30}$$

* An enhanced inertia of the flux tube with respect to transversal motions due to the acceleration of material in the exterior is not considered here. It would only affect growth rates (or oscillation frequencies) but does not change the stability criteria. In the case $\beta = 8\pi p_0/B_0^2 \gg 1$ which we consider later the enhanced inertia can be crudely taken account of by multiplying the inertial term of the normal component of the equation of motion by a factor 2 (cf. Spruit and van Ballegooijen, 1982).

which gives

$$v_{\perp 1} \;\equiv\; (\mathbf{v}_e \cdot \hat{\mathbf{n}})_1^2 \;=\; 2(\mathbf{v}_{e0} \cdot \hat{\mathbf{n}}_0) \left[(\mathbf{w}_{e1} \cdot \hat{\mathbf{n}}_0) \;-\; \dot{\varepsilon} \;-\; (\mathbf{v}_{e0} \cdot \hat{\mathbf{l}}_0) \left(\frac{\eta}{R_0} \;+\; \frac{\partial \varepsilon}{\partial l_0} \right) \right]. \tag{5.31}$$

Note that $v_{\perp 1}$ may have positive or negative sign. Using Eq. (5.28/29) we obtain

$$\begin{aligned} (\mathbf{w}_{e1} \cdot \hat{\mathbf{n}}_0) \;&=\; \left[\varepsilon(\hat{\mathbf{x}} \cdot \hat{\mathbf{n}}_0) + \eta(\hat{\mathbf{x}} \cdot \hat{\mathbf{l}}_0) \right] \left(\frac{\partial \mathbf{v}_e}{\partial x}\bigg|_{\mathbf{r}_0} \cdot \hat{\mathbf{n}}_0 \right) \;-\; \left[\varepsilon(\hat{\mathbf{g}}_0 \cdot \hat{\mathbf{n}}_0) + \eta(\hat{\mathbf{g}}_0 \cdot \hat{\mathbf{l}}_0) \right] \left(\frac{\partial \mathbf{v}_e}{\partial z}\bigg|_{\mathbf{r}_0} \cdot \hat{\mathbf{n}}_0 \right) \\ &\equiv\; \left[\varepsilon(\hat{\mathbf{x}} \cdot \hat{\mathbf{n}}_0) + \eta(\hat{\mathbf{x}} \cdot \hat{\mathbf{l}}_0) \right] w_x \;-\; \left[\varepsilon(\hat{\mathbf{g}}_0 \cdot \hat{\mathbf{n}}_0) + \eta(\hat{\mathbf{g}}_0 \cdot \hat{\mathbf{l}}_0) \right] w_z \,. \end{aligned} \tag{5.32}$$

Now we can write down the perturbation of the drag term:

$$\left(\frac{C_D \rho_e (\mathbf{v}_e \cdot \hat{\mathbf{n}})^2 \mathrm{sgn}(\mathbf{v}_e \cdot \hat{\mathbf{n}})}{\pi a} \right)_1 \;=\; \frac{C_D \rho_{e0} (\mathbf{v}_{e0} \cdot \hat{\mathbf{n}}_0)^2 \mathrm{sgn}(\mathbf{v}_{e0} \cdot \hat{\mathbf{n}}_0)}{\pi a_0} \left(\frac{v_{\perp 1}}{(\mathbf{v}_{e0} \cdot \hat{\mathbf{n}}_0)^2} + \frac{\rho_{e1}}{\rho_{e0}} - \frac{a_1}{a_0} \right). \tag{5.33}$$

The last term on the r.h.s. can be rewritten using the conservation of magnetic flux, $Ba^2 = \mathrm{const.}$, which yields

$$\frac{a_1}{a_0} \;=\; -\frac{B_1}{2B_0}. \tag{5.34}$$

We combine Eqs. (5.24), (5.26) and (5.33/34) and obtain for the normal component of the perturbed equation of motion by inserting into Eq. (3.26):

$$\begin{aligned} \ddot{\varepsilon} \;=\; & \frac{\rho_1 - \rho_{e1}}{\rho_0}\, g_0 (\hat{\mathbf{g}}_0 \cdot \hat{\mathbf{n}}_0) \;-\; \left(1 - \frac{\rho_{e0}}{\rho_0} \right) g_0 \left[(\hat{\mathbf{g}}_0 \cdot \hat{\mathbf{n}}_0) s\Delta + (\hat{\mathbf{g}}_0 \cdot \hat{\mathbf{l}}_0) \left(\frac{\eta}{R_0} + \frac{\partial \varepsilon}{\partial l_0} \right) \right] \\ & + \; \frac{B_0^2}{4\pi R_0 \rho_0} \left(\frac{2B_1}{B_0} + \frac{\varepsilon}{R_0} + R_0 \frac{d^2 \varepsilon}{dl_0^2} - \frac{\eta}{R_0} \frac{\partial R_0}{\partial l_0} \right) \\ & + \; \frac{C_D \rho_{e0} (\mathbf{v}_{e0} \cdot \hat{\mathbf{n}}_0)^2 \mathrm{sgn}(\mathbf{v}_{e0} \cdot \hat{\mathbf{n}}_0)}{\pi a_0 \rho_0} \left(\frac{v_{\perp 1}}{(\mathbf{v}_{e0} \cdot \hat{\mathbf{n}}_0)^2} + \frac{\rho_{e1}}{\rho_{e0}} + \frac{B_1}{2B_0} \right). \end{aligned} \tag{5.35}$$

Since it is our aim to obtain a set of two coupled equations for the displacements η and ε alone, we have to eliminate the other perturbations $(B_1, \rho_1, \rho_{e1}, p_1, ...)$ in favor of η, ε, and equilibrium quantities. This has already been achieved for ρ_{e1} with Eqs. (5.25) and (5.14) and for $v_{\perp 1}$ in Eqs. (5.31/32). For the remaining quantities we use Eq. (3.13), the equation of continuity, which can be written to first order in the perturbations (after a time integration) in the form

$$\frac{\rho_1}{\rho_0} \;-\; \frac{B_1}{B_0} \;+\; \frac{\partial \eta}{\partial l_0} \;-\; \frac{\varepsilon}{R_0} \;=\; 0\,, \tag{5.36}$$

the equation of state for adiabatic perturbations,

$$\frac{dp}{dt} \;=\; \frac{\gamma p}{\rho} \frac{d\rho}{dt}\,, \tag{5.37}$$

which yields (to first order, after time integration)

$$\frac{p_1}{p_0} \;=\; \gamma \frac{\rho_1}{\rho_0}\,, \tag{5.38}$$

and the condition of instantaneous pressure equilibrium, Eq. (3.23), which gives

$$\frac{p_1}{p_0} \;+\; \frac{2}{\beta}\frac{B_1}{B_0} \;=\; \frac{p_{e1}}{p_0} \tag{5.39}$$

with $\beta = 8\pi p_0/B_0^2$. Assuming hydrostatic equilibrium in the environment and using the equilibrium pressure balance condition, $p_0 + B_0^2/8\pi = p_{e0}$, we rewrite Eq. (5.39) in the form

$$\frac{p_1}{p_0} \;+\; \frac{2}{\beta}\frac{B_1}{B_0} \;=\; -\left(1+\frac{1}{\beta}\right)\frac{z_1}{H_{pe}}\,. \tag{5.40}$$

Eqs. (5.36) and (5.38/39) are used to obtain

$$\frac{B_1}{B_0} \;=\; \left(\frac{\beta\gamma}{\beta\gamma+2}\right)\left(\frac{\partial\eta}{\partial l_0} - \frac{\varepsilon}{R_0}\right) \;-\; \left(\frac{\beta+1}{\beta\gamma+2}\right)\frac{z_1}{H_{pe}} \tag{5.41}$$

$$\frac{\rho_1}{\rho_0} \;=\; \left(\frac{\beta\gamma}{\beta\gamma+2} - 1\right)\left(\frac{\partial\eta}{\partial l_0} - \frac{\varepsilon}{R_0}\right) \;-\; \left(\frac{\beta+1}{\beta\gamma+2}\right)\frac{z_1}{H_{pe}} \tag{5.42}$$

$$\frac{p_1}{p_0} \;=\; \gamma\left(\frac{\beta\gamma}{\beta\gamma+2} - 1\right)\left(\frac{\partial\eta}{\partial l_0} - \frac{\varepsilon}{R_0}\right) \;-\; \gamma\left(\frac{\beta+1}{\beta\gamma+2}\right)\frac{z_1}{H_{pe}}\,. \tag{5.43}$$

Using the abbreviations

$$\frac{\beta\gamma}{\beta\gamma+2} \;\equiv\; \alpha_1, \qquad \frac{\beta+1}{\beta\gamma+2} \;\equiv\; \alpha_2 \tag{5.44}$$

we insert Eqs. (5.42/43) into Eq. (5.23) and obtain for the equation which determines the time evolution of the longitudinal displacement η (primes denote derivatives with respect to l_0):

$$\begin{aligned}
\ddot{\eta} \;=\; & \varepsilon\Bigg\{-(\alpha_1-1)\frac{\gamma p_0}{\rho_0}\frac{R_0'}{R_0^2} \;+\; \frac{1}{\rho_0 R_0}\left[\gamma p_0(\alpha_1-1)\right]' \;+\; \frac{1}{\rho_0}\left[\frac{\alpha_2 p_0'}{H_{pe}} - \left(\frac{\gamma p_0 \alpha_2}{H_{pe}}\right)'\right](\hat{\mathbf{g}}_0\cdot\hat{\mathbf{n}}_0) \\
& \quad -\frac{\alpha_1 p_0'}{\rho_0 R_0} \;+\; \frac{\gamma p_0 \alpha_2}{\rho_0 H_{pe} R_0}(\hat{\mathbf{g}}_0\cdot\hat{\mathbf{l}}_0) \;-\; \frac{g_0 s}{z_0}(\hat{\mathbf{g}}_0\cdot\hat{\mathbf{l}}_0)(\hat{\mathbf{g}}_0\cdot\hat{\mathbf{n}}_0)\Bigg\} \\
& + \varepsilon'\left\{(\alpha_1-1)\frac{\gamma p_0}{\rho_0 R_0} + \left(g_0 \;-\; \frac{\gamma p_0\alpha_2}{\rho_0 H_{pe}}\right)(\hat{\mathbf{g}}_0\cdot\hat{\mathbf{n}}_0)\right\} \\
& + \eta\Bigg\{\left[\frac{\alpha_2 p_0'}{\rho_0 H_{pe}} - \frac{1}{\rho_0}\left(\frac{\gamma p_0\alpha_2}{H_{pe}}\right)'\right](\hat{\mathbf{g}}_0\cdot\hat{\mathbf{l}}_0) \\
& \quad + \left(\frac{g_0}{R_0} \;-\; \frac{\gamma p_0\alpha_2}{\rho_0 H_{pe} R_0}\right)(\hat{\mathbf{g}}_0\cdot\hat{\mathbf{n}}_0) - \frac{g_0 s}{z_0}(\hat{\mathbf{g}}_0\cdot\hat{\mathbf{l}}_0)^2\Bigg\} \\
& + \eta'\left\{-\frac{1}{\rho_0}\Big[\gamma p_0(\alpha_1-1)\Big]' \;+\; \frac{p_0'\alpha_1}{\rho_0} \;-\; \frac{\gamma p_0\alpha_2}{\rho_0 H_{pe}}(\hat{\mathbf{g}}_0\cdot\hat{\mathbf{l}}_0)\right\} \\
& + \eta''\left\{-(\alpha_1-1)\frac{\gamma p_0}{\rho_0}\right\}.
\end{aligned} \tag{5.45}$$

In order to derive Eq. (5.45) we have used Eqs. (5.14), (5.16) and the relation

$$\left[\varepsilon\,(\hat{\mathbf{g}}_0\cdot\hat{\mathbf{n}}_0)+\eta\,(\hat{\mathbf{g}}_0\cdot\hat{\mathbf{l}}_0)\right]' \;=\; \left(\eta' \,-\, \frac{\varepsilon}{R_0}\right)(\hat{\mathbf{g}}_0\cdot\hat{\mathbf{l}}_0) \;+\; \left(\varepsilon' \,+\, \frac{\eta}{R_0}\right)(\hat{\mathbf{g}}_0\cdot\hat{\mathbf{n}}_0). \tag{5.46}$$

In a similar way we obtain the equation which determines the time evolution of ε, the displacement in normal direction, by inserting into Eq. (5.35):

$$\begin{aligned}
\ddot{\varepsilon} \;=\; \eta\Bigg\{ & -\frac{2p_0R_0'}{\rho_0\beta R_0^2} \;+\; \frac{4p_0\alpha_2}{\rho_0\beta R_0 H_{pe}}(\hat{\mathbf{g}}_0\cdot\hat{\mathbf{l}}_0) \;+\; \frac{g_0}{H_{pe}}\left[\alpha_2 \;+\; \frac{\rho_{e0}}{\rho_0}(\nabla-1)\right](\hat{\mathbf{g}}_0\cdot\hat{\mathbf{l}}_0)(\hat{\mathbf{g}}_0\cdot\hat{\mathbf{n}}_0) \\
& -\;\left(1-\frac{\rho_{e0}}{\rho_0}\right)\left[\frac{g_0 s}{z_0}(\hat{\mathbf{g}}_0\cdot\hat{\mathbf{l}}_0)(\hat{\mathbf{g}}_0\cdot\hat{\mathbf{n}}_0) \;+\; \frac{g_0}{R_0}(\hat{\mathbf{g}}_0\cdot\hat{\mathbf{l}}_0)\right] \\
& +\;\frac{C_D\rho_{e0}\mathrm{sgn}(\mathbf{v}_{e0}\cdot\hat{\mathbf{n}}_0)(\mathbf{v}_{e0}\cdot\hat{\mathbf{n}}_0)^2}{\pi a_0\rho_0}\Bigg[\frac{2}{(\mathbf{v}_{e0}\cdot\hat{\mathbf{n}}_0)}\Big((\hat{\mathbf{x}}\cdot\hat{\mathbf{l}}_0)w_x-(\hat{\mathbf{g}}_0\cdot\hat{\mathbf{l}}_0)w_z\Big) \\
& -\;\frac{2(\mathbf{v}_{e0}\cdot\hat{\mathbf{l}}_0)}{R_0(\mathbf{v}_{e0}\cdot\hat{\mathbf{n}}_0)} \;-\; \frac{1}{H_{pe}}\left(\nabla\,-\,1\,-\,\frac{\alpha_2}{2}\right)(\hat{\mathbf{g}}_0\cdot\hat{\mathbf{l}}_0)\Bigg]\Bigg\} \\
+\;\eta'\Bigg\{ & \frac{4p_0\alpha_1}{\rho_0\beta R_0} \;+\; g_0(\alpha_1-1)(\hat{\mathbf{g}}_0\cdot\hat{\mathbf{n}}_0) \;+\; \frac{C_D\rho_{e0}(\mathbf{v}_{e0}\cdot\hat{\mathbf{n}}_0)^2\mathrm{sgn}(\mathbf{v}_{e0}\cdot\hat{\mathbf{n}}_0)\alpha_1}{2\pi a_0\rho_0}\Bigg\} \\
+\;\varepsilon\Bigg\{ & -\frac{4p_0\alpha_1}{\rho_0\beta R_0^2} \;+\; \frac{4p_0\alpha_2}{\rho_0\beta R_0 H_{pe}}(\hat{\mathbf{g}}_0\cdot\hat{\mathbf{n}}_0) \;+\; \frac{2p_0}{\rho_0 R_0^2\beta} \;-\; \frac{g_0 s}{z_0}\left(1-\frac{\rho_{e0}}{\rho_0}\right)(\hat{\mathbf{g}}_0\cdot\hat{\mathbf{n}}_0)^2 \\
& -\;\left[\frac{g_0}{R_0}(\alpha_1-1) \;-\; \frac{g_0}{H_{pe}}\left(\alpha_2+\frac{\rho_{e0}}{\rho_0}(\nabla-1)\right)(\hat{\mathbf{g}}_0\cdot\hat{\mathbf{n}}_0)\right](\hat{\mathbf{g}}_0\cdot\hat{\mathbf{n}}_0) \\
& +\;\frac{C_D\rho_{e0}\mathrm{sgn}(\mathbf{v}_{e0}\cdot\hat{\mathbf{n}}_0)(\mathbf{v}_{e0}\cdot\hat{\mathbf{n}}_0)^2}{\pi a_0\rho_0}\Bigg[\frac{2}{(\mathbf{v}_{e0}\cdot\hat{\mathbf{n}}_0)}\left((\hat{\mathbf{x}}\cdot\hat{\mathbf{n}}_0)w_x-(\hat{\mathbf{g}}_0\cdot\hat{\mathbf{n}}_0)w_z\right) \\
& -\;\frac{1}{H_{pe}}\left(\nabla\,-\,1\,-\,\frac{\alpha_2}{2}\right)(\hat{\mathbf{g}}_0\cdot\hat{\mathbf{n}}_0) \;-\; \frac{\alpha_1}{2R_0}\Bigg]\Bigg\} \\
+\;\varepsilon'\Bigg\{ & -g_0\left(1-\frac{\rho_{e0}}{\rho_0}\right)(\hat{\mathbf{g}}_0\cdot\hat{\mathbf{l}}_0) \;-\; \frac{2C_D\rho_{e0}\mathrm{sgn}(\mathbf{v}_{e0}\cdot\hat{\mathbf{n}}_0)}{\pi a_0\rho_0}(\mathbf{v}_{e0}\cdot\hat{\mathbf{n}}_0)(\mathbf{v}_{e0}\cdot\hat{\mathbf{l}}_0)\Bigg\} \\
+\;\varepsilon''\Bigg\{ & \frac{2p_0}{\rho_0\beta}\Bigg\} \\
-\;\dot{\varepsilon}\Bigg\{ & \frac{2C_D\rho_{e0}(\mathbf{v}_{e0}\cdot\hat{\mathbf{n}}_0)\mathrm{sgn}(\mathbf{v}_{e0}\cdot\hat{\mathbf{n}}_0)}{\pi a_0\rho_0}\Bigg\}.
\end{aligned} \tag{5.47}$$

In the case of a non-constant molecular weight, the term $(1-\nabla)/H_{pe}$ has to be replaced by $1/H_{\rho e}$ (cf. Eq. 5.25). A form of Eqs. (5.45/5.47) which is more convenient for our purposes is obtained below by considering the limit $\beta \gg 1$ and a suitable non-dimensionalization.

5.4 Non-dimensionalization and the case $\beta \gg 1$

As we have discussed in Sec. 5.2, the value of β for equipartition flux tubes in the deep layers of the solar convection zone is very large. Having this application in mind, it is convenient to rewrite and simplify Eqs. (5.45/47) in the limit $\beta \gg 1$ and to introduce non-dimensional quantities. As units for all quantities we use their values in the interior of the flux tube at the reference level, $z = z_m$, which has already been defined in Eq. (5.13). As length scale we choose the internal scale height, $H_{pm} \equiv H_{p0}(z_m)$, and the units of magnetic field, pressure, density etc. are defined by $B_m \equiv B_0(z_m)$, $p_m \equiv p_0(z_m)$, $\rho_m \equiv \rho_0(z_m)$ etc., respectively. As time unit, τ, we take, similar to Spruit and van Ballegooijen (1982)

$$\tau \;=\; \left(\frac{\beta_m H_{pm}}{g_m}\right)^{1/2} \tag{5.48}$$

with $\beta_m = 8\pi p_m/B_m^2$. It is easy to see that τ is $\sqrt{2}$ times the Alfvén travel time across one scale height. For values of β_m of the order $10^5 ... 10^7$, $H_{pm} = 10^9$ cm, $g_m = 6 \cdot 10^4$ cm^2$\cdot$s^{-1} we find $\tau = 10^5 ... 10^6$s $\approx$ 1...2 days. The velocity unit is defined as $V = H_{pm}/\tau = v_A/\sqrt{2}$ where $v_A = B_m/\sqrt{4\pi\rho_m}$ is the Alfvén speed at the reference height. Since Eqs. (5.45/47) are linear and homogeneous, we can separate the time dependence by writing $f \propto \exp(i\omega t)$ for all quantities where ω is a (generally complex) frequency. This leads to

$$(\ddot{\eta}, \ddot{\varepsilon}) \;=\; -\omega^2(\eta, \varepsilon)\,. \tag{5.49}$$

We insert Eq. (5.49) into Eqs. (5.45/47) and take the limit $\beta \gg 1$ such that only terms of order unity and order β^{-1} are retained. It turns out that the terms of order unity cancel. Consequently, non-dimensionalization by multiplication of the resulting equations with $\tau^2 = \beta_m H_{pm}/g_m$ leads to terms of order unity and to terms of the form $\beta\delta$, βr, and $\beta(1-\rho_{e0}/\rho_0)$ which are also of order unity (δ is the superadiabaticity of the external gas and r is defined in Eq. 5.5). For example, a flux tube in temperature equilibrium with its surroundings ($T_0 = T_{e0}$) has $\beta(1 - \rho_{e0}/\rho_0) = -1$ and, using a standard mixing-length model, Spruit and van Ballegooijen (1982) found a value of $\beta\delta = 3.6$ for an equipartition flux tube in the deep parts of the solar convection zone. Thus for $\beta\delta \ll 1$ we have fields strong compared to the equipartition value, for $\beta\delta \gg 1$ we have weak fields.

We give some examples of how the transformation of the coefficients in Eqs. (5.45/47) is carried out but avoid a presentation of the whole calculation. The algebra is straightforward although lengthy and tedious, filling dozens of pages. Let us first write down the quantities α_1 and α_2 up to first order in β^{-1} (cf. Eq. 5.44), viz.

$$\begin{aligned} \alpha_1 \;&=\; 1 \;-\; \frac{2}{\beta\gamma} \;+\; O(\beta^{-2}) \\ \alpha_2 \;&=\; \frac{1}{\gamma} \;+\; \frac{1}{\beta\gamma}\left(1 - \frac{2}{\gamma}\right) \;+\; O(\beta^{-2})\,. \end{aligned} \tag{5.50}$$

It is easy to show that for α_1 and α_2 the operations of taking the limit $\beta \gg 1$ and taking the derivative with respect to l_0 can be interchanged. This simplifies the calculation of the coefficients which contain derivatives of these quantities. We now consider the first coefficient on the r.h.s. of Eq. (5.45) and use Eq. (5.50) to obtain the limit for large β:

$$-(\alpha_1 - 1)\frac{\gamma p_0}{\rho_0}\frac{R_0'}{R_0^2} \;=\; \frac{B_0^2}{4\pi\rho_0}\,\frac{R_0'}{R_0^2} \;+\; O\left(\beta^{-2}\right). \tag{5.51}$$

The non-dimensional form is found by multiplication with $\beta_m H_{pm}/g_m$ which yields

$$\frac{B_0^2}{4\pi\rho_0}\frac{R_0'}{R_0^2}\cdot\frac{8\pi p_m H_{pm}}{B_m^2 g_m} = \frac{2\tilde{B}_0^2}{\tilde{\rho}_0}\frac{\tilde{R}_0'}{\tilde{R}_0^2}. \tag{5.52}$$

The tilde denotes dimensionless quantities (e.g. $\tilde{\rho}_0 = \rho_0/\rho_m$) and we have used the hydrostatic relation $p_m/g_m = \rho_m H_{pm}$. A similar procedure is carried out for all other coefficients. Sometimes it is helpful to use the relation between the derivative along the flux tube and the derivative with respect to z for quantities which only depend on height such as ρ_0, p_0 and B_0:

$$f' = \hat{\mathbf{l}}_0\cdot\nabla f = -(\hat{\mathbf{g}}_0\cdot\hat{\mathbf{l}}_0)\frac{df}{dz}. \tag{5.53}$$

An often needed quantity is the z-derivative of a scale height (external or internal) which can be written for the case of constant mean molecular weight, $\bar{\mu}$, in the form

$$\frac{dH_p}{dz} = \frac{d}{dz}\left(\frac{\mathcal{R}T}{\bar{\mu}g}\right) = \frac{\mathcal{R}}{\bar{\mu}g}\frac{dT}{dz} + \frac{\mathcal{R}T}{\bar{\mu}}\frac{d}{dz}\left(\frac{1}{g}\right) = -\nabla - \frac{sH_p}{z} \tag{5.54}$$

where we have used the equation of state for a perfect gas. $\mathcal{R}$ is the gas constant and T denotes the temperature. Another helpful relation is given by the condition of internal hydrostatic equilibrium, i.e. $p_0/H_{p0} = \rho_0 g_0$. We give another example for the transformation of a coefficient which is not quite straightforward. Consider the large β limit for the third term on the r.h.s. of Eq. (5.45):

$$\frac{1}{\rho_0}\left[\frac{\alpha_2 p_0'}{H_{pe}} - \left(\frac{\gamma p_0\alpha_2}{H_{pe}}\right)'\right] \rightarrow \frac{1}{\rho_0}\left\{\left[\frac{1}{\gamma}+\frac{1}{\beta\gamma}\left(1-\frac{2}{\gamma}\right)\right]\frac{p_0'}{H_{pe}} - \left[\frac{\gamma p_0}{H_{pe}}\left(\frac{1}{\gamma}+\frac{1}{\beta\gamma}\left(1-\frac{2}{\gamma}\right)\right)\right]'\right\}$$
$$= \frac{1}{\rho_0}\left\{\frac{p_0'}{\gamma H_{pe}} + \frac{p_0'}{\beta\gamma H_{pe}}\left(1-\frac{2}{\gamma}\right) - \left(\frac{p_0}{H_{pe}}\right)' - \left[\frac{p_0}{\beta H_{pe}}\left(1-\frac{2}{\gamma}\right)\right]'\right\}. \tag{5.55}$$

We denote the superadiabaticity of the external gas by $\delta = \nabla - \nabla_{ad}$, take $\nabla_{ad} = (\gamma-1)/\gamma$, such that $1/\gamma = 1 - \nabla + \delta$ and write using Eqs. (5.53/54)

$$\frac{p_0'}{\gamma H_{pe}} - \left(\frac{p_0}{H_{pe}}\right)' = -(\hat{\mathbf{g}}_0\cdot\hat{\mathbf{l}}_0)\left[\frac{\delta}{H_{pe}}\frac{dp_0}{dz} + \nabla\frac{p_0}{H_{pe}^2}\left(\frac{H_{pe}}{H_{p0}}-1\right) - \frac{p_0 s}{H_{pe}z_0}\right]. \tag{5.56}$$

Inserting Eq. (5.56) and using $dp_0/dz = -p_0/H_{p0} = -\rho_0 g_0$ we find for the r.h.s. of Eq. (5.55):

$$\begin{aligned}
... &= -(\hat{\mathbf{g}}_0\cdot\hat{\mathbf{l}}_0)\frac{1}{\rho_0}\left\{-\frac{\delta p_0}{H_{pe}H_{p0}} + \nabla\frac{p_0}{H_{pe}^2}\left(\frac{H_{pe}}{H_{p0}}-1\right) - \frac{p_0 s}{H_{pe}z_0}\right.\\
&\qquad \left. -\left(1-\frac{2}{\gamma}\right)\frac{p_0}{\beta\gamma H_{pe}H_{p0}} - \left(1-\frac{2}{\gamma}\right)\left[\frac{1}{H_{pe}}\frac{d}{dz}\left(\frac{p_0}{\beta}\right) + \frac{p_0}{\beta}\frac{d}{dz}\left(\frac{1}{H_{pe}}\right)\right]\right\}\\
&= (\hat{\mathbf{g}}_0\cdot\hat{\mathbf{l}}_0)\left\{\frac{g_0}{H_{pe}}\left[\delta - \nabla\left(1-\frac{H_{p0}}{H_{pe}}\right) + \frac{sH_{p0}}{z_0}\right]\right.\\
&\qquad \left. + \left(1-\frac{2}{\gamma}\right)\frac{1}{\rho_0 H_{pe}}\left[\frac{d}{dz}\left(\frac{B_0^2}{8\pi}\right) + \frac{B_0^2}{8\pi H_{pe}}\left(\frac{H_{pe}}{\gamma H_{p0}} + \nabla + \frac{sH_{pe}}{z_0}\right)\right]\right\}.
\end{aligned} \tag{5.57}$$

By multiplication with $\beta_m H_{pm}/g_m$ which can be rewritten as

$$\frac{\beta_m H_{pm}}{g_m} \;=\; \frac{\beta_m H_{pm}}{g_m \beta}\beta \;=\; \frac{H_{pm}^2 \rho_m B_0^2}{g_0 H_{p0} \rho_0 B_m^2}\beta \tag{5.58}$$

and

$$\frac{\beta_m H_{pm}}{g_m} \;=\; \frac{8\pi H_{pm}^2 \rho_m}{B_m^2}, \tag{5.59}$$

Eq. (5.57) is transferred to non-dimensional form:

$$\begin{aligned} ... \;\rightarrow\; (\hat{\mathbf{g}}_0 \cdot \hat{\mathbf{l}}_0)\frac{\tilde{B}_0^2}{\tilde{\rho}_0 \tilde{H}_{pe}} \Bigg\{ \frac{1}{\tilde{H}_{p0}} \left[\beta\delta \;-\; \nabla\beta \left(1 - \frac{\tilde{H}_{po}}{\tilde{H}_{pe}}\right) \;+\; \frac{\beta s \tilde{H}_{p0}}{\tilde{z}_0} \right] \\ + \left(1 - \frac{2}{\gamma}\right) \left[\frac{1}{\tilde{B}_0^2}\frac{d\tilde{B}_0^2}{d\tilde{z}} + \frac{1}{\tilde{H}_{pe}} \left(\frac{\tilde{H}_{pe}}{\gamma \tilde{H}_{p0}} + \nabla + \frac{s\tilde{H}_{pe}}{\tilde{z}_0} \right) \right] \Bigg\}. \end{aligned} \tag{5.60}$$

In what follows we shall omit the tildes and tacitly assume that all quantities are non-dimensional unless the contrary is explicitly stated. The procedures described above have been applied to each term in Eqs. (5.45/47). For equipartition flux tubes in the deep solar convection zone we have $H_{pe}/H_{p0} - 1 = O(\beta^{-1})$, $\rho_{e0}/\rho_0 - 1 = O(\beta^{-1})$ and we can take $H_{pe}/H_{p0} \approx 1$, $\rho_{e0}/\rho_0 \approx 1$ unless such a term is multiplied by β. Under these conditions we have

$$\beta \left(1 - \frac{H_{pe}}{H_{p0}}\right) \;+\; 1 \;=\; \beta \left(\frac{\rho_{e0}}{\rho_0} - 1 \right) \;+\; O(\beta^{-2}). \tag{5.61}$$

Another useful relation is

$$\frac{1}{B_0^2}\frac{dB_0^2}{dz} \;=\; \frac{8\pi}{B_0^2}\frac{d}{dz}(p_{e0} - p_0) \;=\; \frac{\beta}{H_{p0}} \left(1 - \frac{\rho_{e0}}{\rho_0}\right). \tag{5.62}$$

After some tedious algebra, Eqs. (5.45/5.47) in their final form are given by

$$\begin{aligned} -\omega^2 \frac{\rho_0}{B_0^2}\eta \;=\; \varepsilon \Bigg\{ &(\hat{\mathbf{g}}_0 \cdot \hat{\mathbf{l}}_0) \left[\frac{1}{R_0 H_{p0}} \beta \left(1 - \frac{\rho_{e0}}{\rho_0}\right) - \frac{2}{R_0^2}\frac{dR_0}{dz} \right] \\ &+ (\hat{\mathbf{g}}_0 \cdot \hat{\mathbf{l}}_0)(\hat{\mathbf{g}}_0 \cdot \hat{\mathbf{n}}_0) \left(-\frac{s}{z_0 H_{p0}} \left[\beta \left(1 - \frac{\rho_{e0}}{\rho_0}\right) + \frac{2}{\gamma} \right] \;+\; \frac{1}{H_{p0}^2} \left[\beta\delta - \frac{1}{\gamma} - \frac{\beta}{\gamma} \left(1 - \frac{\rho_{e0}}{\rho_0}\right) \right] \right) \Bigg\} \\ &+ \; \varepsilon' \left\{ -\frac{2}{R_0} \;+\; (\hat{\mathbf{g}}_0 \cdot \hat{\mathbf{n}}_0) \frac{1}{H_{p0}} \left[\beta \left(1 - \frac{\rho_{e0}}{\rho_0}\right) + \frac{2}{\gamma} \right] \right\} \\ &+ \; \eta \Bigg\{ (\hat{\mathbf{g}}_0 \cdot \hat{\mathbf{l}}_0)^2 \left(-\frac{s}{z_0 H_{p0}} \left[\beta \left(1 - \frac{\rho_{e0}}{\rho_0}\right) + \frac{2}{\gamma} \right] \;+\; \frac{1}{H_{p0}^2} \left[\beta\delta - \frac{1}{\gamma} - \frac{\beta}{\gamma} \left(1 - \frac{\rho_{e0}}{\rho_0}\right) \right] \right) \\ &+ (\hat{\mathbf{g}}_0 \cdot \hat{\mathbf{n}}_0) \frac{1}{R_0 H_{p0}} \left[\beta \left(1 - \frac{\rho_{e0}}{\rho_0}\right) + \frac{2}{\gamma} \right] \Bigg\} \\ &+ \; \eta' \left\{ -(\hat{\mathbf{g}}_0 \cdot \hat{\mathbf{l}}_0) \frac{1}{H_{p0}} \beta \left(1 - \frac{\rho_{e0}}{\rho_0}\right) \right\} \;+\; 2\eta'' \end{aligned} \tag{5.63}$$

for the longitudinal displacement and

$$
\begin{aligned}
-\omega^2 \frac{\rho_0}{B_0^2}\varepsilon \;=\; & \eta \left\{ (\hat{\mathbf{g}}_0 \cdot \hat{\mathbf{l}}_0) \left[\frac{2}{R_0^2}\frac{dR_0}{dz} + \frac{2}{\gamma R_0 H_{p0}} - \frac{1}{R_0 H_{p0}}\beta \left(1 - \frac{\rho_{e0}}{\rho_0}\right) \right] \right. \\
& \quad + (\hat{\mathbf{g}}_0 \cdot \hat{\mathbf{l}}_0)(\hat{\mathbf{g}}_0 \cdot \hat{\mathbf{n}}_0)\frac{1}{H_{p0}^2}\left[\beta\delta - \frac{sH_{p0}}{z_0} + \frac{1}{\gamma}\left(1 - \frac{2}{\gamma}\right)\right] \\
& \quad \left. + \frac{\beta r m}{H_{p0}} \left(\frac{2}{\mathbf{v}_{e0}\cdot\hat{\mathbf{n}}_0}\left[(\hat{\mathbf{x}}\cdot\hat{\mathbf{l}}_0)w_x - (\hat{\mathbf{g}}_0\cdot\hat{\mathbf{l}}_0)w_z - \frac{\mathbf{v}_{e0}\cdot\hat{\mathbf{l}}_0}{R_0}\right] + \frac{1}{2\gamma H_{p0}}(\hat{\mathbf{g}}_0\cdot\hat{\mathbf{l}}_0) \right) \right\} \\
& + \eta' \left\{ \frac{4}{R_0} - (\hat{\mathbf{g}}_0 \cdot \hat{\mathbf{n}}_0)\frac{2}{\gamma H_{p0}} + \frac{\beta r m}{2H_{p0}} \right\} \\
& + \varepsilon \left\{ -\frac{2}{R_0^2} + (\hat{\mathbf{g}}_0 \cdot \hat{\mathbf{n}}_0)\frac{4}{\gamma R_0 H_{p0}} + (\hat{\mathbf{g}}_0 \cdot \hat{\mathbf{n}}_0)^2 \frac{1}{H_{p0}^2}\left[\beta\delta + \frac{1}{\gamma}\left(1 - \frac{2}{\gamma}\right) - \frac{sH_{p0}}{z_0}\beta\left(1 - \frac{\rho_{e0}}{\rho_0}\right)\right] \right. \\
& \quad \left. + \frac{\beta r m}{H_{p0}} \left(\frac{2}{\mathbf{v}_{e0}\cdot\hat{\mathbf{n}}_0}\left[(\hat{\mathbf{x}}\cdot\hat{\mathbf{n}}_0)w_x - (\hat{\mathbf{g}}_0\cdot\hat{\mathbf{n}}_0)w_z \right] + \frac{1}{2\gamma H_{p0}}(\hat{\mathbf{g}}_0\cdot\hat{\mathbf{n}}_0) - \frac{1}{2R_0} \right) \right\} \\
& + \varepsilon' \left\{ -(\hat{\mathbf{g}}_0 \cdot \hat{\mathbf{l}}_0)\frac{1}{H_{p0}}\beta\left(1 - \frac{\rho_{e0}}{\rho_0}\right) - \frac{2\beta r m(\mathbf{v}_{e0}\cdot\hat{\mathbf{l}}_0)}{H_{p0}(\mathbf{v}_{e0}\cdot\hat{\mathbf{n}}_0)} \right\} \\
& + 2\varepsilon'' - i\omega\varepsilon \frac{2\beta r m}{H_{p0}(\mathbf{v}_{e0}\cdot\hat{\mathbf{n}}_0)}
\end{aligned}
\tag{5.64}
$$

for the displacement in normal direction. In Eq. (5.64) we have abbreviated $\mathrm{sgn}(\mathbf{v}_{e0}\cdot\hat{\mathbf{n}}_0) \equiv m$ and used the equilibrium condition, Eq. (5.4), in some places. In the special case of a horizontal flux tube in static equilibrium and uniform gravity ($R_0 \to \infty$, $(\hat{\mathbf{g}}_0 \cdot \hat{\mathbf{l}}_0) = 0$, $(\hat{\mathbf{g}}_0 \cdot \hat{\mathbf{n}}_0) = -1$, $s = 0$, $\mathbf{v}_e = 0$, $\rho_0 = \rho_{e0}$, $B_0^2 = \rho_0 = 1$) Eqs. (5.63/64) take the form

$$
\begin{aligned}
-\omega^2 \eta \;&=\; 2\eta'' - \varepsilon' \frac{2}{\gamma} \\
-2\omega^2 \varepsilon \;&=\; 2\varepsilon'' + \eta' \frac{2}{\gamma} + \varepsilon\left(\beta\delta + \frac{1}{\gamma} - \frac{2}{\gamma^2}\right).
\end{aligned}
\tag{5.65}
$$

In order to compare with the result of Spruit and van Ballegooijen (1982) we have multiplied the inertial term in the equation for ε by a factor 2 intending to describe the enhanced inertia of the flux tube with respect to transversal motions in the same way as done by these authors. Since the coefficients are constant we are permitted to write $(\eta, \varepsilon) \propto \exp(ikl_0)$ with wavenumber k in the longitudinal (here: horizontal) direction. Inserting this into Eq. (5.65) we obtain the dispersion relation

$$
\omega^4 + \omega^2 \left[-3k^2 + \frac{\beta\delta}{2} + \frac{1}{2\gamma}\left(1 - \frac{2}{\gamma}\right)\right] + 2k^2\left(k^2 - \frac{\beta\delta}{2} - \frac{1}{2\gamma}\right) = 0 \tag{5.66}
$$

which is identical to the relation found by Spruit and van Ballegooijen (1982, their Eq. 39).

5.5 Symmetric form for static equilibrium

If we ignore the drag force there is no dissipation in the system and the force operator is self-adjoint (Spruit, 1981b). Hence, in the case $\mathbf{v}_{e0} = 0$ (static equilibrium) the perturbation equations (5.63/64) must lead to a self-adjoint eigenvalue problem with real eigenvalues.* Symbolically, we can write Eqs. (5.64/65) in the form

$$-\omega^2 \begin{pmatrix} \eta \\ \varepsilon \end{pmatrix} = \mathbf{F} \begin{pmatrix} \eta \\ \varepsilon \end{pmatrix} \tag{5.67}$$

where the operator $\mathbf{F}$ is defined by

$$\mathbf{F} \begin{pmatrix} \eta \\ \varepsilon \end{pmatrix} = \begin{pmatrix} A\varepsilon + B\varepsilon' + C\eta + D\eta' + E\eta'' \\ F\eta + G\eta' + H\varepsilon + D\varepsilon' + E\varepsilon'' \end{pmatrix}. \tag{5.68}$$

The functions $A(l_0), ..., H(l_0)$ can be obtained from the r.h.s. of Eqs. (5.64/65) by multiplication with B_0^2/ρ_0 and setting $\mathbf{v}_{e0} = 0$. Using the equilibrium condition given by Eq. (5.4) is readily shown that in this (static) case we have $B = -G$. However, the operator $\mathbf{F}$ is not yet written in a form in which its self-adjointness becomes apparent. Such a form is necessary for application of variational methods like the energy principle (Bernstein et al., 1958). It is also useful for numerical calculations since it leads to symmetric matrices which are much easier to deal with. A symmetric form can be obtained by transforming the eigenvector as

$$\begin{pmatrix} \eta \\ \varepsilon \end{pmatrix} = \begin{pmatrix} ax \\ by \end{pmatrix} \tag{5.69}$$

where x and y are the new variables and the functions $a(l_0)$ and $b(l_0)$ are determined such that the eigenvalue problem given by Eqs. (5.67/68) attains the form

$$-\omega^2 \begin{pmatrix} x \\ y \end{pmatrix} = \begin{pmatrix} Ky + \frac{1}{2}[(By)' + By'] + Mx + \frac{1}{2}[(Ex)'' + Ex''] \\ Kx - \frac{1}{2}[(Bx)' + Bx'] + Ny + \frac{1}{2}[(Ey)'' + Ey''] \end{pmatrix} \tag{5.70}$$

which possesses the same eigenvalues as Eqs. (5.67/68). Inserting Eq. (5.69) into Eq. (5.67) leads to the following pair of equations:

$$\begin{aligned} -\omega^2 x = {} & y\frac{b}{a}\left(A + B\frac{b'}{b} - \frac{1}{2}B'\right) + \frac{b}{2a}[(By)' + By'] + x\left(C + D\frac{a'}{a} + E\frac{a''}{a} - \frac{1}{2}E''\right) \\ & + x'\left(D + 2E\frac{a'}{a} - E'\right) + \frac{1}{2}[(Ex)'' + Ex''] \end{aligned} \tag{5.71}$$

$$\begin{aligned} -\omega^2 y = {} & x\frac{a}{b}\left(F - B\frac{a'}{a} + \frac{1}{2}B'\right) - \frac{a}{2b}[(Bx)' + Bx'] + y\left(H + D\frac{b'}{b} + E\frac{b''}{b} - \frac{1}{2}E''\right) \\ & + y'\left(D + 2E\frac{b'}{b} - E'\right) + \frac{1}{2}[(Ey)'' + Ey'']. \end{aligned} \tag{5.72}$$

* Since the drag force is quadratic in the relative velocity between flux tube and environment, its perturbation vanishes if $\mathbf{v}_{e0} = 0$.

By comparison with the desired form given by Eq. (5.70) we find that the functions $a(l_0)$ and $b(l_0)$ are determined by the requirement that the terms which multiply x' in Eq. (5.71) and y' in Eq. (5.72), respectively, must vanish:

$$\begin{aligned} D \,+\, 2E\,\frac{a'}{a} - E' \;&=\; 0 \\ D \,+\, 2E\,\frac{b'}{b} - E' \;&=\; 0\,. \end{aligned} \tag{5.73}$$

Consequently, we have $a'/a = b'/b$ and since a and b may be multiplied by any constant number we can take $a \equiv b$ without loss of generality. Eq. (5.73) may be integrated to give

$$\ln a \;=\; \frac{1}{2}\ln E \;-\; \int \frac{D}{2E}\,dl_0\,. \tag{5.74}$$

The coefficient functions M and N in Eq. (5.70) are determined using Eq. (5.73) which leads to the condition

$$\begin{aligned} M \;&=\; C \,+\, \frac{(E')^2 - D^2}{4E} \,+\, E\left(\frac{E'-D}{2E}\right)' - \frac{E''}{2} \\ N \;&=\; H \,+\, \frac{(E')^2 - D^2}{4E} \,+\, E\left(\frac{E'-D}{2E}\right)' - \frac{E''}{2}. \end{aligned} \tag{5.75}$$

The requirement that the function which multiplies y in the first term on the r.h.s. of Eq. (5.71) is identical to that which multiplies x in the first term on the r.h.s. of Eq. (5.72) in order to conform with Eq. (5.70) leads to

$$A \,+\, B\frac{b'}{b} \,-\, \frac{B'}{2} \;=\; K \;=\; F \,-\, B\frac{a'}{a} \,+\, \frac{B'}{2}\,. \tag{5.76}$$

This implies the compatibility relation

$$F \,-\, A \;=\; \frac{B(E'-D)}{E} \,-\, B' \tag{5.77}$$

which must be fulfilled if the system is self-adjoint. Hence, we may use Eq. (5.77) in order to check the correctness of the algebraic manipulations and the consistency of the approximation which led to Eqs. (5.63/64). It turns out, after some lengthy algebra, that Eq. (5.77) indeed is valid for our problem, i.e. the self-adjointness of the problem is reflected in the symmetric structure of the resulting system of equations. Defining

$$\xi \;\equiv\; \begin{pmatrix} x \\ y \end{pmatrix}$$

it is easy to show that Eq. (5.70) indeed is selfadjoint, i.e. the equality

$$\int \tilde{\xi}\cdot\mathbf{G}(\xi)\,dV \;=\; \int \xi\cdot\mathbf{G}(\tilde{\xi})\,dV \tag{5.78}$$

holds. **G** denotes the operator on the r.h.s. of Eq. (5.70), the tilde indicates the complex conjugate, and the integration is taken over an appropriate volume. Since integrations by parts are necessary to demonstrate the validity of Eq. (5.78) the volume of integration must be chosen large enough such that the displacements can be assumed to vanish at the boundaries.

5.6 Horizontal tubes with vertical external flow

The preceding sections give a basis for the determination of the stability properties of rather general flux tube equilibrium structures. For realistic convection zone models and flow patterns an equilibrium can only be determined by numerical means (e.g. van Ballegooijen, 1982a; Anton, 1984; Anton and Schüssler, unpublished) and thus the perturbation equations, Eqs. (5.63/64), have to be transformed into a numerically tractable matrix eigenvalue problem. Such an undertaking is outside the scope of the present investigation and has to be deferred to future work. In what follows we shall consider a couple of analytically tractable cases instead to which we nevertheless attribute some general relevance.

As a first simple application of the formalism we consider the case $R_0 \to \infty$, $(\hat{\mathbf{g}}_0 \cdot \hat{\mathbf{l}}_0) = 0$, $(\hat{\mathbf{g}}_0 \cdot \hat{\mathbf{n}}_0) = -1$, $s = 0$, $\mathbf{v}_e = v(z)\hat{\mathbf{z}}$, i.e. a horizontal, straight flux tube whose equilibrium is determined by a balance between the buoyancy and drag forces (cf. Eq. 5.4/5):

$$\beta \left(1 - \frac{\rho_{e0}}{\rho_0}\right) = \beta r m \,. \tag{5.79}$$

Here we have $m = \mathrm{sgn}(\mathbf{v}_{e0} \cdot \hat{\mathbf{n}}_0) = \mathrm{sgn}(v(z_0))$, i.e. $m = 1$ describes an upflow, $m = -1$ a downflow. Defining

$$\frac{C_D v_0^2}{\pi a_0 g_0} \equiv q \tag{5.80}$$

with $v_0 = |v(z_0)|$ we obtain the equilibrium density contrast as function of the positive number q as

$$1 - \frac{\rho_{e0}}{\rho_0} = \frac{q}{m+q} \,. \tag{5.81}$$

It is clear from Eq. (5.81) that q is limited to $q < 1$ in the case of a downflow ($m = -1$) since the tube becomes completely evacuated for $q \to 1$ and the buoyancy force cannot be increased beyond that limit. On the other hand, for an upflow ($m = 1$) the range of values for q is not restricted because the internal density can be made large enough to balance any upward directed drag force.

If we insert Eq. (5.79) into the perturbation equations, Eqs. (5.63/64), and have regard to the properties of the equilibrium as described in the beginning of this section we obtain the following pair of equations:

$$-\omega^2 \eta = -\varepsilon' \left(\beta r m + \frac{2}{\gamma}\right) + 2\eta'' \tag{5.82}$$

$$\begin{aligned} -\omega^2 \varepsilon = {} & \eta' \left(\frac{\beta r m}{2} + \frac{2}{\gamma}\right) + \varepsilon \left[\beta\delta + \frac{1}{\gamma}\left(1 - \frac{2}{\gamma}\right) + \beta r m \left(\frac{2}{v_0}\frac{dv_0}{dz} - \frac{1}{2\gamma}\right)\right] \\ & + 2\varepsilon'' - i\omega\varepsilon \frac{2\beta r}{v_0} \end{aligned} \tag{5.83}$$

Here we have written $|v(z_0)| \equiv v_0$ and the notation dv_0/dz has been used to abbreviate $d|v(z)|/dz$ taken at $z = z_0$. Let us first consider displacements which do not depend on the horizontal coordinate $l_0 \equiv x$. All derivatives vanish in this case and we find $\eta \equiv 0$ from Eq. (5.82). The equation for ε is transformed into the dispersion relation

$$\omega^2 \;-\; i\omega\frac{2\beta r}{v_0} \;+\; \left[\beta\delta + \frac{1}{\gamma}\left(1 - \frac{2}{\gamma}\right) + \beta r m \left(\frac{2}{v_0}\frac{dv_0}{dz} - \frac{1}{2\gamma}\right)\right] \;=\; 0\,. \tag{5.84}$$

Writing

$$\frac{\beta r}{v_0} \;\equiv\; S \geq 0 \tag{5.85}$$

and

$$\beta\delta + \frac{1}{\gamma}\left(1 - \frac{2}{\gamma}\right) + \beta r m \left(\frac{2}{v_0}\frac{dv_0}{dz} - \frac{1}{2\gamma}\right) \;\equiv\; T \tag{5.86}$$

we find from Eq. (5.84)

$$\omega_\pm \;=\; iS \;\pm\; \left(-S^2 - T\right)^{1/2} \tag{5.87}$$

and by multiplication with the imaginary unit we obtain

$$i\omega_\pm \;=\; -S \;\mp\; \left(S^2 + T\right)^{1/2}. \tag{5.88}$$

We now have to consider two cases. Firstly, if $S^2+T<0$, the square root in Eq. (5.88) is imaginary and the growth rate (real part of $i\omega_\pm$) becomes equal to $-S$. Consequently, we have a damped oscillation in this case and the equilibrium is stable. In the second case, $S^2+T>0$, both the square root and $i\omega_\pm$ are real. Depending on the sign of the latter, the perturbation will grow or decay monotonically. It is easy to see that the stability in this case depends solely on the sign of T: If $T<0$ we have $i\omega_\pm<0$ and the displacement decays, if $T>0$ we have $i\omega_->0$ and a monotonic growth of the perturbation ensues. Combining the results for both cases we find

$$T \begin{cases} >0 \;:\; \text{monotonic growth} \\ <0 \;:\; \begin{cases} S^2+T<0 \;:\; & \text{damped oscillation} \\ S^2+T>0 \;:\; & \text{monotonic decay} \end{cases} \end{cases}$$

Hence, the stability of the flux tube depends only on the sign of T while the imaginary term in Eq. (5.83) influences the way in which stable perturbations decay, monotonically or oscillatory. This behavior is plausible from the fact that this term, being proportional to $\dot{\varepsilon}$, describes the drag force caused by the perturbation itself and therefore only has a damping effect. Similar to a damped oscillator the case of 'creeping motion' is achieved if the damping rate (described by S) exceeds a critical value. The equilibrium is unstable if $T>0$, i.e. if the superadiabaticity satisfies the inequality

$$\beta\delta \;>\; \frac{1}{\gamma}\left(\frac{2}{\gamma} - 1\right) + \beta r m \left(\frac{1}{2\gamma} - \frac{2}{v_0}\frac{dv_0}{dz}\right)\,. \tag{5.89}$$

Consequently, positive terms on the r.h.s. of Eq. (5.89) have a stabilizing influence. For constant velocity, i.e. $dv_0/dz=0$, we find that an upflow ($m=1$) has a stabilizing effect while a downflow ($m=-1$) is destabilizing. This behavior is caused by the changes in flux tube radius and external density. An upward displacement leads to an expansion of the tube and a decrease of external density. Consequently, the drag force decreases (cf. Eq. 5.33). Similarly, for a downward displacement we find an increase of the drag force. If we now have a flux tube which is in equilibrium with a downflow, for both upward and downward displacements the perturbation of the (downward) drag force tends to increase the displacement and thus favors instability while the reverse is true for an upflow.

For $dv_0/dz \neq 0$, the situation is more complicated. Whether the change of velocity with height acts stabilizing or destabilizing depends on its sign and on the direction of the flow. For example, an upflow ($m = 1$) whose velocity increases with height ($dv_0/dz > 0$) leads to a perturbation of the drag force which tends to increase an initial displacement and thus favors instability. The influence of the velocity term on the stability properties in the case of purely vertical displacements is summarized Tab. 1:

m	dv_0/dz	$1/2\gamma$	$(1/2\gamma) - (2/v_0)(dv_0/dz)$
1	$> 0 \rightarrow$ destabilizing	stabilizing	?
1	$< 0 \rightarrow$ stabilizing	stabilizing	stabilizing
-1	$> 0 \rightarrow$ stabilizing	destabilizing	?
-1	$< 0 \rightarrow$ destabilizing	destabilizing	destabilizing

Tab. 1: Influence of the velocity-related terms in the stability criterion (Eq. 5.89) for horizontal magnetic flux tubes and purely vertical displacement (infinite longitudinal wavelength).

The combined effect of both terms in Eq. (5.89) which are affected by the external velocity is indicated in the last column. A question mark indicates that one term is stabilizing and the other destabilizing such that it depends on their relative sizes which one dominates. In dimensionalized form, the term involving the velocity derivative can be written as

$$\frac{2}{\tilde{v}_0}\frac{d\tilde{v}_0}{d\tilde{z}} \;\rightarrow\; \frac{2H_{p0}}{v_0}\frac{dv_0}{dz} \;\equiv\; \frac{2H_{p0}}{H_v} \tag{5.90}$$

where H_v is the scale height of the external velocity. If we assume a flow with constant mass flux density, ρv, and assume further that the temperature varies much more slowly with height than the density, we have $p_0 v_0 = \text{const.}$ and thus $H_{p0} \approx H_v$. The relation between the two terms in the second bracket on the r.h.s. of Eq. (5.89) is then given by

$$\frac{(1/2\gamma)}{(2/v_0)(dv_0/dz)} \;\approx\; \frac{1}{4\gamma} \;=\; \frac{3}{20} \tag{5.91}$$

for $\gamma = 5/3$. We see that for a flow with constant mass flux density the stability properties are mainly determined by the velocity gradient. Since density decreases with height, the flow velocity increases and we see from the table above that an upflow has a destabilizing influence, while a downflow stabilizes.

If we now consider all terms in Eq. (5.89) we find that a flow can stabilize/destabilize a convectively unstable/stable flux tube. For a flux tube in temperature equilibrium ($T_0 = T_{e0}$, $\beta r m = -1$) and a downflow with constant mass flux density instability requires

$$\beta\delta \;>\; \frac{2}{\gamma^2} - \frac{3}{2\gamma} + 2 \;=\; 1.82 \tag{5.92}$$

Since equipartition flux tubes in the deep convection zone of the Sun have $\beta\delta \approx 3.6$ (Spruit and van Ballegooijen, 1982) they cannot be stabilized by a flow of this kind. On the other hand, Eq. (5.92) predicts stability for flux tubes located in a downflow within an overshoot region which have $\beta\delta \leq 0$.

The case of purely vertical displacements which do not depend on the horizontal coordinate treated so far excludes an important destabilizing mechanism, the flow from the crests to the troughs of a wavelike disturbance of the flux tube which is the mechanism for the so-called Parker instability (Parker, 1966). If we allow for a dependence of the displacements η and ε on the horizontal coordinate, x, we may write

$$\eta\,,\varepsilon \;\propto\; e^{ikx} \tag{5.93}$$

with (real) wavenumber k since the coefficients in Eqs. (5.82/83) are constant. Using the symbols η and ε again for the (constant) *amplitudes* of the perturbations we obtain by inserting Eq. (5.93) into Eqs. (5.82/83):

$$-\omega^2\eta \;=\; -ik\varepsilon\left(\beta rm + \frac{2}{\gamma}\right) \;-\; 2k^2\eta \tag{5.94}$$

$$\begin{aligned} -\omega^2\varepsilon \;=\; & ik\eta\left(\frac{\beta rm}{2} + \frac{2}{\gamma}\right) \;+\; \varepsilon\left[\beta\delta + \frac{1}{\gamma}\left(1-\frac{2}{\gamma}\right) + \beta rm\left(\frac{2}{v_0}\frac{dv_0}{dz} - \frac{1}{2\gamma}\right)\right] \\ & -\; 2k^2\varepsilon \;-\; i\omega\varepsilon\frac{2\beta r}{v_0}. \end{aligned} \tag{5.95}$$

This linear, homogeneous system of equations has non-trivial solutions for eigenvalues ω which satisfy the dispersion relation

$$\begin{aligned} (\omega^2 - 2k^2)&\left[\omega^2 - i\omega\frac{2\beta r}{v_0} - 2k^2 + \beta\delta + \frac{1}{\gamma}\left(1-\frac{2}{\gamma}\right) + \beta rm\left(\frac{2}{v_0}\frac{dv_0}{dz} - \frac{1}{2\gamma}\right)\right] \\ & -\; k^2\left(\frac{2}{\gamma} + \frac{\beta rm}{2}\right)\left(\frac{2}{\gamma} + \beta rm\right) \;=\; 0\,. \end{aligned} \tag{5.96}$$

Eq. (5.96) can be written as a fourth order polynomial in $i\omega \equiv \hat{\omega}$ with real coefficients:

$$\hat{\omega}^4 \;+\; A\hat{\omega}^3 \;+\; B\hat{\omega}^2 \;+\; C\hat{\omega} \;+\; D \;=\; 0 \tag{5.97}$$

with

$$\begin{aligned} A \;&=\; \frac{2\beta r}{v_0} \\ B \;&=\; 4k^2 - \beta\delta - \frac{1}{\gamma}\left(1-\frac{2}{\gamma}\right) - \beta rm\left(\frac{2}{v_0}\frac{dv_0}{dz} - \frac{1}{2\gamma}\right) \\ C \;&=\; \frac{4k^2\beta r}{v_0} \\ D \;&=\; 2k^2\left[2k^2 - \beta\delta - \frac{1}{\gamma} - \beta rm\left(\frac{2}{v_0}\frac{dv_0}{dz} + \frac{1}{\gamma}\right) - \frac{(\beta r)^2}{4}\right] \end{aligned}$$

Since the coefficients are real, the roots of this polynomial can be real numbers and pairs of complex conjugates. A positive, real root means monotonic instability, i.e. exponential growth of the perturbation, while a complex root with positive real part represents overstability, i.e. oscillations or waves with exponentially growing amplitude. In order to establish a sufficient condition for monotonic instability we may utilize Descartes' sign rule:

The number of positive, real roots of a fourth order polynomial with real coefficients is smaller than or equal to the number of sign changes in the sequence of its coefficients. The difference is an even number.

Since in our case we have $A \geq 0$ and $C \geq 0$ the number of sign changes is determined by the signs of B and D as indicated in Tab. 2:

Case	B	D	Sign changes	Positive, real roots
1	> 0	< 0	1	1
2	> 0	> 0	0	0
3	< 0	< 0	3	1 or 3
4	< 0	> 0	2	0 or 2

Tab. 2: Estimate of the number of positive, real roots (i.e. monotonically unstable modes) of Eq. (5.97) using the number of sign changes in the sequence of its coefficients (Descartes' rule). Since A and C are positive, this number depends only on the signs of B and D.

In the cases 1 and 3 we have at least one positive root. Consequently, $D < 0$ *is a sufficient condition for monotonic instability.* In case 2 there is no monotonic instability (but possibly overstability) while for case 4 no definite statement can be made at this stage. The condition $D < 0$ can be transformed into a condition for the wavenumber, k:

$$k^2 \ < \ k_0^2 \ \equiv \ \frac{1}{2}\left[\beta\delta + \frac{1}{\gamma} + \beta r m\left(\frac{2}{v_0}\frac{dv_0}{dz} + \frac{1}{\gamma}\right) + \frac{(\beta r)^2}{4}\right] \tag{5.98}$$

Since any value of k is allowed in our cartesian model (in contrast to a spherical system where the wavelength cannot be larger than the circumference), the flux tube is monotonically unstable if only $k_0^2 > 0$, i.e.

$$\beta\delta \ > \ -\frac{1}{\gamma} + \beta r m\left(-\frac{1}{\gamma} - \frac{2}{v_0}\frac{dv_0}{dz}\right) - \frac{(\beta r)^2}{4}\,. \tag{5.99}$$

We immediately see that a flow with constant velocity ($dv_0/dz = 0$) cannot stabilize a tube within a superadiabatic environment: For an upflow ($m = +1$) both remaining velocity terms are negative while it is easy to see that for a downflow ($m = -1$) the r.h.s. of Eq. (5.99) is always negative since $\gamma > 1$. If the flow speed depends on depth, stabilization is possible. A downflow whose speed decreases with depth such that the mass flux density stays constant [$m = -1$, $(2/v_0)(dv_0/dz) = 2$] leads to positive values of the r.h.s. of Eq. (5.99) provided that $0.23 < \beta r < 10.16$, i.e. within a certain range of values for the parameter βr.

Due to the last term in Eq. (5.99) a flux tube is always monotonically unstable for sufficiently large values of βr, irrespective of the flow direction. This is caused by the change of the flux tube radius in the course of a wave-like displacement, a mechanism which can be understood with aid of the heuristic approach followed in Sec. 5.7.3.

For the example discussed in conjunction with the criterion Eq. (5.92) (temperature equilibrium, $T_0 = T_{e0}$, and downflow with constant mass flux density, $\beta r m = -1$) we find from Eq. (5.99) the criterion $\beta\delta > 1.75$ for monotonic instability, i.e. a slightly smaller critical value than that obtained for the case of purely vertical displacements. Generally we find that the condition given in Eq. (5.99) leads to instability for smaller values of the $\beta\delta$, i.e. monotonic instability is easier to excite for wave-like perturbations (even if $k \to 0$) than for those with $k \equiv 0$. This is similar to the case without external flow treated by Spruit and van Ballegooijen (1982) whose results may be recovered by setting $\beta r = 0$. However, in our case flux tubes embedded in a subadiabatic region ($\beta\delta \leq 0$) are stable with respect to wave-like perturbations while in the case without external flow instability results if $\beta\delta > -1/\gamma$.

The general properties of the roots of Eq. (5.97) unfortunately are not as easily obtained as the sufficient condition for positive, real roots. However, since the coefficients A and C result from the imaginary term in Eq. (5.83) which mainly has a damping effect and does not affect the stability conditions for the case $k = 0$, we may conjecture that this is the case for $k \neq 0$ as well. We therefore consider a reduced dispersion relation by setting $A = C = 0$ in Eq. (5.97). The conclusions drawn from the discussion of this equation have been verified by (numerical) determination of the roots of the full equation (5.97).* For $A = C = 0$ Eq. (5.97) is transformed into a biquadratic equation which is readily solved, viz.

$$\hat{\omega}^2 \;=\; -\frac{B}{2} \pm \left(\frac{B^2}{4} - D\right)^{1/2} . \tag{5.100}$$

We see immediately that we recover the sufficient condition for monotonic instability, $D < 0$, since in this case always one solution $\hat{\omega}^2 > 0$ exists. A second possibility for monotonic instability is the case $B < 0$ and $0 \leq D \leq B^2/4$ while the case $B > 0$, $0 \leq D \leq B^2/4$ leads to stable solutions ($\hat{\omega}^2 < 0$). Complex roots which signify oscillatory instability (overstability) appear for $B^2/4 - D < 0$, irrespective of the sign of B. Since we have

$$\frac{B^2}{4} - D \;=\; k^2 \left[\frac{4}{\gamma^2} + \frac{(\beta r)^2}{2} + \frac{3}{\gamma}\beta r m\right] \;+\; \frac{1}{4}\left[\beta\delta + \frac{1}{\gamma}\left(1 - \frac{2}{\gamma}\right) + \beta r m \left(\frac{2}{v_0}\frac{dv_0}{dz} - \frac{1}{2\gamma}\right)\right]^2 \tag{5.101}$$

complex roots exist only if the first term on the r.h.s. is negative. This requires $m = -1$ (downflow) and

$$\frac{2}{\gamma} \;<\; \beta r \;<\; \frac{4}{\gamma} . \tag{5.102}$$

For $\gamma = 5/3$ this range is given by $1.2 < \beta r < 2.4$. If both conditions are satisfied we see from Eq. (5.101) that the wavenumber can always be made large enough to give $B^2/4 - D < 0$. Hence, the condition for overstability is $k^2 > k_1^2$ with

$$k_1^2 \;=\; \frac{1}{4}\left[-\frac{4}{\gamma^2} - \frac{(\beta r)^2}{2} - \frac{3}{\gamma}\beta r m\right]^{-1} \left[\beta\delta + \frac{1}{\gamma}\left(1 - \frac{2}{\gamma}\right) + \beta r m \left(\frac{2}{v_0}\frac{dv_0}{dz} - \frac{1}{2\gamma}\right)\right]^2 . \tag{5.103}$$

Note that in order to observe the limits set by the approximation of slender flux tubes the radius of the flux tube has to be much smaller than the perturbation wavelength. This can be a severe restriction if overstability appears only for very small wavelength (very large wavenumber). If we have $k^2 > k_1^2$ the four solutions of Eq. (5.100) are given by

$$\hat{\omega} \;=\; \pm\frac{1}{2}\left(2D^{1/2} - B\right)^{1/2} \;\pm\; \frac{1}{2}i\left(2D^{1/2} + B\right)^{1/2} . \tag{5.104}$$

We see that if the conditions for complex roots are satisfied there are always unstable solutions, i.e. roots with a positive real part. The overstability is caused by the drag force which is added

* The general algorithm for the determination of roots of quartic equations in closed form is not used here because, given the complicated structure of the coefficients, it leads to lengthy algebraic expressions which give no direct insight in the properties of the stability problem.

to the restoring force due to magnetic tension such that an oscillation with growing amplitude results. The conditions for overstability depend only on the sign and the amplitude of the velocity (cf. Eq. 5.102). In particular, they are independent of the velocity gradient, a fact which is due to the linear approach.

Numerical solutions of the exact dispersion relation, Eq. (5.97), basically confirm the criteria derived on the basis of the discussion of the reduced form, Eq. (5.100). In most cases, finite values of A and C only affect the growth or decay rates or change oscillatory into monotonic decay. A notable exception is the result that finite values of A and C lead to positive growth rates of oscillatory modes whenever the conditions $m = -1$ and Eq. (5.102) are fulfilled, even for wave numbers which give $B^2/4 - D > 0$. The second possibility for monotonic instability mentioned above, $B < 0$ and $0 \leq D \leq B^2/4$, does not appear in practice since it requires that the conditions $m = -1$ and Eq. (5.102) are fulfilled which immediately lead to oscillatory instability. Hence, we can summarize the stability properties as follows:

> *A horizontal flux tube whose equilibrium is determined by a balance between buoyancy and drag force exerted by an external, vertical flow is monotonically unstable if the condition $D < 0$ (cf. Eq. 5.99) is satisfied. In particular, flux tube equilibria with a sufficiently large value of βr are always unstable, irrespective of the flow direction. A flux tube may exhibit oscillatory instability (overstability) if the external flow is a downflow and the value of βr is within a certain range (cf. Eq. 5.102).*

Oscillatory instability can be excited whenever the conditions $m = -1$ and $2/\gamma < \beta r < 4/\gamma$ are fulfilled. This excludes isothermal flux tubes which require $\beta r m = -1$. Overstability cannot be stabilized by the stratification, however subadiabatic it may be. Consequently, it is potentially relevant for all flux tubes, irrespective of their location in convection zones, overshoot layers or regions in radiative equilibrium. Since βr depends on the field strength and radius of the tube as well as on the flow velocity, for given values of two of these parameters Eq. (5.102) defines a range of the third parameter which leads to overstability. The tube radius, however, must always be small enough to stay consistent with the utilization of the approximation of slender flux tubes.

While the convective and Parker-type instabilities are most easily excited for large wavelength along the flux tube, overstable modes have their largest growth rates for small wavelengths. Consequently, we expect that overstability is not only relevant for horizontal flux tubes but also for more general forms of equilibrium. If we restrict ourselves to perturbation wavelengths which are much smaller than the wavelength of the equilibrium path of a flux tube a kind of local analysis is possible. Overstable modes can be revealed by this kind of treatment while the convective and Parker-type instabilities are suppressed since they only appear for large enough wavelengths. An example of such a local analysis is given in Sec. 5.7.1 below.

Let us finally consider the influence of the coefficients A and C on the growth rates of unstable modes. Tab. 3 below illustrates the dependence of $\hat{\omega}$ on the value of v_0 which determines the size of A and C for given values of βr (cf. Eq. 5.97). We consider two examples: Monotonic instability of equipartition flux tubes ($\beta\delta = 3.6$) in temperature equilibrium with the environment ($\beta r m = -1$) and overstability of equipartition tubes with $\beta r m = -1.8$.

* Strictly spoken, $v_0 \to \infty$ is inconsistent with the assumption of a finite value for βr unless the flux tube diameter becomes infinite, too. We nevertheless consider this case (which gives $A = C = 0$) for the purpose of comparison with the results for finite values of v_0.

v_0	$\beta rm = -1.$, $k = 0.$ (monotonic)		$\beta rm = -1.8$, $k = 1.$ (overstable)	
	$\mathrm{Re}(\hat{\omega})$	$\mathrm{Im}(\hat{\omega})$	$\mathrm{Re}(\hat{\omega})$	$\mathrm{Im}(\hat{\omega})$
∞^*	1.334	0.	0.137	1.345
10.	1.238	0.	0.077	1.348
1.	0.667	0.	0.012	1.413
0.1	0.089	0.	0.001	1.414

Tab. 3: Dependence of growth rate, $\mathrm{Re}(\hat{\omega})$, and oscillation frequency, $\mathrm{Im}(\hat{\omega})$, on the the vertical velocity v_0 which determines the size of the coefficients of the damping terms A and C. Two cases are considered: Monotonic instability of equipartition flux tubes ($\beta\delta = 3.6$) in temperature equilibrium with the environment ($\beta rm = -1$) and overstability of equipartition tubes with $\beta rm = -1.8$. While $\mathrm{Im}(\hat{\omega})$ is barely affected, the growth rate decreases drastically for small values of v_0 and fixed βr.

As explained in Sec. 5.4, the velocity v_0 is measured in units of $v_A/\sqrt{2}$ and the time unit is of the order of one day for the deep layers of the solar convection zone. Smaller values of v_0 (for fixed values of βr, see discussion below) entail larger values of A and C which lead to smaller growth rates of both monotonic and oscillatory instabilities. The overstable modes which typically have much smaller growth rates than the monotonic modes are more strongly affected by this damping mechanism. The *growth time* $2\pi/\mathrm{Re}(\hat{\omega})$ of the overstable mode in our example increases from about 80 days for $v_0 = 10.$ to 17 years for $v_0 = 0.1$ while for the monotonic mode the numbers are 7 days and 70 days, respectively. On the other hand, the oscillation frequencies are hardly affected.

We may estimate the value of v_0 associated with a given value of βr with aid of Eq. (5.6) which may be simplified by assuming $\beta \gg 1$ and $2C_D/\pi \approx 1$. Written in non-dimensional quantities we obtain

$$\beta r \;\approx\; \frac{v_0^2}{a_0}. \tag{5.105}$$

Here a_0 is the flux tube radius in units of the external pressure scale height. For the interesting range $\beta r = O(1)$ we have

$$v_0 \;\approx\; \sqrt{a_0} \tag{5.106}$$

We see that for *fixed* βr the quantity v_0 effectively is a measure of the flux tube radius. Tab. 3 shows that small flux tubes are more strongly influenced by the drag forces and suffer from a stronger damping than those with larger radius. For $\beta r = 1$ and $H_{p0} = 5 \cdot 10^4$ km we find the range $v_0 \approx 0.03...0.3$ for flux tube radii between 50 km and 5000 km. Consequently, we have to expect a strong effect of the damping terms on the growth rates, especially in the case of overstable modes.

5.7 Symmetric loops with vertical external flow

As an example of a flux tube equilibrium with a curved path we investigate a planar loop which is symmetric with respect to a vertical line through its maximum or minimum. Since we shall consider the stability only in the vicinity of the point of extremum, the results are relevant also for flux tubes which wind like a serpentine line, i.e. consist of a sequence of (symmetric) loops with alternating maxima and minima. Such configurations are of practical interest since one could imagine that the kink instability of a horizontal (or toroidal) flux tube in a convection zone leads to ‘sea serpent’ structures, i.e. a series of erupted active regions connected by loops with minima in the convection zone. Another interesting question is whether ‘dived sea serpents’, a series of minimum and maximum loops fully within the convection zone represent a stable alternative to the unstable horizontal tubes.

As in the preceding section we assume a purely vertical external velocity field which does not depend on x, the coordinate in the horizontal direction, and continue to use the notation of the velocity terms introduced there. The equilibrium is determined by a balance of buoyancy, curvature and drag force which is described by Eq. (5.4). For the point of extremum with $(\hat{\mathbf{g}}_0 \cdot \hat{\mathbf{n}}_0) = -1$ in the case of a minimum and $(\hat{\mathbf{g}}_0 \cdot \hat{\mathbf{n}}_0) = +1$ in the case of a maximum we have (in non-dimensional form)

$$\mp\beta\left(1 - \frac{\rho_{e0}}{\rho_0}\right) \;=\; \frac{2}{R_0} \;+\; \beta rm\,. \tag{5.107}$$

The upper sign on the l.h.s. applies for a maximum, the lower sign for a minimum. In both cases we have $(\hat{\mathbf{g}}_0 \cdot \hat{\mathbf{l}}_0) = 0$, i.e. the tangent vector has a horizontal direction at the point of extremum.

5.7.1 Local analysis

Overstable modes of a symmetric loop can be treated analytically by way of a local stability analysis assuming perturbations with small wavelength (large wavenumber) in the direction along the flux tube. We consider the extremum point (maximum or minimum) of a symmetric loop and investigate its stability with respect to growing oscillations of short wavelength in the neighborhood of this point.

We assume wave-like perturbations, i.e. $\varepsilon, \eta \propto \exp(ikx)$ whose wavelength $\lambda = 2\pi/k$ is small enough such that we can take all quantities describing the equilibrium flux tube $(R_0, H_{p0}, \rho_0, (\hat{\mathbf{g}}_0 \cdot \hat{\mathbf{l}}_0), (\hat{\mathbf{g}}_0 \cdot \hat{\mathbf{n}}_0)...)$ to be constant within a wavelength. On the other hand, the approximation of slender flux tubes demands $\lambda \gg a_0$ where a_0 is the radius of the tube. Consequently, we require $a_0 \ll \lambda \ll R_0$ and also $\lambda \ll (8R_0H_{p0})^{1/2}$ which results from the requirement that the height increment of the path of the equilibrium flux tube within one wavelength must be small compared to the scale height. Both conditions lead to

$$\frac{2\pi}{a_0} \;\gg\; k \;\gg\; \frac{2\pi}{\min(R_0,\, 8R_0H_{p0})^{1/2}}. \tag{5.108}$$

Since overstability often requires that the wavenumber exceeds some critical value one has to keep in mind that the following results are only applicable within the limits of the approximation of slender flux tubes if the tube radius satisfies the left part of the above relation. For wavenumbers which satisfy Eq. (5.108) we may use Eq. (5.107) to rewrite the general perturbation equations, Eqs. (5.63/64), taking the extremum as reference point, z_m, for the non-dimensionalization of all quantities and obtain

$$-\omega^2\eta \;=\; ik\varepsilon\left(-\frac{4}{R_0} - \beta rm \pm \frac{2}{\gamma}\right) \;+\; \eta\frac{1}{R_0}\left(-\frac{2}{R_0} - \beta rm \pm \frac{2}{\gamma}\right) \;-\; 2k^2\eta \tag{5.109}$$

$$\begin{aligned} -\omega^2\varepsilon \;=&\; ik\eta\left(\frac{4}{R_0} + \frac{\beta rm}{2} + \frac{2}{\gamma}\right) \;-\; 2k^2\varepsilon \;-\; i\omega\varepsilon\frac{2\beta r}{v_0} \\ &+\; \varepsilon\left[-\frac{2}{R_0^2} \pm \frac{4}{\gamma R_0} + \beta\delta + \frac{1}{\gamma}\left(1 - \frac{2}{\gamma}\right) + \beta rm\left(\mp\frac{2}{v_0}\frac{dv_0}{dz} \pm \frac{1}{2\gamma} - \frac{1}{2R_0}\right)\right]. \end{aligned} \tag{5.110}$$

Note that for the lower signs ($(\hat{\mathbf{g}}_0 \cdot \hat{\mathbf{n}}_0) = -1$) and in the limit $R_0 \to \infty$ these equations pass over to Eqs. (5.94/95) for a horizontal flux tube. We follow the same procedure as in the preceding section and determine from Eqs. (5.109/110) a dispersion relation for $i\omega \equiv \hat{\omega}$, again of a fourth order polynomial with real coefficients:

$$\hat{\omega}^4 \,+\, A\hat{\omega}^3 \,+\, B\hat{\omega}^2 \,+\, C\hat{\omega} \,+\, D \,=\, 0 \tag{5.111}$$

$$A \,=\, \frac{2\beta r}{v_0}$$

$$B \,=\, 4k^2 + \frac{2}{R_0}\left(\frac{2}{R_0} \mp \frac{3}{\gamma}\right) - \beta\delta - \frac{1}{\gamma}\left(1 - \frac{2}{\gamma}\right) + \beta rm\left(\pm\frac{2}{v_0}\frac{dv_0}{dz} \mp \frac{1}{2\gamma} + \frac{3}{2R_0}\right)$$

$$C \,=\, \frac{2\beta r}{v_0}\left[2k^2 + \frac{1}{R_0}\left(\frac{2}{R_0} + \beta rm \mp \frac{2}{\gamma}\right)\right]$$

$$\begin{aligned} D \,=\,& 2k^2\left[2k^2 - \beta\delta - \frac{1}{\gamma} + \frac{2}{R_0}\left(\pm\frac{1}{\gamma} - \frac{2}{R_0}\right) + \beta rm\left(\pm\frac{2}{v_0}\frac{dv_0}{dz} \pm \frac{1}{\gamma} - \frac{3}{2R_0}\right) - \frac{(\beta r)^2}{4}\right] \\ &+\, \frac{1}{R_0}\left\{\frac{4}{R_0^2}\left(\frac{1}{R_0} \mp \frac{3}{\gamma}\right) + \frac{2}{\gamma R_0}\left(\frac{6}{\gamma} - 1\right) \pm \frac{2}{\gamma^2}\left(1 - \frac{2}{\gamma}\right) + \beta\delta\left(-\frac{2}{R_0} - \beta rm \pm \frac{2}{\gamma}\right)\right. \\ &+\, \left.\beta rm\left[\frac{2}{v_0}\frac{dv_0}{dz}\left(\frac{2}{\gamma} \mp \frac{2}{R_0}\right) + \frac{1}{\gamma}\left(\frac{3}{\gamma} - \frac{6}{R_0} - 1\right) + \frac{3}{R_0^2}\right] + (\beta r)^2\left(\mp\frac{2}{v_0}\frac{dv_0}{dz} \mp \frac{1}{2\gamma} + \frac{1}{2R_0}\right)\right\} \end{aligned}$$

In analogy to the treatment in Sec. 5.6 we consider a reduced dispersion relation obtained by setting $A = C = 0$ in Eq. (5.111) which leads to

$$\hat{\omega}^2 \,=\, -\frac{B}{2} \pm \left(\frac{B^2}{4} - D\right)^{1/2}. \tag{5.112}$$

We have obtained a number of numerical solutions of the full dispersion relation, Eq. (5.111), which confirm the criteria derived below on the basis of Eq. (5.112). Finite values of A and C only affect the growth or decay rates. Monotonic instability for large values of k requires extreme values for $\beta\delta$ or βr which are unrealistic for a convection zone. Oscillatory instability, on the other hand, which sets in if $B^2/4 - D < 0$ can be well described by local analysis. This expression is given by

$$\begin{aligned} \frac{B^2}{4} - D \,=\,& k^2\left[\frac{4}{\gamma^2} + \frac{(\beta r)^2}{2} + 3\beta rm\left(\frac{2}{R_0} \mp \frac{1}{\gamma}\right) + \frac{16}{R_0}\left(\frac{1}{R_0} \mp \frac{1}{\gamma}\right)\right] \\ &+\, \frac{1}{4}\left[-\frac{2}{R_0}\left(\frac{2}{R_0} \mp \frac{3}{\gamma}\right) + \beta\delta + \frac{1}{\gamma}\left(1 - \frac{2}{\gamma}\right) - \beta rm\left(\pm\frac{2}{v_0}\frac{dv_0}{dz} \mp \frac{1}{2\gamma} + \frac{3}{2R_0}\right)\right]^2 \\ &-\, \frac{1}{R_0}\left\{\frac{4}{R_0^2}\left(\frac{1}{R_0} \mp \frac{3}{\gamma}\right) + \;...\; + (\beta r)^2\left(\mp\frac{2}{v_0}\frac{dv_0}{dz} \mp \frac{1}{2\gamma} + \frac{1}{2R_0}\right)\right\} \end{aligned} \tag{5.113}$$

where the term in braces is the same as the last term in the above definition of D. Since local analysis demands large values of k we conclude that the sign of $B^2/4 - D$ is determined by the sign of the term multiplied by k^2 in Eq. (5.113). Note that the superadiabaticity does not enter into this term, i.e. the excitation condition for oscillatory instability is independent of the stability of the external stratification which may only affect the wavelength range of overstable modes. This applies also to horizontal flux tubes (cf. Eqs. 5.101/103). A simple calculation shows that the term under consideration is negative if

$$(\beta r)_{\min} \;<\; \beta r \;<\; (\beta r)_{\max} \tag{5.114}$$

where

$$(\beta r)_{\min} \;=\; \min\left[(\beta r)_1, (\beta r)_2\right], \qquad (\beta r)_{\max} \;=\; \max\left[(\beta r)_1, (\beta r)_2\right] \tag{5.115}$$

with

$$\begin{aligned} (\beta r)_1 \;&=\; (3m-1)\left(\pm\frac{1}{\gamma} - \frac{2}{R_0}\right) \\ (\beta r)_2 \;&=\; (3m+1)\left(\pm\frac{1}{\gamma} - \frac{2}{R_0}\right). \end{aligned} \tag{5.116}$$

Since βr is a positive quantity and $(\beta r)_1$ and $(\beta r)_2$ always have the same sign, overstability is only possible if both are positive, too. We now have to distinguish 4 cases, i.e. maximum/minimum and upflow/downflow, respectively. Note that since $m = \mathrm{sgn}(\mathbf{v}_{e0} \cdot \hat{\mathbf{n}}_0)$ the value $m = 1$ signifies an upflow for a minimum and a downflow for a maximum while $m = -1$ corresponds to a downflow for a minimum and an upflow for a maximum. Tab. 4 summarizes the stability properties for the four possible cases. The fourth column gives necessary conditions on R_0 for overstability while the last column shows the range of values of βr which lead to overstability. Cases 3 and 4 with $R_0 \to \infty$ pass over to the case of a horizontal flux tube treated in the preceding section (cf. Eq. 5.102).

Case	Extremum	m	Condition	Oscillatory instability for
1	maximum	-1 (up)	$R_0 < 2\gamma$	$2(2/R_0 - 1/\gamma) < \beta r < 4(2/R_0 - 1/\gamma)$
2	maximum	$+1$ (down)	$R_0 > 2\gamma$	$2(1/\gamma - 2/R_0) < \beta r < 4(1/\gamma - 2/R_0)$
3	minimum	-1 (down)		$2(1/\gamma + 2/R_0) < \beta r < 4(1/\gamma + 2/R_0)$
4	minimum	$+1$ (up)		no overstability

Tab. 4: Range of values for βr which lead to overstability of symmetric loops with fixed radius of curvature, R_0. The four possible cases (maximum/minimum, upflow/downflow) are given. For the first pair of cases necessary conditions for overstability exist which are indicated in the fourth column.

We must keep in mind, however, that the quantities R_0 and βr generally cannot be chosen independently since they are related through the equilibrium condition given by Eq. (5.107). If the relation between internal and external temperature and the value of $\beta r m$ are given, the radius of curvature is fixed. Hence, Eq. (5.116) and Tab. 4 are only applicable if the internal temperature and βr are chosen in such a way that R_0 stays constant. For more realistic cases we must prescribe the relation between external and internal temperature and determine R_0 according to Eq. (5.107) for any given value of βr.

In what follows we discuss the case of an *isothermal* flux tube, i.e. internal equal to external equilibrium temperature. In this case the equilibrium (written in dimensionless form) is given by

$$\frac{2}{R_0} + \beta r m = \pm 1 . \tag{5.117}$$

We notice that no equilibrium is possible for a minimum with upflow. This is due to the fact that an isothermal flux tube has an upward directed buoyancy force and the curvature force in case of a minimum has the same direction. Consequently, force balance can only be achieved by a downflow. In other cases there are restrictions on βr: For a minimum with downflow we must have $\beta r \geq 1$ while a maximum with downflow requires $\beta r \leq 1$ and $R_0 \geq 1$. In the case of a maximum with upflow any value of βr is permitted. We insert Eq. (5.117) into Eq. (5.113) and determine the range of oscillatory instability by the same procedure which led to Eqs. (5.114-116). We find

$$(\beta r)_1 = \frac{(\pm 5m - 1)}{3}\left(1 - \frac{1}{\gamma}\right), \qquad (\beta r)_2 = \frac{(\pm 5m + 1)}{3}\left(1 - \frac{1}{\gamma}\right). \tag{5.118}$$

Since we certainly have $\gamma \geq 1$ the sign of $(\beta r)_{1,2}$ for a given equilibrium is determined only by m. The stability criteria for the isothermal case as they follow from Eqs. (5.114/118) are summarized in Tab. 5:

Case	Extremum	m	Oscillatory instability for
1	maximum	-1 (up)	no overstability
2	maximum	$+1$ (down)	$(4/3)(1-1/\gamma) < \beta r < 2(1-1/\gamma)$
3	minimum	-1 (down)	$(4/3)(1-1/\gamma) < \beta r < 2(1-1/\gamma)$
4	minimum	$+1$ (up)	no equilibrium

Tab. 5: Range of values for βr which lead to overstability of *isothermal,* symmetric loops. Only configurations with an external downflow are liable to overstability.

For $\gamma = 5/3$ the range of values of βr which lead to overstability in cases 2 and 3 is given by

$$0.53 < \beta r < 0.8 \tag{5.119}$$

Since the equilibrium condition given by Eq. (5.117) requires $\beta r \geq 1$ for case 3 (minimum with downflow) there is no possibility for overstability in this case if the flux tube is isothermal. Consequently, *the minimum region of a symmetric loop formed by a flux tube which is in temperature equilibrium with the external gas is always stable with respect to growing oscillations and a maximum with a downflow is the only configuration which can lead to overstability of an isothermal loop.* For $R_0 \to \infty$ in all cases we have $\beta r \to 1$ and we thus recover the result of the preceding section, namely that an isothermal, horizontal flux tube does not show overstability.

Another interesting special case is the *neutrally buoyant flux tube,* $\rho_0 = \rho_{e0}$, whose equilibrium is determined by a balance between curvature force and drag force. Eq. (5.107) then leads to (non-dimensional form)

$$\frac{2}{R_0} = -\beta r m \tag{5.120}$$

and it is clear that this kind of equilibrium requires $m = -1$, i.e. either a minimum with a downflow or a maximum with an upflow. Inserting Eq. (5.120) into Eq. (5.113) with $m = -1$ we now obtain

$$
\begin{aligned}
(\beta r)_1 &= \frac{\pm 5 - 1}{3\gamma} \\
(\beta r)_2 &= \frac{\pm 5 + 1}{3\gamma} \,.
\end{aligned}
$$

Consequently, the minimum region of a neutrally buoyant flux loop is always stable with respect to growing oscillations while a maximum may show overstability. For a maximum loop and $\gamma = 5/3$ we find $(\beta r)_1 = 0.8$ and $(\beta r)_2 = 1.2$. Consequently, overstability of a neutrally buoyant loop can occur if it has a maximum with a radius of curvature of about 2 scale heights.

5.7.2 Constant vertical displacement

If we assume that the perturbation wavelength along the equilibrium flux tube is infinite and consider purely vertical displacements (in z-direction) the perturbation equations can be simplified considerably and are analytically solvable in the case of symmetric loops. In this way we can investigate *monotonic instability.* As in the preceding section we consider an extremum point (local minimum or maximum) of a flux tube whose path has the form of a symmetric loop. We assume that the whole structure is displaced vertically by a constant amount, z_1. Since the tube is not stretched by this operation we have $l = l_0$ and conclude from Eq. (5.8) that

$$
\eta' = \frac{\varepsilon}{R_0} \,. \tag{5.121}
$$

At the point of extremum we have for reasons of symmetry

$$
\eta = \eta'' = \varepsilon' = 0 \tag{5.122}
$$

and since the radius of curvature is unaffected by this kind of displacement ($R = R_0$) we find from Eq. (5.11)

$$
\varepsilon'' = -\frac{\varepsilon}{R_0^2} \,. \tag{5.123}
$$

Furthermore, we have $(\hat{\mathbf{g}}_0 \cdot \hat{\mathbf{l}}_0) = 0$ and $(\hat{\mathbf{g}}_0 \cdot \hat{\mathbf{n}}_0) = \pm 1$ at an extremum point. Using this together with Eqs. (5.121-123) we find that both sides of Eq. (5.63) vanish and Eq. (5.64) has non-trivial solutions provided that

$$
\omega^2 - i\omega \frac{2\beta r}{v_0} + \left[\beta\delta + \frac{1}{\gamma}\left(1 - \frac{2}{\gamma}\right) \pm \frac{2}{\gamma R_0} + \beta r j \left(\frac{2}{v_0}\frac{dv_0}{dz} - \frac{1}{2\gamma} \right) \right] = 0 \tag{5.124}
$$

where (as before) the upper (+) sign applies for a maximum and the lower (−) sign for a minimum. In this equation we have introduced $j \equiv \mathrm{sgn}(\mathbf{v}_{e0} \cdot \hat{\mathbf{z}}) = \mp m$ such that for both cases (minimum and maximum) $j = +1$ indicates an upflow and $j = -1$ a downflow. The quantities have been non-dimensionalized with respect to their values at the point of extremum. As in the preceding sections we have assumed a constant gravitational acceleration ($s = 0$) in order to simplify the discussion. The influence of a variation of $\mathbf{g}$ on the stability properties is marginal, however. Note that in the case of a horizontal tube ($R_0 \to \infty$) Eq. (5.124) transforms into Eq. (5.84), the dispersion relation for vertical displacements of a horizontal tube.* The same line of arguments as in that case shows

* In the derivation of Eq. (5.84) we have assumed $(\hat{\mathbf{g}}_0 \cdot \hat{\mathbf{n}}_0) = -1$ such that we have $j = m$ in this case.

that a necessary and sufficient criterion for instability is that the expression in square brackets in Eq. (5.124) is positive, viz.

$$\beta\delta + \frac{1}{\gamma}\left(1 - \frac{2}{\gamma}\right) \pm \frac{2}{\gamma R_0} + \beta r j \left(\frac{2}{v_0}\frac{dv_0}{dz} - \frac{1}{2\gamma}\right) \;>\; 0\,. \tag{5.125}$$

The effect of the terms which depend on the external velocity is identical to the case of a horizontal tube, i.e. the curvature of the tube does not change the effect of the flow on the stability of the point of extremum. This is not obvious from the original equations (5.63/64) since we find terms there which depend on both velocity *and* curvature. In the special case of purely vertical displacements these terms cancel, however.

For the heuristic argumentation presented in the following subsection it is important to note here that the stability criterion given by Eq. (5.125) can be also obtained by considering the perturbations of the buoyancy, curvature and drag forces brought about by a vertical displacement of the point of extremum. The sign of the resulting perturbation of the total force then determines the stability properties of the equilibrium. In the present case we assume that a purely vertical displacement does not lead to a flow of matter along the tube ($\eta \equiv 0$) such that the ratio B/ρ is constant and the perturbations (indicated by an index *1*) are related to the equilibrium quantities as $B_1/B_0 = \rho_1/\rho_0$. Together with the adiabaticity of the perturbations (Eq. 5.38) and the condition of pressure equilibrium (Eq. 5.39) this leads to the following relation for the magnetic field perturbation as function of the displacement z_1:

$$\frac{B_1}{B_0} \;=\; -\left(\frac{\beta+1}{\beta\gamma+2}\right)\frac{z_1}{H_{pe}}\,. \tag{5.126}$$

Consequently, for $\beta \gg 1$ (ignoring terms of order β^{-1}) we find for the perturbation of the curvature force (with $R_1 = 0$):

$$F_{C1} \;=\; \mp\frac{B_0 B_1}{2\pi R_0} \;=\; \pm\frac{B_0^{\,2} z_1}{2\pi\gamma R_0 H_{p0}}\,. \tag{5.127}$$

In a similar way we determine the perturbations of the buoyancy and drag forces as functions of z_1 and the equilibrium quantities. We add all force perturbations together, take the limit $\beta \gg 1$, and non-dimensionalize with respect to the values of the quantities at the point of extremum. Taking then $z_1 \propto \exp(i\omega t)$ we obtain *exactly* the stability criterion given by Eqs. (5.124/125). This result lends some support to the treatment presented in the subsequent section where a similar heuristic approach is used for displacements with large but finite wavelength.

The perturbation of the curvature force given by Eq. (5.127) is helpful for understanding the effect of curvature on the stability of the loop which is expressed by the term $\pm 2/\gamma R_0$ in Eq. (5.124). Since the magnetic field decreases for an upward displacement and increases for a downward displacement (cf. Eq. 5.126), the absolute value of the curvature force always decreases for an upward displacement and increases for a downward displacement. Now consider a *minimum*: The curvature force is directed upward (positive) and is reduced by an upward displacement and increased by a downward displacement; the result is a restoring force which acts against the displacement – this stabilizing effect of curvature shows up in the negative sign of the term $2/\gamma R_0$ in the case of a minimum. An analogous consideration shows that in the case of a *maximum* the effect of curvature is destabilizing. Tab. 6 below summarizes the effect of the different terms in Eq. (5.125) on the stability properties of the loop. Regarding the stratification of the convection zone we assume that the flow speed decreases with depth.

Extremum	Flow	$\pm 2/(\gamma R_0)$	$(2/v_0)(dv_0/dz) > 0$	$-1/(2\gamma) < 0$
minimum	up	stabilizing	destabilizing	stabilizing
maximum	up	destabilizing	destabilizing	stabilizing
minimum	down	stabilizing	stabilizing	destabilizing
maximum	down	destabilizing	stabilizing	destabilizing

Tab. 6: Influence of individual terms in the stability criterion (Eq. 5.125) for various configurations of a symmetric loop in the case of purely vertical displacements. The term given in the third column describes the direct effect of curvature while the terms in the fourth and fifth column represent the effect of the external velocity.

According to Eq. (5.91) we expect that the velocity gradient term dominates over the last term in Eq. (5.125) such that in particular minimum loops with a downflow are possible examples of stable configurations.

In order to estimate the quantitative effect of the curvature term we consider the case of a flux tube in thermal equilibrium with the environment, i.e. $T_0 = T_{e0}$ and $\beta(\rho_{e0}/\rho_0 - 1) = 1$, such that the equilibrium condition, Eq. (5.107), can be written in non-dimensional form as

$$1 + \beta r j = \pm \frac{2}{R_0} . \tag{5.128}$$

We see that for a minimum (lower sign) we must have a downflow ($j = -1$) of sufficient strength since in temperature equilibrium the internal density is always smaller than the external density leading to an upward directed buoyancy force. Inserting Eq. (5.128) into the instability criterion Eq. (5.125) and assuming a constant flow velocity ($dv_0/dz = 0$) we find instability for

$$\beta\delta + \frac{2}{\gamma}\left(1 - \frac{1}{\gamma}\right) + \frac{\beta r j}{2\gamma} > 0 . \tag{5.129}$$

The fact that in this case a downflow always stabilizes while an upflow destabilizes can be understood by considering Eq. (5.128): With the exception of the small range $-1 \le \beta r j \le 0$ a downflow leads to a minimum and an upflow to a a maximum. In both cases the effect of the flow is to decrease R_0, the radius of curvature. Thus the stabilizing effects of curvature for a minimum (downflow) and its destabilizing effects for a maximum (upflow) are amplified by the flow.

In the absence of a flow we only can have a maximum and the criterion for instability reads

$$\beta\delta > -\frac{2}{\gamma}\left(1 - \frac{1}{\gamma}\right) = -0.48 \tag{5.130}$$

for $\gamma = 5/3$. If we compare this with the criterion for a horizontal tube without flow, i.e. $\beta\delta > +0.12$ (cf. Eq. 5.89) we see that the effect of curvature is quite significant: While for the horizontal tube a positive superadiabaticity was necessary in the case of purely vertical perturbations, the static, isothermal loop is unstable even in a moderately subadiabatic environment. On the other hand, an external downflow of sufficient amplitude leads to stable local minimum configurations for any value of the superadiabaticity. Take for example the value $\beta\delta = 3.6$ for equipartition flux tubes in the deep solar convection zone. With $j = -1$ we find from Eq. (5.129) that such an equilibrium is stable if $\beta r > 13.6$. From Eq. (5.105) we see that this condition is realized for flux tube radii smaller than about $H_{p0}/13.6 \approx 4000$ km if the external velocity is of the order of the typical convective velocities obtained from mixing length theory.

5.7.3 Heuristic approach for perturbations with large wavelength

As far as monotonic instability is concerned, it has already been shown by Spruit and van Ballegooijen (1982) that for horizontal flux tubes without external flow the most unstable perturbations are those which lead to wave-like displacements of very large, *but finite,* wavelength. In this case a Parker-type/convective instability with a flow along the tube can be excited which is largely undisturbed by curvature forces. We have generalized this result to horizontal tubes with external flow and we suspect that this kind of perturbation is also decisive for the monotonic instability of symmetric loops for which we until now have only considered very small and infinite wavelength (subsections 5.7.1 and 5.7.2, respectively). Unfortunately, finite wavelength perturbations for non-horizontal flux tube equilibria in most cases do not permit analytical treatment since the coefficients in the perturbation equations, Eqs. (5.63/64), become variable. One then has to resort to a numerical solution of the eigenvalue problem for any given equilibrium tube. However, for symmetric loops and displacements with very large, but finite, wavelength which turned out to be most unstable kind of perturbation for horizontal tubes we can extend the heuristic approach sketched in the preceding subsection. Since in contrast to the treatment there we cannot check against the exact result, no definite proof can be given that the approach described below is correct. However, we will show that in the limit of horizontal tubes ($R_0 \to \infty$) the result becomes identical to the exact criterion for monotonic instability and $k \to 0$ (but finite, cf. Eqs. 5.98/99). Together with the success of the method for purely vertical displacements demonstrated in the preceding subsection this gives some confidence in its validity.

We consider a symmetric loop in a vertical flow and determine the perturbations of the various forces (buoyancy, curvature, drag) at the point of extremum which are brought about by a vertical displacement. In contrast to the previous treatment we now assume a perturbation with finite wavelength such that the flux tube is not displaced as a whole – parts of the equilibrium tube are lifted while other parts are displaced downward. Since in our cartesian model the wavelength of the perturbation can be made arbitrarily large, it can in particular be chosen large enough such that the perturbations of the tube geometry (arc length, radius of curvature etc.) can be neglected in comparison with the relative perturbations of the other quantities. For example, for a displacement z_1 with wavenumber k, the perturbation of the radius of curvature at the extremum point of a symmetric loop is given by

$$|R_1| \;=\; k^2 R_0^2 |z_1| \tag{5.131}$$

where we have used Eqs. (5.11/14) and the symmetry properties. We see that for any given displacement we can make R_1 as small as we want by decreasing k sufficiently, i.e. by increasing the wavelength of the perturbation.

The important difference to the treatment in the preceding subsection lies in the determination of the perturbations of internal density and pressure. Since the wavelength of the displacement is now finite (albeit very large) parts of the equilibrium tube are lifted while other parts are displaced downward such that an internal flow along the tube sets in which tends to establish hydrostatic equilibrium along the magnetic field lines according to the principle of communicating tubes. We therefore determine the perturbed internal density and pressure by assuming that the flow along the tube has already restored hydrostatic equilibrium at the point of extremum, viz.

$$p_1 \;=\; -\frac{p_0}{H_{p0}} z_1 \tag{5.132}$$

which entails for adiabatic perturbations (cf. Eq. 5.38)

$$\rho_1 \;=\; -\frac{\rho_0}{\gamma H_{p0}} z_1 \,. \tag{5.133}$$

By assuming that hydrostatic equilibrium is reestablished we probably loose information about growth rates and we also cannot reproduce the overstable modes but we conjecture that the stability criteria for monotonic instabilities are correctly described by this approach. We shall prove this below for the special case of horizontal tubes for which the exact solution is available.

We continue by determining F_{B1}, the perturbation of the buoyancy force, which is given by

$$F_{B1} \;=\; (\rho_{e1} - \rho_1) g_0 \tag{5.134}$$

where we have assumed that the gravitational acceleration is constant ($s = 0$). With $\nabla_{ad} = (\gamma - 1)/\gamma$, $\delta = \nabla - \nabla_{ad}$ and using Eqs. (5.25) and (5.133) we find, after some algebra

$$F_{B1} \;=\; \frac{B_0^2}{8\pi H_{p0}^2} \left\{ (1-\nabla) \left[\beta \left(1 - \frac{\rho_{e0}}{\rho_0} \right) + \frac{\rho_{e0}}{\rho_0} \frac{H_{p0}}{H_{pe}} \, \beta \left(\frac{H_{pe}}{H_{p0}} - 1 \right) \right] + \beta\delta \right\} z_1 \,. \tag{5.135}$$

We now perform the same procedure as in Sec. 5.4 and take the limit $\beta \gg 1$ such that all terms of order β^{-1} are neglected unless they are multiplied by β. In this limit we have

$$\beta \left(\frac{H_{pe}}{H_{p0}} - 1 \right) = 1 \;+\; \beta \left(1 - \frac{\rho_{e0}}{\rho_0} \right) \;+\; O(\beta^{-1}) \tag{5.136}$$

as well as $1 - \nabla = 1/\gamma + O(\beta^{-1})$, $\rho_{e0}/\rho_0 = 1 + O(\beta^{-1})$, $H_{p0}/H_{pe} = 1 + O(\beta^{-1})$, and Eq. (5.135) is transformed into

$$F_{B1} \;=\; \frac{B_0^2}{8\pi H_{p0}^2} \left[\beta\delta + \frac{1}{\gamma} + \frac{2}{\gamma} \beta \left(1 - \frac{\rho_{e0}}{\rho_0} \right) \right] z_1 \,. \tag{5.137}$$

The perturbation of the magnetic field is determined by the condition of pressure balance, Eq. (5.39), which yields together with Eqs. (5.25) and (5.132/233)

$$\frac{B_1}{B_0} \;=\; \beta \left(1 - \frac{\rho_{e0}}{\rho_0} \right) \frac{z_1}{2H_{p0}} \,. \tag{5.138}$$

Inserting into the first (general) part of Eq. (5.127) we obtain the perturbation of the curvature force

$$F_{C1} \;=\; \mp \frac{B_0^2}{4\pi H_{p0} R_0} \, \beta \left(1 - \frac{\rho_{e0}}{\rho_0} \right) z_1 \,. \tag{5.139}$$

Note that we have assumed a sufficiently large wavelength of the displacement such that the perturbation of the radius of curvature can be neglected. Finally we determine F_{D1}, the perturbation of the drag force. As in the preceding sections we assume a purely vertical external velocity field and continue to use the notation introduced in Eqs. (5.83) and (5.124). Since our present approach cannot adequately describe impulsive motion of the flux tube we omit the contribution to F_{D1} due to the motion of the tube itself which gives rise to the last term in Eq. (5.64). We have discussed at some length in Sec. 5.6 that this term does only affect the growth rates but *not* the stability criteria. A derivation along the lines of Eqs. (5.27-5.33) applied to the special case discussed here yields

$$F_{D1} \;=\; \frac{C_D \rho_{e0} v_0^2 j}{\pi a_0} \left(\frac{v_{\perp 1}}{v_0^2} + \frac{\rho_{e1}}{\rho_{e0}} + \frac{B_1}{2B_0} \right) . \tag{5.140}$$

Using Eqs. (5.25), (5.90) and (5.138) and taking the limit $\beta \gg 1$ we obtain, after some algebra

$$F_{D1} \;=\; \frac{B_0^2}{8\pi H_{p0}^2}\,\beta r j \left[\frac{2H_{p0}}{H_{v0}} - \frac{1}{\gamma} + \frac{1}{4}\beta\left(1 - \frac{\rho_{e0}}{\rho_0}\right)\right] z_1 \tag{5.141}$$

where $H_{v0} \equiv v_0 (dv_0/dz)^{-1}$ denotes the scale height of the external velocity. The total force perturbation is obtained by adding Eqs. (5.137), (5.139), (5.141), and using the equilibrium condition, Eq. (5.4), which gives

$$\begin{aligned} F_{B1} + F_{C1} + F_{D1} \;=\; \frac{B_0^2}{8\pi H_{p0}^2} \Bigg[& \beta\delta + \frac{1}{\gamma} + \frac{4H_{p0}}{R_0}\left(\frac{H_{p0}}{R_0} \mp \frac{1}{\gamma}\right) + \frac{(\beta r)^2}{4} \\ & + \beta r j \left(\frac{2H_{p0}}{H_{v0}} + \frac{1}{\gamma} \pm \frac{5}{2}\frac{H_{p0}}{R_0}\right)\Bigg] z_1 . \end{aligned} \tag{5.142}$$

The equilibrium is unstable if the expression within square brackets is positive which means that the perturbation of total force has the same sign as the displacement and thus tends to increase the latter. The exact result for a horizontal tube obtained in Sec. 5.6 is recovered by taking $R_0 \to \infty$ which yields as condition for monotonic instability

$$\beta\delta + \frac{1}{\gamma} + \frac{(\beta r)^2}{4} + \beta r j \left(\frac{2H_{p0}}{H_{v0}} + \frac{1}{\gamma}\right) \;>\; 0\,. \tag{5.143}$$

Regarding Eq. (5.90) we find that this is *identical* to Eq. (5.99),* the exact criterion in the limit of very large wavelength. For $\beta r = 0$ the result of Spruit and van Ballegooijen (1982) is recovered. For finite radius of curvature the general criterion for monotonic instability is

$$\beta\delta + \frac{1}{\gamma} + \frac{4H_{p0}}{R_0}\left(\frac{H_{p0}}{R_0} \mp \frac{1}{\gamma}\right) + \frac{(\beta r)^2}{4} + \beta r j \left(\frac{2H_{p0}}{H_{v0}} + \frac{1}{\gamma} \pm \frac{5}{2}\frac{H_{p0}}{R_0}\right) \;>\; 0. \tag{5.144}$$

This could easily be transformed to a non-dimensional form by formally taking $H_{p0} \equiv 1$ but we do not change the notation here. Let us now discuss the influence of a finite curvature of the equilibrium flux tube on its stability which is expressed in the terms containing the ratio H_{p0}/R_0. The third term on the l.h.s. of Eq. (5.144) is always positive and therefore destabilizing for a minimum (lower sign) while for a maximum (upper sign) it is stabilizing if $H_{p0}/R_0 < 1/\gamma$. However, since $\gamma \geq 1$ it is easy to show that the sum of the second and the third term on the l.h.s. of Eq. (5.144) is always positive, i.e.

$$\frac{1}{\gamma} + \frac{4H_{p0}}{R_0}\left(\frac{H_{p0}}{R_0} \mp \frac{1}{\gamma}\right) \;>\; 0 \tag{5.145}$$

such that *without external velocity curvature cannot stabilize a flux tube in a superadiabatic environment* ($\beta\delta > 0$). For a minimum the effect of curvature always is destabilizing, in contrast to the case of a constant vertical displacement (cf. Eq. 5.125). This is caused by the perturbation of the curvature force. If we take $\beta r = 0$ the equilibrium condition (Eq. 5.4) for a minimum reads

$$\beta\left(1 - \frac{\rho_{e0}}{\rho_0}\right) \;=\; \mp\frac{2H_{p0}}{R_0} \tag{5.146}$$

* Since we have taken $(\hat{\mathbf{g}}_0 \cdot \hat{\mathbf{n}}_0) = -1$ in Sec. 5.6 we have $j = m$.

and we find from Eq. (5.139)

$$F_{C1} \;=\; +\frac{B_0^2 z_1}{2\pi R_0^2} \tag{5.147}$$

such that the perturbation of the curvature always tends to increase the displacement.

We summarize the influence of the velocity terms in Eq. (5.144) on the stability properties of a loop in Tab. 7 below, assuming that the flow speed decreases with depth ($H_{v0} > 0$).

Extremum	Flow	$2H_{p0}/H_{v0} + 1/\gamma > 0$	$\pm(5/2)(H_{p0}/H_{v0})$
minimum	up	destabilizing	stabilizing
maximum	up	destabilizing	destabilizing
minimum	down	stabilizing	destabilizing
maximum	down	stabilizing	stabilizing

Tab. 7: Influence of velocity-related terms in the criterion for monotonic instability (Eq. 5.144) for various configurations of a symmetric loop in the case of displacements with large wavelength. The fourth term in the criterion, $(\beta r)^2/4$, is always positive and destabilizing.

The sum of the second, third and fourth term in Eq. (5.144) is always positive (destabilizing) such that in a superadiabatic environment a maximum loop with an upflow cannot be stabilized by a flow with $H_{v0} > 0$. The other three configurations can be stabilized provided that certain conditions are fulfilled.

As example let us consider the *isothermal* case, $T_0 = T_{e0}$, for which the equilibrium is determined by Eq. (5.128). If we insert this condition into the criterion given by Eq. (5.144) we find

$$\beta\delta \,+\, 1 \,-\, \frac{1}{\gamma} \,+\, \frac{5}{2}(\beta r)^2 \,+\, \beta r j \left(\frac{2H_{p0}}{H_{v0}} \,-\, \frac{1}{\gamma} \,+\, \frac{13}{4}\right) \;>\; 0\,. \tag{5.148}$$

In the static case ($\beta r = 0$) which leads to a loop with a maximum (cf. Eq. 5.128) we have

$$\beta\delta \;>\; \frac{1}{\gamma} \,-\, 1 \;=\; -0.4 \tag{5.149}$$

for $\gamma = 5/3$ (this value will also be used in the following numerical examples). Consequently, a static isothermal loop is unstable in both superadiabatic and slightly subadiabatic regions. If we include the velocity terms and assume a constant velocity ($H_{v0} \to \infty$) we find, similar to the case of displacements with infinite wavelength (Eq. 5.129), that an upflow ($j = +1$) always destabilizes while a downflow ($j = -1$) may exert a stabilizing influence provided that

$$\frac{5}{2}(\beta r)^2 \;-\; \beta r\left(\frac{13}{4} - \frac{1}{\gamma}\right) \;<\; 0 \tag{5.150}$$

which means

$$0 \;<\; \beta r \;<\; 1.06 \tag{5.151}$$

For $\beta r > 1$ the loop form changes from a maximum to a minimum. The smallest value that the expression on the l.h.s. of Eq. (5.150) can reach is -0.7 (for $\beta r = 0.53$) which leads to the criterion $\beta\delta > -0.4 + 0.7 = 0.3$. Although some stabilization has been achieved, a constant downflow cannot stabilize an isothermal equipartition loop in the deep convection zone of the Sun where we have $\beta\delta = 3.6$.

In which way does a velocity gradient affect the stability of an isothermal loop? From Eq. (5.148) we see that a velocity which increases with height ($H_{v0} > 0$) has a stabilizing effect in the case of a downflow and a destabilizing effect for an upflow (and vice versa). In the case of a flow with constant mass flux density we have seen in Sec. 5.6 that $H_{v0} \approx H_{p0}$ such that we find the criterion

$$\beta\delta + 0.4 + \frac{5}{2}(\beta r)^2 + 4.65(\beta r j) > 0\,. \tag{5.152}$$

Consequently, a downflow has a stabilizing effect for $0 < \beta r < 1.86$. The velocity terms attain their most negative value for $\beta r = 0.93$ which gives as condition for instability

$$\beta\delta > 1.76 \tag{5.153}$$

Thus an equipartition tube with $\beta\delta = 3.6$ is still unstable. In principle we may expect larger velocity gradients for convective downflows near the bottom of the convection zone or within an overshoot region where the flows are strongly decelerated due to the strong subadiabaticity of the radiative region below. Take for example a large equipartition flux tube ($a_0 = 10^4$ km) near the bottom of the solar convection zone ($H_{p0} = 5 \cdot 10^4$ km, $v_0 = v_{A0} = 100$ m/s which gives $\beta r = 2.5$, $\beta\delta = 3.6$). We find from Eq. (5.148) that a minimum loop formed by such a tube is stable in a downflow provided that $H_{v0}/H_{p0} < 0.4$ or $H_{v0} < 2 \cdot 10^4$ km, a value which does not appear unrealistic. On the other hand, a smaller tube with $a_0 = 10^3$ km and $\beta r = 25$ already requires a value of $H_{v0} < 160$ km in order to be stabilized which is clearly unrealistic. We conclude that minimum loops formed by relatively large, isothermal flux tubes can possibly be stabilized by a strongly decelerating downflow near the bottom of the solar convection zone.

The considerations above were for the isothermal case, i.e. a flux tube which is in temperature equilibrium with its environment. Although there is a natural tendency towards this state due to radiative energy exchange the relevant time scale becomes very large in the deep layers of a convection zone. If a loop has evolved out of an initially horizontal tube and hydrostatic equilibrium along the field lines has been established adiabatically, a temperature difference with respect to a superadiabatic environment is the consequence. A loop with a minimum would be somewhat cooler and a loop with a local maximum somewhat hotter than its surroundings. In order to assess the influence of such a temperature difference on the stability of a loop we define the parameter

$$\alpha \equiv \beta\left(\frac{\rho_{e0}}{\rho_0} - 1\right) \tag{5.154}$$

which expresses the relation between external and internal temperature: If we assume that the mean molecular weight is the same inside and outside the tube we find from Eq. (5.136):

$$\beta\left(\frac{\rho_{e0}}{\rho_0} - 1\right) = 1 - \beta\left(\frac{T_{e0}}{T_0} - 1\right) \tag{5.155}$$

where T_{e0} and T_0 denote external and internal temperature, respectively. Consequently, temperature equilibrium entails $\alpha = 1$ while for a cooler interior we find $\alpha < 1$ and for a hotter interior we have $\alpha > 1$. If the temperature difference $\Delta T \equiv T_0 - T_{e0}$ is small compared to the external temperature we can approximate Eq. (5.155) as

$$\alpha \approx 1 + \beta\frac{\Delta T}{T_{e0}} \tag{5.156}$$

and for equipartition flux tubes near the bottom of the solar convection zone ($T_{e0} = 2 \cdot 10^6$ K, $\beta = 10^6$) we have

$$\alpha \approx 1 + \frac{\Delta T}{2} \tag{5.157}$$

where ΔT is assumed to be given in degrees Kelvin. Using Eq. (5.154) the equilibrium condition (Eq. 5.4) at the point of extremum is written as

$$\alpha + \beta r j = \pm \frac{2H_{p0}}{R_0} . \tag{5.158}$$

If we insert Eq. (5.158) into Eq. (5.144) we obtain the following condition for instability:

$$\beta\delta + \alpha^2 + \frac{1}{\gamma}(1 - 2\alpha) + \frac{5}{2}(\beta r)^2 + \beta r j \left(\frac{2H_{p0}}{H_{v0}} - \frac{1}{\gamma} + \frac{13}{4}\alpha \right) > 0 . \tag{5.159}$$

For given values of $\beta\delta$ and $\beta r j$ we can determine a range of values of α for which the l.h.s. of Eq. (5.159) is *negative* describing a stable loop. For the case $H_{v0} = H_{p0}$ and $\gamma = 5/3$ this is achieved by solving the quadratic inequality

$$\alpha^2 + \alpha P + Q < 0 \tag{5.160}$$

where

$$\begin{aligned} P &= \frac{13}{4}(\beta r j) - \frac{6}{5} \\ Q &= \beta\delta + \frac{5}{2}(\beta r)^2 + \frac{7}{5}(\beta r j) + \frac{3}{5} \end{aligned}$$

This inequality has a range of real solutions provided that $W \equiv P^2/4 - Q \geq 0$ which leads to the condition

$$\frac{9}{64}(\beta r)^2 - \frac{67}{20}(\beta r j) - \frac{6}{25} - \beta\delta \geq 0 . \tag{5.161}$$

For an equipartition flux tube in an external downflow ($j = -1$) within the deep layers of the convection zone ($\beta\delta = 3.6$) we find that Eq. (5.161) is satisfied for $\beta r > 1.1$. For example, if we take $\beta r j = -2$, Eq. (5.160) is fulfilled for $2. < \alpha < 5.7$, i.e. if the tube is slightly hotter than its environment. The equilibrium condition (Eq. 5.158) shows that this case refers to a loop with a maximum. Minima can be stabilized by an upflow ($j = +1$) in which case Eq. (5.161) is satisfied for $\beta r > 24.9$. For example, if we take $\beta r j = 25.$ we find that Eq. (5.160) is fulfilled for $-40.57 < \alpha < -39.48$, i.e. a cool loop which forms a minimum. Generally we can conclude from Eqs. (5.160/161) and (5.158) that in the case $H_{v0} = H_{p0}$ and $\beta\delta = 3.6$ only *cool minima in an upflow and hot maxima in a downflow represent a stable configuration* provided that the temperature difference and the flow velocity correspond to the relationship expressed by the above inequalities.

From the bottom to the middle parts of the solar convection zone the integrated temperature difference between adiabatic and actual stratification amounts to only $\Delta T \approx 1$K (Parker, 1987) such that Eq. (5.157) gives rather small values for the parameter α. Consequently, the estimates discussed above suggest that unless more efficient cooling or heating takes place (e.g. if a loop sinks down from the top layers of the convection zone) thermal effects in conjunction with drag forces cannot effectively stabilize flux tubes with or without loops in a stellar convection zone.

5.8 Summary of the stability properties

The formalism derived in Secs. 5.3/4 provides a tool which can be used to investigate the stability of a wide class of flux tube equilibrium structures. In most cases, however, a numerical treatment of the resulting eigenvalue problem is necessary. Such an undertaking is intended for the future but outside the scope of the work presented here. However, we have been able to determine analytically the stability properties in a number of cases which are not without general relevance. We have considered in particular

- horizontal flux tubes with purely vertical and wave-like displacements (Sec. 5.6),
- symmetric loops with perturbations of small wavelength (Sec. 5.7.1),
- symmetric loops with purely vertical displacements (infinite wavelength) (Sec. 5.7.2), and
- symmetric loops with displacements of large wavelength (Sec. 5.7.3).

For *horizontal flux tubes* we have generalized the results of Spruit and van Ballegooijen (1982) to the case of a vertical external flow. The monotonic instability found by these authors can be stabilized if the flow speed has a large gradient, for example by a downflow whose velocity strongly decreases with depth. If perturbations with finite wavelength along the flux tube are considered the value of the quantity βr has to be within a specific range for this stabilization to become effective. Irrespective of the direction or gradient of the flow, sufficiently large values of βr (due to small field strength, small radius, or large velocity) provoke monotonic instability caused by the radius change of the tube during its displacement. An estimate based on the properties of the deep layers of the solar convection zone shows that the effect of a downflow with constant mass flux density is insufficient to prevent isothermal equipartition flux tubes from monotonic instability due to the superadiabatic stratification.

The monotonic mode has been investigated also for the case of a *symmetric loop* structure with a horizontal tangent vector at the point of extremum (maximum or minimum). We have derived the exact solution for constant vertical displacements (infinite longitudinal wavelength) and used it as a guideline and test for a heuristic approach which allowed to treat also the case of large (but finite) wavelength. This represents the most unstable perturbation for horizontal tubes and it turned out that this is true also for symmetric loop structures. In the absence of an external flow, all loops (maximum or minimum) are monotonically unstable in a superadiabatic or slightly subadiabatic environment. A flow may exert a stabilizing influence: For an isothermal tube, a downflow with values of βr within a certain range stabilizes. In particular, a strongly decelerating downflow leads to a stable minimum loop even if $\beta\delta = 3.6$. If the tube is non-isothermal, cool minima in an upflow or hot maxima in a downflow may be stabilized in a superadiabatic region provided that the temperature difference and, again, the value of βr are within specific intervals. As for horizontal tubes, sufficiently large values of βr always lead to instability.

While monotonic instability preferentially evolves for displacements with large (but finite) wavenumber in the longitudinal direction, another mode of instability preferentially appears for large wavenumbers, i.e. *overstable transversal oscillations.* In the case of overstability, the drag force conspires with the magnetic tension force such that oscillations with growing amplitude result. For a horizontal tube this requires a downflow and is restricted to a certain interval of values for βr. The fact that overstability occurs preferentially for large wavenumbers suggests a local analysis for non-horizontal equilibrium tubes. We have carried out such an analysis for symmetric loops and found that from the four possible combinations of loop geometry (minimum/maximum) and flow (up/down) overstability is excluded for the minimum loop with an upflow. For the other cases overstability may appear within specific intervals for βr. In the case of an *isothermal* flux tube, however, overstability is restricted to maximum loops with downflow while a *neutrally buoyant* loop may only become overstable if it represents a maximum with an upflow. Since the approximation of slender flux tubes demands that the perturbation wavelength is large compared to the flux tube radius while overstability requires small wavelengths, the applicability of the present results is restricted to tubes of sufficiently small radius. Apart from the effects discussed so far, the introduction of external flows and drag forces leads to a decrease of the growth rates of unstable perturbations which is most significant for oscillatory instability.

The excitation of the overstable mode depends only on the direction of the flow and the value of βr; in particular, it cannot be stabilized by the stratification and therefore may appear also in convectively stable layers like overshoot zones or regions in radiative equilibrium. Excited locally, for instance in a loop formed by a downflow or an upflow, such oscillations could propagate as transversal tube waves. Under the influence of rotationally induced Coriolis forces these waves may even exhibit helicity and contribute to the field-regeneration mechanism which is necessary for the operation of a dynamo. In order to investigate this conjecture we have to extend the present formalism by moving to spherical geometry and including a (differential) rotation.

Convective flows in the deep parts of the solar convection zone have a typical time scale of the order of a month. Even a stable, stationary flux tube configuration within the convection zone cannot be expected to exist for a significantly longer time. This is in general accordance with the lifetime of large active regions. We have found that stable flux tube equilibria within a superadiabatic region require fine-tuned relations between the various parameters which determine the equilibrium such that they probably are not of great practical importance. A realistic convection zone, of course, is much more complicated than can be expressed by the simple analytical examples treated here. For example, the superadiabaticity probably shows significant spatial variations, be it between upflow and downflow regions or related to differential rotation (Durney, 1989). Hence, the estimates given in the preceding sections must not be taken too serious; however, they strongly indicate that, in the long run, the unstable stratification of the convection zone itself cannot be overcome.

6. Dynamics of flux tubes in a convection zone

In the preceding chapters we have investigated in some detail certain aspects of the structure and dynamics of concentrated fields. We may have obtained some pieces of a yet unfinished jigsaw puzzle in this way but we certainly are not in a position to present a full theory. In the present chapter we shall nevertheless try to sketch a tentative picture of the magnetic field dynamics in stellar convection zones, based upon our own results and on the work of other researchers. This picture is largely based on heuristic arguments, sometimes supported by more solid results. It is not thought as a comprehensive model but more as an orientation and stimulus for further work.

6.1 Size distribution

We have already discussed in Ch. 2 that the magnetic Rayleigh-Taylor instability and other fragmentation processes tend to produce magnetic structures with sizes of less than 100 km within the convection zone. Fragmentation proceeds until the fragments are so small that they merge by magnetic diffusion as fast as they are formed, i.e. until the diffusive time scale becomes equal to the growth time of the instability considered. For the case of the interchange instability this minimum fragment size, d_i, is given by Eq. (2.12) which we repeat here:

$$d_i \;=\; \left(\frac{2\,R\,\eta^2}{v_A^2}\right)^{1/3} \qquad (2.12) = (6.1)$$

(R: radius of curvature, η: magnetic diffusivity, v_A: Alfvén velocity). Taking equipartition fields, i.e. Alfvén velocity equal to v_c, the typical velocity of convective flows, and R equal to L, the length scale of the convective flows, we can determine d_i for different depths in the solar convection zone using the model of Spruit (1977b). For this rough estimate we use the depth as typical size of the dominant convective cell. The result is given in the following table:

Depth (cm)	η (cm^2·s^{-1})	v_c (cm·s^{-1})	d_i (cm)	d_r (cm)	τ_r (s)	τ_s (s)
$1.0 \cdot 10^8$	$1.5 \cdot 10^6$	$1.3 \cdot 10^5$	$3.0 \cdot 10^3$	$3.4 \cdot 10^4$	$7.7 \cdot 10^2$	$3.0 \cdot 10^{-1}$
$1.0 \cdot 10^9$	$1.0 \cdot 10^5$	$3.2 \cdot 10^4$	$2.7 \cdot 10^3$	$5.6 \cdot 10^4$	$3.1 \cdot 10^4$	$9.1 \cdot 10^2$
$1.0 \cdot 10^{10}$	$7.8 \cdot 10^3$	$9.1 \cdot 10^3$	$2.5 \cdot 10^3$	$9.3 \cdot 10^4$	$1.1 \cdot 10^6$	2.1
$1.8 \cdot 10^{10}$	$7.5 \cdot 10^3$	$4.9 \cdot 10^3$	$4.4 \cdot 10^3$	$1.7 \cdot 10^5$	$3.7 \cdot 10^6$	2.3

Tab. 8: Properties of magnetic filaments as a function of depth in the solar convection zone. η: molecular magnetic diffusivity; v_c: convective velocity; d_i: diffusive scale for the interchange instability; d_r: resistive boundary layer thickness; $\tau_r = d_r^2/\eta$: resistive diffusion time; τ_s: radiative diffusion time on spatial scale d_i.

The table also gives d_r, the thickness of the resistive boundary layer:

$$d_r = \left(\frac{L\,\eta}{v_c}\right)^{1/2}. \tag{6.2}$$

This quantity is determined by the balance of magnetic diffusion and advection by convective flows and represents the scale of structures formed by kinematical magnetic flux expulsion. The relevant time scale for this process is the eddy turnover time, L/v_c, which is equal to the resistive diffusion time on the spatial scale d_r, viz.

$$\tau_r = \frac{d_r^2}{\eta}. \tag{6.3}$$

In the dynamical case Eq. (6.2) still gives a lower limit: Structures smaller than d_r diffuse too rapidly to be held together by the convective cell and therefore cannot be sustained individually. On the other hand, we see from Table 6.1 that always $d_i < d_r$ which means that the growth time for the interchange instability for a structure of size d_r is shorter than its diffusion time, i.e. the time scale of flux expulsion. Consequently, even if flux expulsion produces structures with sizes larger than d_r, these are actually bundles of smaller filaments with a typical size d_i. It is the very influence of the collecting flow itself which leads to fragmentation: It provokes interchanging by deforming the magnetic structures as well as by exerting a destabilizing pressure gradient at the interface between magnetic and non-magnetic gas (see the discussion in Schüssler, 1984b).

The last column in Table 6.1 gives the radiative diffusion time, the time scale which determines the heat exchange between a fragment of size d_i and its environment,

$$\tau_s = \frac{d_i^2}{\eta_s}, \tag{6.4}$$

with the radiative diffusivity η_s given by

$$\eta_s = \frac{16\,\sigma\,T^3}{3\,\rho^2 c_V \kappa_R} \tag{6.5}$$

(σ: Stefan's radiation constant; T: temperature; c_V: specific heat capacity; κ_r: Rosseland mean opacity). For both resistive and thermal diffusion we have assumed that turbulence on length scales smaller than the filament size which could give rise to turbulent diffusivities is suppressed by the magnetic field. If the field is in equipartition with flows on the dominant convective scale it will always be stronger than the respective equipartition field on any other scale of the convective/turbulent velocity field.

We find from Table 6.1 that τ_s is very small compared to any relevant dynamical time scale throughout the whole convection zone. This statement remains valid if the larger spatial scale d_r is used in Eq. (6.4). Furthermore, since we always have $d_i < d_r$, the diffusion time on the scale of the filaments, d_i, is shorter than the dynamical time scale $L/v_c = \tau_r$. Consequently, for magnetic structures which have been fragmented down to the resistive diffusion limit, $d_i < 100$ m, as well as for structures of the size of the resistive boundary layer, $d_r \approx 1$ km, which are formed by flux expulsion, two statements can be made which become important in the following sections:

- The magnetic diffusion time is small enough to allow *mass exchange* between magnetic structures and their surroundings within a dynamical time scale (e.g. while being stretched by differential rotation), and
- the thermal diffusion time is sufficiently small to ensure *temperature equilibrium* between interior and exterior of a filament during its dynamical evolution.

As we have seen above, convective flows accumulate magnetic flux and form larger structures which appear in the form of bundles of small filaments, not monolithic flux tubes. For spatial scales which are much larger than the filament size a mean field treatment can be employed (cf. Parker, 1982b) and appropriate turbulent diffusivities have to be used. Knobloch (1981; see also Knobloch and Rosner, 1981, and references therein) has taken this approach and used the scaling laws given by Galloway et al. (1978) for nonlinear Boussinesq magnetoconvection to estimate a size spectrum of magnetic structures in a turbulent fluid for which he assumed a Kolmogorov spectrum with a (viscous) cut-off. Even without taking into account fragmentation processes he found that most of the structures have sizes at or below the length scale defined by the cut-off. He comes to the conclusion that larger structures can only be formed in the form of flux tube bundles whose size distribution is difficult to obtain.

This may not be the whole story though: A mechanism not mentioned so far is *coalescence* of two parallel twisted flux tubes with the same sense of twist (Parker, 1982e, 1983a,b; Bogdan, 1984; Choudhuri, 1988). If the tubes collide a neutral sheet forms at their interface, the azimuthal field reconnects and builds a binding sheath of magnetic flux about both tubes. An azimuthal field component at the same time exerts a stabilizing influence with respect to the interchange and Kelvin-Helmholtz instabilities. Consequently, besides advection by convective flows and fragmentation, coalescence may be another important factor which determines the size spectrum of flux tubes in the convection zone. First attempts to include this effect in a consistent treatment of the size distribution have been made by Bogdan and Lerche (1985) and by Bogdan (1985) who found that, in principle, sunspot-size structures can be produced within the convection zone. However, the models used so far are very idealized and it is not clear whether the results hold under more realistic conditions, i.e. non-straight flux tubes, inclusion of fragmentation processes, convective and Parker-type instability, advection by large scale flows, magnetic buoyancy. All these effects tend to either fragment large structures or to quickly remove them from the deeper layers of the convection zone. It seems doubtful that under these conditions sunspot-size structures can be formed but this claim can be substantiated or disproved only by more detailed models which include also the more subtle effects of flux tubes and flux tube arrays in a convectively unstable medium like ‘convective counterflow’ (Parker, 1985a,b) and ‘convective propulsion’ (Parker, 1979e).

How can we reconcile our picture of the magnetic field in the deep convection zone as an ensemble of very thin flux tubes with observations of the surface fields where a whole spectrum of structures from large spots to small magnetic elements is present? The key to an answer seems to be the fact that except for the first phase of flux emergence in an active region only *fragmentation* of large structures into smaller structures is observed, never the opposite process: Old active regions do not ‘rejuvenate’ and again form pores or spots unless new magnetic flux erupts. The lognormal distribution of sunspot umbral areas found by Bogdan et al. (1988) also is consistent with their origin in a fragmentation sequence.

We can understand the observation of large sunspots in view of a convection zone which continually shreds and fragments magnetic structures if the magnetic flux does not originate there but is injected in large portions from below (where it resides in a non-fragmented form) and rises rapidly to the surface. Indeed, flux emergence and the appearance of large structures at the surface always take place within the very first days of the life of an active region. The simulations of Moreno-Insertis (1984, 1986) show that a kink-unstable large flux tube traverses the convection zone and breaks out at the surface within a few days. Even within this short time fragmentation apparently has occurred since a whole spectrum of structures appears at the photosphere and large sunspots always form out of a number of pieces (McIntosh, 1981) which seem to know where to go (the “rising magnetic tree” of Zwaan, 1978): Initially the rise and emergence of only weakly fragmented parts of the erupting flux tube is faster than the ongoing fragmentation processes.

After flux emergence has come to an end, fragmentation proceeds until all magnetic flux at the surface is in the form of small network elements with a size of about 100 km*. In the deep convection zone, all flux tends to become fragmented down to the diffusion limit. The formation of filament bundles by convective flows and flux tube coalescence may lead to somewhat larger structures but their actual size distribution is difficult to determine. In any case, these structures are very fragile: They are always subject to the various instabilities and fragmentation processes and filament bundles are closely coupled to the changing pattern of convective flows. We do not believe that large active regions and sunspots are formed in this way: It seems impossible to store even moderately large flux tubes within the convection zone for a sufficiently long time against their inherent buoyancy and instability. Large active regions probably are direct evidence for the genuine dynamo process operating on a more ordered field in a less unstable environment than the convection zone proper.

6.2 The relation of the basic forces

We have argued in Ch. 2 and Sec. 6.1 that the magnetic field in a stellar convection zone consists of an ensemble of small filaments whose dynamics can be described with aid of the approximation of slender flux tubes discussed in Ch. 3. We found that the evolution of a flux tube is determined by three basic forces, the *buoyancy force* F_B, the *curvature force* F_C and the *drag force* F_D, all of which are directed perpendicular to the flux tube axis while gravity and gas pressure determine the momentum balance in the direction along the field lines.

Let us discuss the relative importance of these forces under the physical conditions in a convection zone. If we presume temperature equilibrium between the flux tube and its environment (a reasonable assumption for small filaments as we have seen in the preceding section) we may use Eqs. (3.26) and (3.28) to obtain the order of magnitude of the various forces per unit length of the flux tube:

$$F_B = \frac{B^2\,a^2}{8\,H_{pe}} \tag{6.6}$$

$$F_C = \frac{B^2\,a^2}{4\,R} \tag{6.7}$$

$$F_D = C_D\,\rho_{e0}\,a\,v_\perp^2 \tag{6.8}$$

(a: flux tube radius, H_{pe}: external pressure scale height, ρ_{e0}: external density, $v_\perp$: velocity component perpendicular to the flux tube due to large scale convection, differential rotation or the motion of the flux tube itself, R: radius of curvature). Ignoring factors of order unity we may write for the ratio of buoyancy and curvature force to drag force, respectively:

$$\frac{F_B}{F_D} = \left(\frac{a}{H_{pe}}\right)\left(\frac{B}{B_e}\right)^2\left(\frac{v_c}{v_\perp}\right)^2 \tag{6.9}$$

$$\frac{F_C}{F_D} = \left(\frac{a}{R}\right)\left(\frac{B}{B_e}\right)^2\left(\frac{v_c}{v_\perp}\right)^2. \tag{6.10}$$

* This size is much larger than the resistive scale because surface fields can temporarily achieve stable configurations and resist further fragmentation. This is further discussed in Sec. 6.3.

Here $B_e = v_c\sqrt{4\pi\rho_{e0}}$ is the equipartition field strength with respect to convective flows of typical velocity v_c. We see from these ratios that for equipartition fields and $v_\perp \approx v_c$ *the drag force dominates the dynamics of a thin flux tube:* $a/H_{pe} \ll 1$ and $a/R \ll 1$ in fact are conditions for the applicability of the approximation of slender flux tubes. For strongly fragmented fields in the deep convection zone they are well met: $a < 1$ km, $H_{pe} \approx 10^4$ km; the curvature force comes into play only for extreme distortions ($R \approx a$) of the filament. Consequently, a magnetic field structured in this way *follows passively any large-scale flow* with relative velocity of the order of the convective velocity, be it convection itself, differential rotation or, possibly, meridional circulation. Only structures with $a \approx H_{pe}$ or larger (flux tubes of sunspot size) or strong fields with $B > B_e$ (partially evacuated flux tubes at the surface) can avoid being severely distorted by large scale flows.

On the other hand, the growing distortion of the tube leads to an increase of its length and, if the mass content stays constant, to an increase of the field strength. In the case $\beta \gg 1$ we find that the change of the magnetic field strength is proportional to the length increment, i.e.

$$\frac{\Delta B}{B} = \frac{\Delta l}{l}\,. \tag{6.11}$$

Doubling the flux tube length doubles the field strength and the curvature force increases by a factor 4. Consequently, a flux tube with constant mass content quickly becomes dynamically active and resists to further distortion and stretching. The curvature force increases rapidly and a balance between curvature and drag force establishes itself. However, the assumption of a constant mass content does not hold for two important cases:

- The distortion of flux tubes is strongest in the upper layers of the convection zone where the flow velocities are large. Here the density is small and if parts of the tube are still located in the deep layers they represent a large mass reservoir: Matter can flow along the tube to fill the volume created by stretching the tube, and
- for small filaments formed by the various fragmentation processes and instabilities we have seen in the preceding section that the diffusive time scale is smaller than the dynamical time scale which governs the distortion process. Consequently, matter can diffuse into the flux tube rapidly enough to fill the volume created by its distortion. This is particularly relevant for the deep layers where no further mass reservoir exists for flux tubes contained within the convection zone.

Of course, both mechanisms can be relevant for the same flux tube. Their effect is to keep the flux tube in a state of passiveness with respect to further stretching. We conclude that due to instability and fragmentation the magnetic field structures that reside in the convection zone for an extended period of time (i.e. longer than about a month, the dynamical time scale in the deep layers) are passive with respect to external flows (convection, differential rotation, meridional circulation), i.e. they are strongly coupled to and distorted/fragmented by these flows and probably never reach an equilibrium.

An exception from this rule are large flux tubes whose radius is of the order of the local scale height or larger. Here all three basic forces may become comparable and the results concerning equilibrium structure and stability obtained in Chs. 4 and 5 can be applied. We have found that in most cases such a flux tube is unstable and parts of it rapidly erupt towards the surface layers while other parts sink down below superadiabatic layers of the convection zone. Although the applicability of the approximation of slender flux tubes is somewhat doubtful for such large tubes we believe that the results are qualitatively correct also in this case. Another exception from the rule of passive magnetic fields are the flux tubes in the surface layers. They will be discussed in the following section.

6.3 The peculiar state of the surface fields

The observable surface layers of a star like the Sun are quite different from the state of the deep convection zone. They represent the transition region between the strongly superadiabatic top of the convection zone and the stably stratified photosphere where most of the energy carried by the overshooting convective motions escapes into space by means of radiation. The gas is strongly stratified since the relatively low temperature leads to a small scale height while the temperature fluctuations become a significant fraction of the temperature itself.

Under these conditions magnetic fields can be concentrated to field strengths far beyond equipartition with convective motions. Magnetic fields are swept to the granular downflow regions and concentrated to about equipartition by the horizontal flows of granular convection. These flows at the same time are responsible for carrying heat to the downflow regions which compensates for the radiative losses. Since the growing magnetic field retards the motions it throttles the energy supply and the magnetic region cools down. This leads to an increase of the magnetic field since the gas pressure in the magnetic region becomes smaller. Furthermore, hydrostatic equilibrium on the basis of a reduced temperature tends to reestablish itself via a downflow which gives rise to the *superadiabatic effect* (Parker, 1978): An adiabatic downflow in a magnetic flux tube which is thermally isolated from its surroundings leads to a cooling of the interior with respect to the superadiabatically stratified surroundings and a partial evacuation of the the upper layers ensues. Pressure equilibrium with the surrounding gas is maintained by a contraction of the flux tube which increases the magnetic pressure. In this way, the magnetic field can be locally intensified to values which are only limited by the confining pressure of the external gas.

It has been shown by a number of authors (Webb and Roberts, 1978; Spruit and Zweibel, 1979; Unno and Ando, 1979) that the superadiabatic effect in the case of a vertical flux tube which is in magnetostatic and temperature equilibrium with its environment drives a *convective instability* in the form of a monotonically increasing up- or downflow. Consequently, the initial downflow due to the radiative cooling is enhanced by this effect leading to an even stronger amplification of the magnetic field, a process which is often referred to as *convective collapse.* A more detailed discussion of this process has been given elsewhere (Schüssler, 1990).

Cooling due to suppression of convective motions and the superadiabatic effect have the consequence that most of the observed magnetic flux in the solar photosphere has a field strength in excess of the equipartition value of a few hundred Gauss. It is organized in a hierarchy of structures which have a magnetic pressure comparable to the gas pressure in their apparently non-magnetic environment. This hierarchy extends from large sunspots (diameter $> 5 \cdot 10^4$ km, field strength up to 4000 Gauss) to small magnetic elements (diameter < 200 km, field strength about 2000 Gauss at optical depth unity). In contrast to the circumstances in the deep convection zone which have been discussed in the preceding section, under these conditions *buoyancy* becomes the dominating force. Taking 500 Gauss for the equipartition field strength and using Eq. (6.9) we find that F_B/F_D, the ratio of the buoyancy to the drag force due to convective motions, is of the order of 10 for magnetic elements ($a = 100$ km, $B = 2000$ Gauss) and amounts to about 3000 for large sunspots ($a = 10^4$ km, $B = 4000$ Gauss). By the dominance of buoyancy the magnetic structures are forced to become straight and vertical in the surface layers: A very small inclination suffices to compensate any drag force exerted by the external velocity fields (Schüssler, 1986, 1987).

Besides the ability to resist from being distorted and deformed by convective motions another peculiarity of the surface fields is the existence of configurations which are (at least temporarily) stable with respect to the interchange instability and other fragmentation processes. Buoyancy and the large field strength prevent the flux concentrations from being disrupted by local convection. Large structures like sunspots (magnetic flux larger than about 10^{19} mx) are stabilized against the interchange instability by buoyancy (Meyer et al., 1977) while small magnetic elements (magnetic flux less than a few times 10^{17} mx) may be stabilized by whirl flows which surround them (Schüssler, 1984b). Such whirls form naturally in the narrow downflow regions of convection in a strongly stratified medium (e.g. Nordlund, 1985a). These downflows are enhanced around small magnetic flux concentrations by thermal effects (Deinzer et al., 1984).

The existence of two regimes of stable magnetic flux tubes connected by a range of magnetic configurations which are subject to the interchange instability certainly should have an influence on the observable size distribution of magnetic structures. On the one hand large sunspots may live for an extended period of time during which they only show a slow decay while, on the other hand, small features exist with sizes up to the limit where the stabilization due to a surrounding whirl flow becomes inefficient. The verticality of the magnetic structures due to the dominating buoyancy force facilitates their organization in a network pattern defined by the downflow regions which are the loci of convergence of the horizontal convective flows. The probability of encounters and coalescence is much larger within such a network than for a more random spatial distribution. For all these reasons we think that observed size distributions of surface fields (e.g. Spruit and Zwaan, 1981) are by no means representative for the conditions in the deep layers of the convection zone where most of the effects which determine the particular properties of surface fields become irrelevant.

The special properties of the surface fields are restricted to the photosphere and the rather narrow layer of strong superadiabaticity in the upper convection zone of about 1000 km depth. As discussed in more detail elsewhere (Schüssler, 1987) the non-observation of a systematic dependence of the dynamics of observed flux concentrations on their size together with a consideration of the dominating forces strongly support the cluster model of sunspots (Parker, 1979c; Spruit, 1981b). This model assumes that a spot is a conglomerate of a large number of small magnetic filaments with a diameter of 100 to 1000 km which are closely packed due to buoyancy in the uppermost layers of the convection zone to form the visible spot umbra. Below some merging level (which is situated not much deeper than 1000 km) the spot splits into its fibril components which are passive with respect to the convective motions which continually stretch and distort them; this causes the slow decay of the spot and the fragmentation of its magnetic flux into the network fields.

We have seen that the observable surface fields probably are in many respects different from the conjectured properties of the magnetic fields in the deep layers of the convection zone. The strong superadiabaticity of the uppermost convective layers and the thermal effects associated with the radiative release of the transported energy into free space entail a number of peculiar effects which cannot be expected to operate in the main body of the convection zone. Only at the surface can we expect the field strength to significantly exceed the equipartition limit and only there do we find mechanisms which can stabilize magnetic flux tubes from being quickly disrupted by instabilities. Consequently, it is improbable that a flux concentration observed at the surface maintains its identity as a single flux tube throughout the whole or even a significant part of the convection zone. Visible sunspots and all other observed structures probably fragment into small filaments below about 1000 km depth. These filaments with sizes down to the diffusion limit are passive with respect to the convective motions, they are stretched and deformed, accumulated and dispersed by the action of the dominating drag forces. Due to their inherent stability, the surface fields can tolerate the distortion of their 'roots' for a certain amount of time until they are forced to react accordingly, be it by slowly dispersing and eventually breaking apart as in the case of sunspots, be it by a continuous rearrangement of the small-scale fields in the supergranular network.

6.4 Consequences for the dynamo problem

The presently favored tool to describe the origin of solar activity is the theory of dynamo action in a turbulent medium which started with the pioneering work of Parker (1955). Beginning in the 1960s the next landmark was placed by the Potsdam group (Krause, Rädler, Rüdiger, Steenbeck and others; see Krause and Rädler, 1980, for an overview) who used a statistical approach (mean field theory) in the kinematical limit (passive magnetic field, no back-reaction on the turbulent flows). They found the so-called α-*effect* which can lead to dynamo action in turbulent fluids which lack mirror symmetry, e.g. due to the influence of rotation. Many large-scale properties of the solar cycle could be successfully reproduced by '$\alpha\omega$-dynamos' which are based on the combined induction effects of turbulence (α) and differential rotation (ω). Reviews of these models have been given, among others, by Stix (1976, 1981a, 1982), Parker (1979a) and Yoshimura (1981).

It was again Parker (1975a) who raised doubt concerning the theory of turbulent dynamo action *within* the convection zone. He argued that, if most of the toroidal magnetic flux is in the form of large flux tubes as indicated by the existence of sunspots and active regions, it cannot be stored in the convection zone for times comparable with the solar cycle period: Buoyancy removes magnetic flux from the convection zone much too fast for the induction mechanisms to operate efficiently, in particular for the differential rotation to generate a sufficient amount of toroidal magnetic flux within a cycle period. The instabilities of flux tubes due to superadiabaticity, flows along the field lines, rotation and external flows investigated by Spruit and van Ballegooijen (1982), van Ballegooijen (1983), Moreno-Insertis (1984, 1986), van Ballegooijen and Choudhuri (1988), and in Ch. 5 of this work aggravate the problem even more.

The assumption of very small flux tubes or of a large turbulent viscosity may reduce the velocity of buoyant rise drastically (Unno and Ribes, 1976; Schüssler, 1977; 1979; Kuznetsov and Syrovatskii, 1979) but, on the other hand, leads to a strong coupling between the flux tubes and the convective flows which would destroy their azimuthal orientation and quickly raise them to the solar surface within the convective time scale of about one month. Again, the flux cannot be contained within the convection zone for a sufficiently long time.

Recently it has been argued by Parker (1987a,d) that the magnetic flux observed to emerge in large complexes of activity of relatively small latitude extension would fill as an equipartion field a considerable part of the underlying convection zone and interfer significantly with the convective energy transport. He proposed that the suppression of vertical convective heat transport by a band of horizontal (azimuthal) field in a convection zone leads to an overlying 'thermal shadow', i.e. a cool region of enhanced density, whose weight could balance the magnetic buoyancy and thus keep the field down within the convection zone. He studied in some detail the convective flows set up by a thermal shadow (Parker, 1987b) and the Rayleigh-Taylor instability caused by the pile-up of heat beneath the magnetic layer (Parker, 1987c). He envisages that a thermal relaxation oscillation evolves which leads to the intermittent eruption of magnetic flux in the form of rising, hot plumes (Parker, 1988a). The dynamical instability of a flux sheet of finite lateral extent with respect to sideways displacements leads to a lateral velocity of the order of a few m/s which he connects with the observed latitudinal motions of the solar activity belts (Parker, 1988b).

Parker's conjecture is based on a number of illustrative calculations of idealized problems in order to permit an analytical treatment. While the thermal shadows may well have important dynamical effects it is not shown that they can keep large amounts of magnetic flux in the superadiabatic parts of the convection zone for time intervals comparable to the period of the solar cycle. Actually, in view of the instabilities discussed by Parker himself (Rayleigh-Taylor instability of top and bottom, lateral dynamical instability) and the quick disruption of a magnetic layer even in a stably stratified region (Cattaneo and Hughes, 1988), this seems to be rather improbable.

However we turn the problem, we run into difficulties if we assume the dynamo to operate within the convection zone proper. If the magnetic field is organized in large, dynamically active structures, these are unstable, buoyant and rapidly lost from the deep layers of the convection zone. If the field is diffuse or consists of very small structures (the latter view is favored in this work), it is passive with respect to the motion of the fluid (convection, rotation, ...) and will be carried to the surface within the convective time scale. Moreover, such a passive field is not in accordance with basic features of solar activity: In a large active region, magnetic flux erupts coherently in large quantities and within a few days; large sunspots form which comprise a significant fraction of the total flux erupting during the cycle; Hale's polarity rules are obeyed nearly strictly, not in a statistical sense. On the other hand, the relative velocities due to differential rotation and the convective velocities are of the same order of magnitude as is well known from surface observations (e.g. Schröter, 1985) and also shown by the rotational splitting of p-modes for the deeper layers of the convection zone (e.g. Duvall et al., 1987; Brown et al., 1989; Dziembowski et al., 1989). How can passive fields be predominantly toroidal and obey the polarity rules under such conditions ?

We cannot avoid the conclusion that the original source region at least of the large, sunspot-forming active regions cannot be the convection zone proper. It cannot be the radiative core of the Sun either since the time scale of 22 years for the magnetic cycle does not allow a penetration into the radiative interior because of its large electrical conductivity which leads to a skin effect. Consequently, a number of authors (Spiegel and Weiss, 1980; Galloway and Weiss, 1981; van Ballegooijen, 1982a,b; Schmitt and Rosner, 1983; Schüssler, 1983; DeLuca and Gilman, 1986; Durney, 1989; Durney et al., 1990) have proposed a boundary layer of overshooting convection below the convection zone proper as a favorable site of the solar dynamo. There, in a region of 'mild' convection and turbulence, we may suppose that differential rotation dominates all other velocity fields and generates predominantly toroidal magnetic fields. The failure of large-scale simulations to reproduce the observed characteristics of solar activity (in particular, the direction of the latitude drift of the activity belts) by dynamically consistent 3D-models of the convection zone (Gilman and Miller, 1981; Gilman, 1983; Glatzmaier, 1985a) led their proponents to the same conclusion (Glatzmaier, 1985b).

The subadiabatic stratification of an overshoot region alleviates the stability problems and a number of mechanisms is available which may hold a growing toroidal magnetic flux there for a time comparable with the cycle period (cf. Schüssler, 1983). We may note in particular the 'turbulent diamagnetism' briefly discussed in Sec. 2.2, which is akin to the flux expulsion process and transports magnetic flux antiparallel to a gradient of turbulent intensity. Krivodubskii (1984, 1987) has given quantitative estimates of the diamagnetic effect using models of the solar convection zone. Since, at least in the kinematical limit, this mechanism operates equally well for vorticity (Schüssler, 1984a) it leads to the formation and maintenance of a magnetic shear layer at the bottom of the convection zone (including the overshoot region), just the situation we envisage as a favorable setup for the operation of the solar dynamo.

Besides differential rotation we need a regeneration mechanism for the poloidal field component in order to close the dynamo cycle. Such a mechanism might be provided by the usual α-effect due to cyclonic convection or by an analogous electromotive force generated by waves propagating along the toroidal field in a rotating system. Examples of such waves are slow magnetostrophic waves driven by the magnetic Rayleigh-Taylor instability (Schmitt, 1984; 1985) or transversal flux tube waves excited by differential rotation (van Ballegooijen, 1983) or overstability in an external flow as described in Ch. 5. A boundary layer dynamo model may thus show many of the properties of the 'classical' $\alpha\omega$-dynamo models which have been so successful in describing basic features of the solar cycle. This supports the conjecture that the mathematical description of the field regeneration mechanism (i.e. a mean current parallel to the mean field) in the mean induction equation is basically correct. Note, however, that a kinematical approach is not justified for a boundary layer dynamo as envisaged above since the magnetic and kinetic energy densities are comparable for equipartition fields. A consistent theory for an α-effect in an overshoot region with a strong magnetic field, shear flow and weak turbulence remains to be developed.

Eventually, magnetic flux is released into the convection zone proper by instability or buoyancy. The length and time scales of the formation of large active regions are well in agreement with the characteristics of the eruption of a kink-unstable large flux tube originally situated near the bottom of the convection zone (Moreno-Insertis, 1984; 1986). Moreover, we could think about a modification of Parker's thermal shadow scenario: If the amount of magnetic flux is small enough that it 'fits' into the subadiabatic overshoot layer there is almost no interference (except from opacity effects, cf. Parker, 1984b) with the energy flux which is mainly carried by radiation – neither a shadow nor a significant pile-up of heat evolve. If the magnetic flux layer intrudes significantly into the superadiabatic convection zone proper a thermal shadow and a pile-up of heat in the magnetic overshoot region are the consequence. Both effects provoke Rayleigh-Taylor instability and the whole magnetic layer is disrupted and erupts towards the surface: a large active region is born. In this picture the thermal shadow does not primarily keep the flux submerged but, on the contrary, is the agent of the eruption of magnetic flux. It is tempting to speculate whether the larger efficiency of differential rotation in generating azimuthal magnetic field near the equator might provide the excess azimuthal flux that drives the magnetic layer unstable and produces large active regions while the azimuthal flux in the polar regions always fits into the subadiabatic region.

As shown by Choudhuri and Gilman (1987) and Choudhuri (1989) the influence of rotation on the dynamics of rising loops might be quite significant. In order to avoid the flux erupting in the polar regions either the flux density in the overshoot region must be quite high, i.e. of the order of 10^5 Gauss – which alleviates the storage space problems pointed out by Parker (1987a) but increases the buoyancy problems – or the transport is dominated by the drag of predominantly radial convective flows whose motion the magnetic fields passively follow. Obviously, the rôle of rotation in the transfer of magnetic fields in a convection zone deserves further consideration.

Altogether, the results obtained here support the picture of a boundary layer dynamo sketched above. We have not been able to find a plausible way by which magnetic structures within the convection zone proper could escape from being extremely distorted, dismembered down to the diffusion limit, and eventually becoming completely passive with respect to the convective flows. Large active regions with their specific properties cannot arise from such a kind of field. On the other hand, if a less fragmented magnetic structure at some instant exists in the convection zone (e.g. having been injected from below) in most cases it will immediately become unstable by one of the mechanisms discussed in Ch. 5, part of it will erupt at the surface while another part sinks down into the subadiabatic boundary layer. After flux emergence has come to an end, the magnetic structures are more and more fragmented and shredded until they are merge into the extremely filamented and distorted genuine convection zone fields.

It has been already remarked by Parker (1982b, see also Weiss, 1981c) that an ensemble of passive flux tubes can be described by a kinematic mean field theory in much the same way as in the theory developed by the Potsdam group (see Krause and Rädler, 1980). We may speculate (e.g. Durney, 1989) that part of the field within the convection zone is maintained by a turbulent dynamo in the classical sense which contributes to the background fields at the surface while a boundary layer dynamo provides the source of the big active regions and the large-scale features of solar activity. Anyway, a major revision of the conventional picture of a convection zone dynamo seems to be in order. How the dynamic boundary layer dynamo operates is not understood yet and the detailed study of the dynamics of concentrated fields in a convection zone and its adjacent lower overshoot layer has just started.

7. Outlook

As it turns out so often, most problems remain to be solved. In view of the unsatisfactory state of our understanding of stellar convection and turbulence, a closed and complete theory of magnetic fields in convection zones is not in sight. The theory of photospheric magnetic fields is much more advanced thanks to the availability of detailed measurements and the close connection between theoretical and observational work. Some information about the internal magnetic field and large-scale velocity structure will be obtained in the future by helioseismology but, perhaps with the exception of differential rotation, we are not too optimistic about the prospects of obtaining much more stringent observational boundary conditions. Consequently, besides the ongoing efforts of numerical simulation and the detailed analysis of model problems this field of research will remain open for conjecture, speculation and the presentation of more or less ingenious scenarios.

Numerical simulations will partially substitute unavailable observations. As the development of ever faster computers and sophisticated numerical methods to adequately use them proceeds, simulations will grow more realistic as three-dimensional, compressible MHD calculations with high spatial resolution become available and will provide an immensely useful tool for understanding the magnetic field dynamics in the convection zone. However, in contrast to some fashionable folklore existing and forthcoming numerical simulations do not make other approaches obsolete. The dynamics of motions and magnetic fields in the solar convection zone extends over huge ranges of temporal and spatial scales which in both cases comprise more than ten decades. Since only a small part of these can be covered by any simulation in the foreseeable future, artificial boundaries have to be introduced, certain scales are ignored and others are included only in a parametrized form. Such parametrizations can only be made in a sensible way if they are based on a sound understanding of processes which determine the properties of flows and fields on the scales which they attempt to describe.

We have given some arguments in favor of the conjecture that magnetic fields in stellar convection zones are strongly fragmented and can be treated on the basis of the approximation of slender flux tubes. In the deep parts of a convection zone the scale height is very large such that the approximation is justified even for structures containing the magnetic flux of a whole active region. The investigation of flux tube dynamics in a realistic convection zone is a promising path for future research. Equilibrium structures, stability and dynamical evolution of flux tubes in prescribed velocity fields can be determined on the basis of the methods described in this work, guided by forthcoming 3D simulations of the large-scale convective flows and observational results on differential rotation. As far as the linear stability analysis is concerned, this requires a transformation of the formalism presented in Ch. 5 to spherical geometry and the inclusion of (differential) rotation. For realistic models of convection zones, the equations describing flux tube equilibria and the perturbation equations will have to be treated numerically. Work in this direction is in progress, being done in cooperation with Antonio Ferriz-Mas.

A possibility to gain information about the size distribution of magnetic structures in a convection zone is the application of methods taken from statistical mechanics. The evolution of the properties of an ensemble of flux tubes may be derived from a collisional Boltzmann equation which includes the effect of large-scale flows, diffusion, fragmentation, coagulation and other processes. Moreover, this approach opens a possibility to put the vague notion of a 'flux tube dynamo' on a firm theoretical basis. A cooperation with Tom Bogdan (Boulder), Antonio Ferriz-Mas and Michael Knölker on such a project is arranged.

Finally, the boundary layer or overshoot layer dynamo will remain a challenge. Kinematical theory probably cannot be applied since kinetic and magnetic energy density are of the same order of magnitude. Future work will focus on two approaches, i.e. the quantitative determination of a field regeneration process and the angular momentum distribution in an overshoot layer, and the investigation of nonlinear dynamo models with a given regeneration process which take into account the particular geometry and thermodynamics of the region as well as expulsion processes and magnetic instabilities. As for most of the discussed problem areas here again comprehensive 3D simulations and idealized/simplified approaches will play complimentary parts: The simulations help to identify the relevant processes and allow us a glimpse at phenomena which are observationally unreachable. They can guide us in picking the relevant pieces of physics to study in detail without falling into the trap of oversimplified or prejudiced concepts. An understanding of the physics governing these processes, of their general properties and the validity of their description in the simulation can only come from a detailed study in the spirit of theoretical physics.

References

Abramovitz, M., Stegun, I.A.: 1965, *Handbook of Mathematical Functions*, Dover, New York
Acheson, D.J.: 1978, *Phil. Trans. Roy. Soc. London*, **A289**, 459
Acheson, D.J.: 1979, *Solar Phys.* **62**, 23
Acheson, D.J., Gibbons, M.P.: 1978, *J. Fluid Mech.* **85**, 743
Achterberg, A.: 1982, *Astron. Astrophys.* **114**, 233
Achterberg, A.: 1988, *Astron. Astrophys.* **191**, 167
Anton, V.: 1984, Diplomarbeit, Universität Göttingen

Batchelor, G.K.: 1967, *An Introduction to Fluid Dynamics*, Cambridge Univ. Press
Bernstein, I.B., Frieman, E.A., Kruskal, M.D., Kulsrud, R.M.: 1958, *Proc. Roy. Soc.* **A244**, 17
Bogdan, T.J.: 1984, *Phys. Fluids* **27**, 994
Bogdan, T.J.: 1985, *Astrophys. J.* **299**, 510
Bogdan, T.J., Lerche, I.: 1985, *Astrophys. J.* **296**, 719
Bogdan, T.J., Gilman, P.A., Lerche, I., Howard, R.: 1988, *Astrophys. J.* **327**, 451
Brandenburg, A., Tuominen, I., Moss, D., Rüdiger, G.: 1990, *Solar Phys.* **128**, 243
Brown, T.M., Christensen-Dalsgaard, J., Dziembowski, W.A., Goode, P., Gough, D.O., Morrow, C.A.: 1989, *Astrophys. J.* **343**, 526

Cadez, V.M.: 1974, thesis, Institute of Physics, Beograd
Cap, F.F.: 1976, *Handbook on Plasma Instabilities*, Vol. **1**, Academic Press, New York
Cattaneo, F., Hughes, D.W.: 1988, *J. Fluid Mech.* **196**, 323
Cattaneo, F., Hughes, D.W., Proctor, M.R.E.: 1988, *Geophys. Astrophys. Fluid Dyn.* **41**, 335
Chou, D.-Y., Fisher, G.H.: 1989, *Astrophys. J.* **341**, 533
Choudhuri, A.R.: 1988, *Geophys. Astrophys. Fluid Dyn.* **40**, 261
Choudhuri, A.R.: 1989, *Solar Phys.* **123**, 217
Choudhuri, A.R., Gilman, P.A.: 1987, *Astrophys. J.* **316**, 788

Defouw, R.J.: 1976, *Astrophys. J.* **209**, 266
Deinzer, W., Hensler, G., Schüssler, M., Weisshaar, E.: 1984, *Astron. Astrophys.* **139**, 435
DeLuca, E.E., Gilman, P.A.: 1986, *Geophys. Astrophys. Fluid Dyn.* **37**, 85
Durney, B.R.: 1989, *Solar Phys.* **123**, 197
Durney, B.R., De Young, D.S., Passot, T.P.: 1990, *Astrophys. J.* **362**, 709
Duvall, T.L., Dziembowski, W.A., Goode, P.R., Gough, D.O., Harvey, J.W., Leibacher, J.W.: 1984, *Nature* **310**, 22
Duvall, T.L., Harvey, J.W., Pomerantz, M.A.: : 1987, in B.R. Durney and S. Sofia (eds.): *The Internal Solar Angular Velocity*, Reidel, Dordrecht, p. 19
Dziembowski, W.A., Goode, P.R., Libbrecht, K.G.: 1989, *Astrophys. J.* **337**, L53

Ferriz-Mas, A., Schüssler, M.: 1989, *Geophys. Astrophys. Fluid Dyn.*, **48**, 217
Ferriz-Mas, A., Schüssler, M, Anton, V.: 1989, *Astron. Astrophys.* **210**, 425

Galloway, D.J.: 1978, in G. Belvedere, L. Paternó (eds.): *Workshop on Solar Rotation*, Catania, p. 352
Galloway, D.J., Proctor, M.R.E., Weiss, N.O.: 1978, *J. Fluid Mech.* **87**, 243
Galloway, D.J., Weiss, N.O.: 1981, *Astrophys. J.* **243**, 945
Garcia de la Rosa, J.I.: 1987, *Solar Phys.* **112**, 49
Gilman, P.A.: 1970, *Astrophys. J.* **162**, 1019
Gilman, P.A.: 1983, *Astrophys. J. Suppl.* **53**, 243
Gilman, P.A., Miller, J.: 1981, *Astrophys. J. Suppl.* **46**, 211

Glatzmaier, G.A., Gilman, P.A.: 1982, *Astrophys. J.* **256**, 316
Glatzmaier, G.A.: 1985a, *Astrophys. J.* **291**, 300
Glatzmaier, G.A.: 1985b, *Geophys. Astrophys. Fluid Dyn.* **31**, 137
Grappin, R., Frisch, U., Léorat, J., Pouquet, A.: 1982, *Astron. Astrophys.* **105**, 6

Hopfinger, E.J., Browand, F.K., Gagne, Y.: 1982, *J. Fluid Mech.* **125**, 505
Howard, R.: 1974, *Solar Phys.* **38**, 59
Howard, R.: 1984, *Ann. Rev. Astron. Astrophys.*, **22**, 131
Howard, R.: 1989, *Solar Phys.* **123**, 285
Hughes, D.W.: 1985a, *Geophys. Astrophys. Fluid Dyn.* **32**, 273
Hughes, D.W.: 1985b, *Geophys. Astrophys. Fluid Dyn.* **34**, 99
Hughes, D.W.: 1987, *Geophys. Astrophys. Fluid Dyn.* **37**, 297
Hughes, D.W., Cattaneo, F.: 1987, *Geophys. Astrophys. Fluid Dyn.* **39**, 297
Hurlburt, N.E., Toomre, J.: 1988, *Astrophys. J.* **327**, 920
Hurlburt, N.E., Toomre, J., Massaguer, J.M.: 1984, *Astrophys. J.* **282**, 557

Knobloch, E.: 1981, *Astrophys. J.* **247**, L93
Knobloch, E., Rosner, R.: 1981, *Astrophys. J.* **247**, 300
Kraichnan, R.H.: 1976, *J. Fluid Mech.* **77**, 753
Krall, N.A., Trivelpiece, A.W.: 1973, *Principles of Plasma Physics*, McGraw-Hill, New York
Krause, F., Rädler, K.-H.: 1980, *Mean-Field Magnetohydrodynamics and Dynamo Theory*, Pergamon, Oxford
Krivodubskii, V.N.: 1984, *Sov. Astron.* **28**, 205
Krivodubskii, V.N.: 1987, *Sov. Astron. Lett.* **13**, 338
Kuznetsov, V.D., Syrovatskii, S.I.: 1979, *Sov. Astron.* **23**, 715

LaBonte, B.J., Howard, R.: 1982, *Solar Phys.* **75**, 161
LaBonte, B.J., Howard, R., Gilman, P.A.:1981, *Astrophys. J.* **150**, 796
Livingston, W., Holweger, H.: 1982, *Astrophys. J.* **252**, 375

McIntosh, P.S.: 1981, in *The Physics of Sunspots*, L.E. Cram, J.H. Thomas (eds.), Sacramento Peak Observatory, p. 7
McEwan, A.D.: 1973, *Geophys. Fluid Dyn.* **5**, 283
McEwan, A.D.: 1976, *Nature* **260**, 126
McWilliams, J.C.: 1984, *J. Fluid Mech.* **146**, 21
Meneguzzi, M., Frisch, U., Pouquet, A.: 1981, *Phys. Rev. Lett.* **47**, 1060
Meneguzzi, M., Pouquet, A.: 1989, *J. Fluid Mech.* **205**, 297
Meyer, F., Schmidt, H.U., Weiss, N.O.: 1977, *Mon. Not. Roy. Astron. Soc.* **179**, 741
Moffatt, H.K.: 1983, *Rep. Prog. Phys.* **46**, 621
Moreno-Insertis, F.: 1983, *Astron. Astrophys.* **122**, 241
Moreno-Insertis, F.: 1984, Dissertation, Universität München
Moreno-Insertis, F.: 1986, *Astron. Astrophys.* **166**, 291
Müller, R., Roudier, Th.: 1984, *Solar Phys.* **94**, 33

Nordlund, Å.: 1983, in J.O. Stenflo (ed.): *Solar and Stellar Magnetic Fields: Origins and Coronal Effects*, IAU-Symp. No. 102, Reidel, Dordrecht , p. 79
Nordlund, Å.: 1984, in S.L. Keil (ed.): *Small-scale Processes in Quiet Stellar Atmospheres*, Sacramento Peak Observatory, Sunspot, p. 174
Nordlund, Å.: 1985, in H.U. Schmidt (ed.): *Theoretical Problems in High Resolution Solar Physics*, MPA 212, Max-Planck Institut für Astrophysik, München, p. 1

Nordlund, Å.: 1986, in W. Deinzer et al. (eds.): *Small Scale Magnetic Flux Concentrations in the Solar Photophere*, Abh. Akad. d. Wiss. Göttingen No. 38, Vandenhoeck & Ruprecht, Göttingen, p. 83

Orszag, S., Tang, C.-H.: 1979, *J. Fluid Mech.* **90**, 129

Piddington, J.H.: 1975, *Astrophys. Space Sci.* **34**, 347
Parker, E.N.: 1955, *Astrophys. J.* **122**, 293
Parker, E.N.: 1963, *Astrophys. J.* **138**, 552
Parker, E.N.: 1966, *Astrophys. J.* **145**, 811
Parker, E.N.: 1975a, *Astrophys. J.* **198**, 205
Parker, E.N.: 1975b, *Solar Phys.* **40**, 291
Parker, E.N.: 1975c, *Astrophys. J.* **201**, 494
Parker, E.N.: 1978, *Astrophys. J.* **221**, 368
Parker, E.N.: 1979a, *Cosmical Magnetic Fields*, Clarendon, Oxford
Parker, E.N.: 1979b, *Astrophys. Sp. Sci.* **62**, 135
Parker, E.N.: 1979c, *Astrophys. J.* **230**, 905
Parker, E.N.: 1979d, *Astrophys. J.* **230**, 914
Parker, E.N.: 1979e, *Astrophys. J.* **232**, 282
Parker, E.N.: 1982a, *Astrophys. J.* **256**, 292
Parker, E.N.: 1982b, *Astrophys. J.* **256**, 302
Parker, E.N.: 1982c, *Astrophys. J.* **256**, 736
Parker, E.N.: 1982d, *Astrophys. J.* **256**, 746
Parker, E.N.: 1982e, *Geophys. Astrophys. Fluid Dyn.* **22**, 195
Parker, E.N.: 1983a, *Astrophys. J.* **264**, 635
Parker, E.N.: 1983b, *Astrophys. J.* **264**, 642
Parker, E.N.: 1984a, *Astrophys. J.* **283**, 343
Parker, E.N.: 1984b, *Astrophys. J.* **286**, 666
Parker, E.N.: 1985a, *Astrophys. J.* **294**, 47
Parker, E.N.: 1985b, *Astrophys. J.* **294**, 57
Parker, E.N.: 1986, in W. Deinzer et al. (eds.): *Small Scale Magnetic Flux Concentrations in the Solar Photophere*, Abh. Akad. d. Wiss. Göttingen No. 38, Vandenhoeck & Ruprecht, Göttingen, p. 13
Parker, E.N.: 1987a, *Astrophys. J.* **312**, 868
Parker, E.N.: 1987b, *Astrophys. J.* **321**, 984
Parker, E.N.: 1987c, *Astrophys. J.* **321**, 1009
Parker, E.N.: 1987d, in B.R. Durney and S. Sofia (eds.): *The Internal Solar Angular Velocity*, Reidel, Dordrecht, p. 289
Parker, E.N.: 1988a, *Astrophys. J.* **325**, 880
Parker, E.N.: 1988b, *Astrophys. J.* **326**, 395
Parker, E.N.: 1988c, *Astrophys. J.* **326**, 407
Parkinson, J.H.: 1983, *Nature* **304**, 518
Pidatella, R.M., Stix, M.: 1986, *Astron. Astrophys.* **157**, 338
Pneuman, G.W., Raadu, M.A.: 1972, *Astrophys. J.* **172**, 739
Pouquet, A.: 1985, in H.U. Schmidt (ed.): *Theoretical Problems in High Resolution Solar Physics*, MPA 212, Max-Planck Institut für Astrophysik, München, p. 34
Proctor, M.R.E., Weiss, N.O.: 1982, *Rep. Progr. Phys.*, **45**, 1317

Rädler, K.H.: 1968, *Z. Naturforsch.* **23a**, 1851 (engl. transl. in Roberts, P.H., Stix, M.: *The Turbulent Dynamo*, Tech. Note 60, NCAR, Boulder, Colorado, 1971)

Roberts, B., Webb, A.R.: 1978, *Solar Phys.* **56**, 5
Roberts, P.H., Stewartson, K.: 1977, *Astron. Nachr.*, **298**, 311

Schmitt, D.: 1985, Dissertation, Universität Göttingen
Schmitt, J.H.M.M., Rosner, R.: 1983, *Astrophys. J.* **265**, 901
Schmitt, J.H.M.M., Rosner, R., Bohn, H.U.: 1984, *Astrophys. J.* **282**, 316
Schröter, E.H.: 1985, *Solar Phys.* **100**, ???
Schüssler, M.: 1977, *Astron. Astrophys.* **56**, 439
Schüssler, M.: 1979, *Astron. Astrophys.* **71**, 79
Schüssler, M.: 1980a, *Astron. Astrophys.* **89**, 26
Schüssler, M.: 1980b, *Nature* **288**, 150
Schüssler, M.: 1983, in J.O. Stenflo (ed.): *Solar and Stellar Magnetic Fields: Origins and Coronal Effects*, IAU-Symp. No. 102, Reidel, Dordrecht , p. 213
Schüssler, M.: 1984a, in T.D. Guyenne and J.J. Hunt (eds.): *The Hydromagnetics of the Sun*, ESA SP-220, p. 67
Schüssler, M.: 1984b, *Astron. Astrophys.* **140**, 453
Schüssler, M.: 1986, in W. Deinzer et al. (eds.): *Small Scale Magnetic Flux Concentrations in the Solar Photophere*, Abh. Akad. d. Wiss. Göttingen No. 38, Vandenhoeck & Ruprecht, Göttingen, p. 103
Schüssler, M.: 1987, in B.R. Durney and S. Sofia (eds.): *The Internal Solar Angular Velocity*, Reidel, Dordrecht, p. 303
Schüssler, M.: 1990, in J.O. Stenflo (ed.): *Solar Photosphere: Structure, Convection and Magnetic Fields*, IAU-Symp. No. 138, Kluwer, Dordrecht, p. 161
Shaviv, G., Salpeter, E.E.: 1983, *Astrophys. J.* **184**, 191
Smirnow, W.I.: 1968, *Lehrgang der Höheren Mathematik*, Bd. II, Akademie-Verlag, Berlin, DDR
Solanki, S.K.: 1990, in J.O. Stenflo (ed.): *Solar Photosphere: Structure, Convection and Magnetic Fields*, IAU-Symp. No. 138, Kluwer, Dordrecht
Spiegel, E.A., Weiss, N.O.: 1980, *Nature* **287**, 616
Spitzer, L.: 1957, *Astrophys. J.* **125**, 525
Spruit, H.C.: 1977a, *Solar Phys.* **55**, 3
Spruit, H.C.: 1977b, thesis, University of Utrecht
Spruit, H.C.: 1981a, *Astron. Astrophys.* **98**, 155
Spruit, H.C.: 1981b, *Astron. Astrophys.* **102**, 129
Spruit, H.C.: 1981c, in *The Physics of Sunspots*, L.E. Cram, J.H. Thomas (eds.), Sacramento Peak Observatory, p. 98
Spruit, H.C.: 1982, *Astron. Astrophys.* **108**, 348
Spruit, H.C., Roberts, B.: 1983, *Nature* **304**, 401
Spruit, H.C., van Ballegooijen, A.A.: 1982, *Astron. Astrophys.* **106**, 58
Spruit, H.C., Zweibel, E.G.: 1979, *Solar Phys.* **62**, 15
Spruit, H.C., Zwaan, C.: 1981, *Solar Phys.* **70**, 207
Stenflo, J.O.: 1989, *Astron. Astrophys. Rev.*, **1**, 3
Stix, M.: 1981a, *Solar Phys.* **74**, 79
Stix, M.: 1981b, *Astron. Astrophys.* **93**, 339
Stix, M.: 1976, in V. Bumba, J. Kleczek (eds.): *Basic Mechanisms of Solar Activity*, IAU-Symp. No. 71, Reidel, Dordrecht, p. 367
Stix, M.: 1982, in W. Fricke, G. Teleki (eds.): *Sun and Planetary System*, 6th European Regional Meeting, Reidel, Dordrecht, p. 63

Title, A.M., Tarbell, T.D., Topka, K.P.: 1987, *Astrophys. J.* **317**, 892

Tsinganos, K.C.: 1980, *Astrophys. J.* **239**, 746

Unno, W., Ando, H.: 1979, *Geophys. Astrophys. Fluid Dyn.* **12**, 107
Unno, W., Ribes, E.: 1976, *Astrophys. J.* **208**, 222

Van Ballegooijen, A.A.: 1982a, *Astron. Astrophys.* **106**, 43
Van Ballegooijen, A.A.: 1982b, *Astron. Astrophys.* **113**, 99
Van Ballegooijen, A.A.: 1983, *Astron. Astrophys.* **118**, 275
Van Ballegooijen, A.A., Choudhuri, A.R.: 1988, *Astrophys. J.* **333**, 965

Webb, A.R., Roberts, B.: 1978, *Solar Phys.* **59**, 249
Weiss, N.O.: 1966, *Proc. Roy. Soc.* **A293**, 310
Weiss, N.O.: 1981a, *J. Fluid Mech.* **108**, 247
Weiss, N.O.: 1981b, *J. Fluid Mech.* **108**, 273
Weiss, N.O.: 1981c, in C. Jordan (ed.): *Solar Activity*, Proc. 3rd European Solar Meeting, Oxford, p. 35
Willson, R.C.: 1984, *Sp. Sci. Rev.* **38**, 203
Wittmann, A., Bonet Navarro, J.A., Wöhl, H.: 1981, in L.E. Cram, J.H. Thomas (eds.): *The Physics of Sunspots*, Sacramento Peak Observatory, p. 424

Yoshimura, H.: 1981, in F. Moriyama, J.C. Hénoux, Proc. of the Japan-France Seminar on Solar Physics, p. 19

Zel'dovich, Ya.B.: 1957, *Sov. Phys. JETP* **4**, 460
Zwaan, C.: 1978, *Solar Phys.* **60**, 213